CHALMERS
UNIVERSITY OF TECHNOLOGY

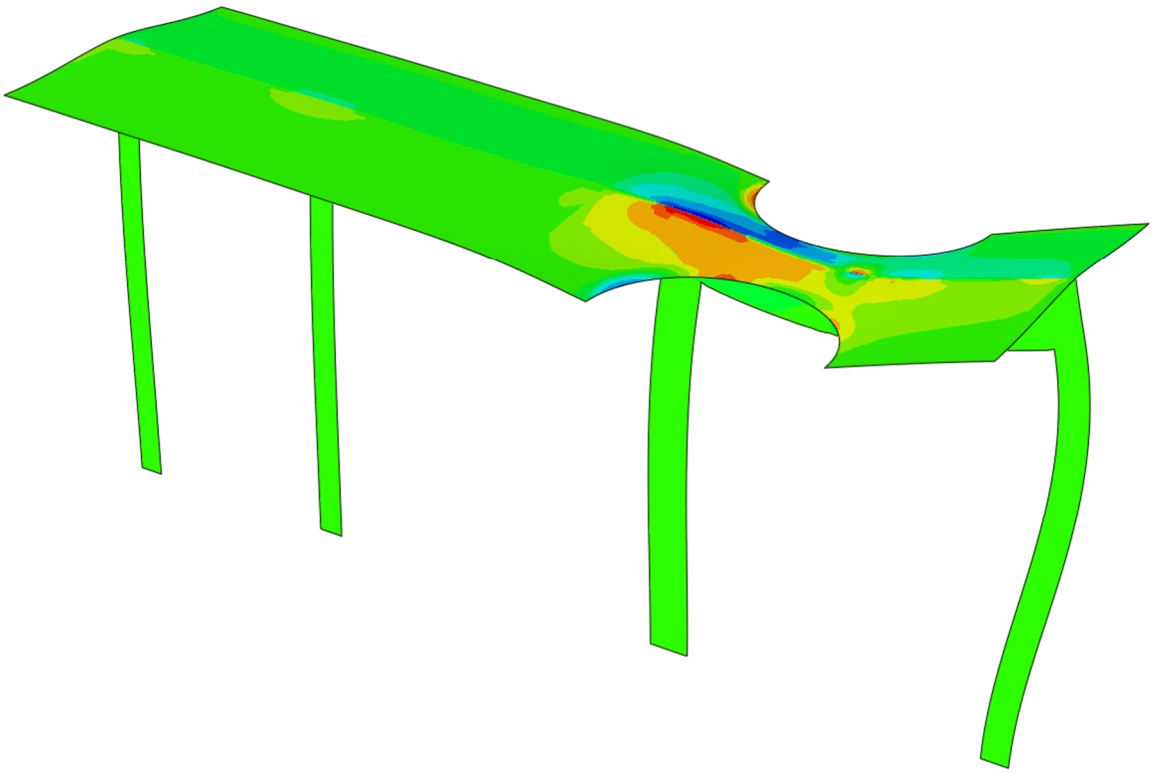

Shear Strengthening of Existing Concrete Slabs

Master's thesis in the Master's Programme Structural Engineering and Building Technology

ANTON HELLBERG
VICTOR ERYD

Department of Architecture and Civil Engineering
Division of Structural Engineering
Concrete Structures
CHALMERS UNIVERSITY OF TECHNOLOGY
Master's Thesis ACEX30-18-11
Gothenburg, Sweden 2018

MASTER'S THESIS ACEX30-18-11

Shear Strengthening of Existing Concrete Slabs

Master's Thesis in the Master's Programme Structural Engineering and Building Technology

ANTON HELLBERG
VICTOR ERYD

Department of Architecture and Civil Engineering
Division of Structural Engineering
Concrete Structures
CHALMERS UNIVERSITY OF TECHNOLOGY
Göteborg, Sweden 2018

Shear Strengthening of Existing Concrete Slabs

Master's Thesis in the Master's Programme Structural Engineering and Building Technology

ANTON HELLBERG

VICTOR ERYD

Examensarbete ACEX30-18-11
Institutionen för arkitektur och samhällsbyggnadsteknik
Chalmers tekniska högskola, 2018

Department of Architecture and Civil Engineering
Division of Structural Engineering
Concrete Structures
Chalmers University of Technology
SE-412 96 Göteborg
Sweden
Telephone: + 46 (0)31-772 1000

Cover:
Contour plot of the transverse shear flow on the deformed shape of the case study, level III analysis.
Department of Architecture and Civil Engineering
Göteborg, Sweden, 2018

Shear Strengthening of Existing Concrete Slabs

Master's thesis in the Master's Programme Structural Engineering and Building Technology

ANTON HELLBERG
VICTOR ERYD
Department of Architecture and Civil Engineering
Division of Structural Engineering
Concrete Structures
Chalmers University of Technology

ABSTRACT

Existing reinforced concrete (RC) slabs have usually been designed without shear reinforcement. Previous design codes have made it possible to assume that the shear capacity of regular reinforced concrete is sufficient. Recent times have shown an increasing need for strengthening existing RC slabs, due to increased load demands or changes in design codes. However, research on this topic is still limited.

This study aimed to further increase the knowledge of shear in RC slabs and provide a review of current shear strengthening methods by literature review. In addition, the study aimed to explore reasons for the increased need of shear strengthening in reinforced concrete slabs that is seen today. When comparing current and previous design codes, it could be seen that the current design code, Eurocode, is more conservative and yields a lower shear capacity than previous design codes. This difference arose due to different approaches when determining the shear resistance.

Further, the study assessed and evaluated the possible need for shear strengthening of a case study. The case study consisted of an industrial building with RC slabs in several spans, supported on beams and columns. In each span, a silo is supported along the perimeter of a hole through the slab. A need to increase the loads of the silos led to an interest of further investigation of the shear behaviour in the structure. Additionally, the case study was meant to provide recommendations for the assessment of similar cases.

The assessment was done through the use of a multi-level structural assessment strategy, consisting of analytical calculations as well as linear and non-linear numerical analyses. The analytical and linear elastic analysis showed that the structure had sufficient shear capacity, while the non-linear analysis determined a need for shear strengthening the structure. Non-linear numerical analyses captured load redistributions due to cracking, which the other models did not. This provided higher shear forces locally in the slab, which led to a conclusion that shear strengthening is needed. However, since a strengthening need was seen for the highest level only, caution must be taken when studying similar cases in the future. It should be made sure the level of assessment is fitting, since higher levels of accuracy require additional time and effort.

Based on the numerical results, an evaluation of the different shear strengthening methods was done. It shown that drilled-in steel bars would be the most appropriate strengthening technique for the case study, due to its low cost and high applicability.
Key words: Shear Strengthening, Concrete, Slab, Finite Element, Assessment

Tvärkraftsförstärkning av Befintliga Betongplattor

Examensarbete inom masterprogrammet Structural Engineering and Building Technology

ANTON HELLBERG
VICTOR ERYD
Institutionen för arkitektur och samhällsbyggnadsteknik
Avdelningen för Konstruktionsteknik
Betongbyggnad
Chalmers tekniska högskola

SAMMANFATTNING

Befintliga betongplattor har vanligen dimensionerats utan särskild tvärkraftsarmering. Tidigare beräkningsnormer har gjort det möjligt att anta att kapaciteten mot tvärkraft av enkelarmerade betongplattor är tillräcklig. På senare tid har det däremot framkommit ett ökat behov av tvärkraftsförstärkningar i betongplattor på grund av ökade laster och förändringar i designkrav. Dock är forskningen angående detta ännu begränsad.

Denna studie ämnade att utöka kunskapen om tvärkraft i armerade betongplattor och tillhandahålla en redogörelse för idag tillgängliga förstärkningsmetoder genom litteraturstudie. Fortsättningsvis syftade studien till att utforska det ökade behovet av tvärkraftsförstärkningar som kan ses idag. Vid en jämförelse mellan nuvarande och tidigare gällande beräkningsnormer visades det att den nu gällande beräkningsnormen, Eurocode, är mer konservativ och ger en lägre tvärkraftskapacitet. Denna skillnad härstammade ifrån olika tillvägagångssätt för att bestämma betongs tvärkraftskapacitet.

Utöver detta utreddes och utvärderades det eventuella behovet av tvärkraftsförstärkning för en fallstudie. Fallstudien bestod av en befintlig industribyggnad, bestående av armerade betongplattor i flera spann vilka i sin tur bärs upp av betongpelare och -balkar. I varje spann finns håltagningar i plattan för autoklaver, vilka är upplagda utmed hålens omkrets. Ett behov av att öka de laster som härstammar från dessa autoklaver föranledde intresset att vidare studera tvärkraftsbeteendet i denna byggnad. Fallstudien skulle också bidra till en riktlinje för hur liknande bärighetsutredningar kan genomföras.

Genom en bärighetsutredning i flera nivåer, bestående av analytiska beräkningar samt linjära och icke-linjära numeriska analyser, påvisades behov för tvärkraftsförstärkning. Den högsta utvärderingsnivån, icke-linjär numerisk analys, beskrev lastomfördelning som tog plats på grund av sprickbildning, vilket lägre nivåer inte gjorde. Denna omfördelning föranledde högre tvärkraft lokalt i plattan vilket ledde till slutsatsen att förstärkning behövs. Då ett förstärkningsbehov endast sågs i den högsta nivån bör liknande utvärderingar göras med försiktighet. Lämplig detaljnivå bör användas, samtidigt som hänsyn tas till den extra tid och möda som krävs för en högre nivå.

Baserat på resultaten från den numeriska analysen gjordes en utvärdering av de presenterade förstärkningsmetoderna. Inborrade stålstänger konstaterades vara det mest lämpliga alternativet tack vare sin låga kostnad och goda applicerbarhet.

Nyckelord: Tvärkraftsförstärkning, Betongplatta, Finita Element, Bärighetsutredning

Contents

Preface

This study was meant to increase the knowledge of shear in reinforced concrete slabs, why an increase in strengthening need is apparent today and how to perform the process concerning a strengthening, if needed. The study was conducted at ÅF Infrastructure in Gothenburg in association with the Division of Structural Engineering at Chalmers University of Technology during the spring of 2018.

We would first and foremost like to thank our supervisor, Valbona Mara from ÅF, without whom the study would not have been possible. The impact from her never-ending interest throughout the entirety of the process cannot be understated. Our examiner, Ignasi Fernandez from Chalmers, have also provided a constant helping hand throughout the project and been an integral part of the end outcome.

Special gratitude goes out as well to Jincheng Yang from Chalmers and Johan Olsson from ÅF with regard to the much needed knowledge in ABAQUS and finite element modelling that they have provided.

We would also like to thank our thesis opponents Felica Carlander-Reuterfelt and Felicia Flink for reviewing and providing constructive criticism throughout the process.

Finally, we would like to thank ÅF Infrastructure for the opportunity to carry out the study with the help from all the colleagues and last but not least, a place to sit.

Gothenburg, May 2018

Anton Hellberg and Victor Eryd

Notations

Roman upper case letters

A	Shear reinforcement area per unit length
$A_{eq.s}$	Equivalent steel area
A_{FRP}	Cross-sectional area of longitudinal FRP reinforcement
A_f	Cross-sectional area of FRP strip
A_{fw}	Cross-sectional area of ETS bars
A_s	Cross-sectional area of bolt stem
A_{sw}	Cross-sectional area of shear reinforcement
B	Diameter of perimeter around a column
$C_{Rd,c}$	Material specific constant
E	Young's modulus
E_{FRP}	Young's modulus for FRP
E_S	Young's modulus for steel
F_{cw}	Force in incline concrete compressive chord
F_{td}	Tensile force in reinforcement
I	Second moment of area
J_1	Bond modelling constant
L_p	Bar perimeter
$L_{Rfi.eq}$	Equivalent average resisting bond length
M_{cr}	Cracking moment
M_{ult}	Ultimate moment
$N^l_{f,int}$	Minimum number of bars that can cross a shear crack
Q_k	Concentrated imposed load
P	Punching force
R	Reaction force
S	First moment of area
V	Shear force
V_{ccd}	Design shear component of the force in compression area in case of inclined compression chord
$V_{R,f}$	Contribution of shear capacity due to strengthening
$V^{max}_{fi,eff}$	Maximum capacity of the average length bar along the shear crack, taken as the minimum value between the resisting bond force an yield force
$V_{Rd,c}$	Design shear resistance of concrete without shear reinforcement
$V_{Rd,cs}$	Design punching shear resistance of concrete with shear reinforcement
$V_{Rd,i}$	Additional design shear capacity due to inclination in regular reinforcement
$V_{Rd,max}$	Design web shear compression resistance
$V_{Rd,s}$	Design shear resistance of yielding shear reinforcement
V_{td}	Design shear component of the force in tensile reinforcement in case of inclined tensile chord

Roman lower case letters

b	Width of cross-section
b_w	Minimum width of cross-section
c	Diameter of a circular area
d	Effective depth

f_{cd}	Design concrete compressive strength
f_{ck}	Characteristic concrete compressive strength
f_{ct}	Characteristic concrete tensile strength
f_{fv}	Tensile strength of FRP material
f_v	Formal concrete shear capacity
f_{yt}	Yield strength of steel
f_{ywd}	Design yield strength of shear reinforcement
$f_{ywd,ef}$	Effective design yield strength of shear reinforcement
h	Height of cross-section
k	Geometric variable
k_1	Constant
m	Bending moment per unit width
n	Normal force per unit width
n_{bar}	Number of installed bars
n_{layer}	Number of layers of FRP strips
q_d	Design distributed load
q_k	Distributed imposed load
s	Shear reinforcement spacing
s_{ebr}	Spacing of externally bonded FRP reinforcement
s_{fw}	Spacing of ETS bars
s_r	Radial shear reinforcement spacing
t	Thickness
u_1	Perimeter length of a punching subjected area
v	Shear force per unit width
v_{Ed}	Design punching shear resistance along a perimeter
v_{min}	Variable depending on concrete compressive strength and geometry
z	Internal lever arm

Greek lower case letters

α	Angle between shear reinforcement and centroidal axis of member
α_A	Reduction factor
α_{cw}	Coefficient taking account of the state of the stress in the compression chord
β	Reduction factor with regard to usable FRP strength
δ_1	Bond slip
θ	Angle between the concrete compressive strut and member axis perpendicular to the shear force
λ	Bond modelling constant
ν	Strength reduction factor for concrete cracked in shear
ξ	Geometric variable
ρ_l	Ratio between reinforcement and concrete cross-sectional areas
σ_a	Allowed tensile stress for shear reinforcement
σ_{cp}	Normal stress in concrete due to external load or prestressing
σ_{cw}	Stress in incline concrete compressive chord
τ	Shear stress
τ_{nom}	Nominal shear stress
τ_0	Shear stress limit
τ_1	Shear stress limit
ϕ_{ETS}	Diameter of ETS bar

1 Introduction

1.1 Background

Existing reinforced concrete (RC) slabs have usually been designed without shear reinforcement. Previous design codes have made possible to assume that the shear capacity of regular reinforced concrete was sufficient. Recent times have shown, however, an increasing need for strengthening existing RC slabs because of changes in loads and design requirements. This has therefore raised an interest in the topic to determine the changes for designing RC slabs against shear and investigate the different existing strengthening techniques.

Recently, ÅF Infrastructure carried out a project with the underlying purpose to evaluate the need of strengthening an industrial building. The building consists of several RC slabs in different spans, which are supported on concrete beams and columns. Each main span carries a silo, which is supported along the perimeter of a go-through-hole in the slab, see Figure 1.1. A need of increasing the loads of these silos led to the interest in further investigation of the shear behaviour of the structure.

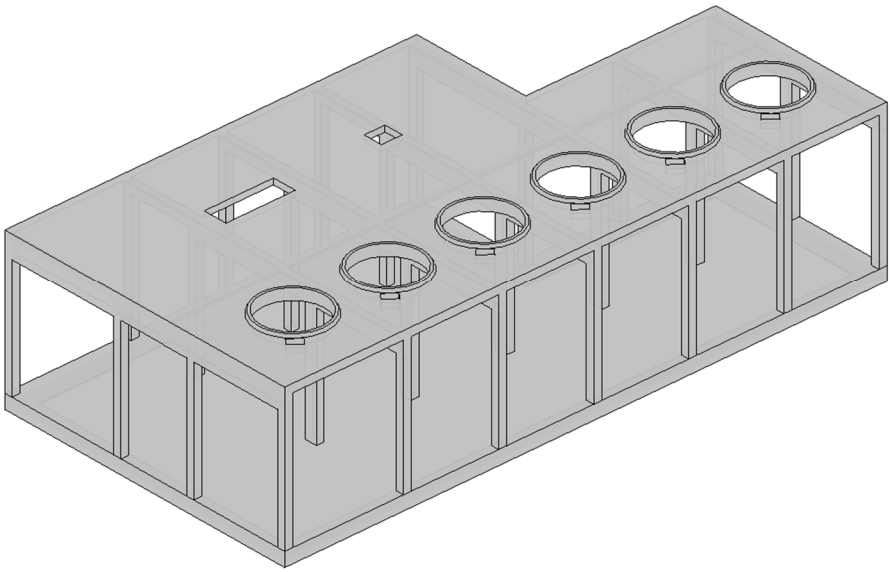

Figure 1.1 3D model of floor from building in case study.

1.2 Aim and objectives

The aim of this study is to provide knowledge about shear behaviour, strengthening techniques and to evaluate different strengthening methods for RC slabs which are suspected to fail in shear. Specifically, the study addresses:

- A general review of shear behaviour and failure mechanisms in reinforced concrete.
- A review regarding substantial changes in design codes, with respect to both loads and shear design.
- A review of different shear strengthening methods available today and the extent of knowledge as well as the state-of-practice in the field today.

- A case study of an existing industrial building which is comprised of two sub-parts:
    - A structural assessment of the building using hand calculations and finite element (FE) analyses in the commercial software ABAQUS/CAE 2017. The assessment should produce an analysis of the shear capacity for the structure and an evaluation of different modelling techniques for composite slab-beam RC structures with regard to computational demand and modelling time, while still being able to describe shear. The assessment should provide recommendations for how similar cases could be evaluated. Additionally, it should determine whether the industrial building is able to carry an increase in load with regard to shear.
    - Based on the result from the previous sub-part, the most suitable method for strengthening the structure should be determined. Analytical expressions should be determined and used to compare relevant strengthening methods against each other in terms of structural performance. The most suitable strengthening method should then be determined based on its applicability and cost. An evaluation of the impact of the already existing flexural strengthening's contribution to the shear capacity will be performed in this step as well.

1.3 Method

The method of the study consists of literature review of the different topics to be addressed, analytical calculations and numerical analyses. The main methodology consists of:

- Reviewing shear behaviour in RC slabs and beams. Investigating the transferability of beam theory to slabs and thereafter identifying shear strengthening techniques and comparing/evaluating the found methods in a case study of a composite slab-beam structure.
- Reviewing and comparing current design codes with previous design codes.
- Modelling and performing FE analyses of the composite slab-beam structure. Comparing and evaluating the numerical results for different levels of modelling detail and against analytical hand-calculations.
- Assessing the need for shear strengthening in the case study and thereafter performing an evaluation of different applicable methods with analytical calculations and evaluations considering the suitability for this specific case.

1.4 Limitations

The study focuses on effects arising from shear stresses in the ultimate limit state (ULS) in non-prestressed RC slabs. The investigated and applied design codes are according to Swedish standards. FE modelling is carried out in the commercial FE software ABAQUS, where anchorage failure of reinforcement is not described. Slabs that are prestressed are out of the scope of this study.

2 Shear in Reinforced Concrete Slabs

This section describes, in general terms, what shear is and how it gives rise to stresses, both for RC beams and slabs. The chapter presents the load carrying behaviour of concrete in shear, in all stages of its lifetime. It concludes in a review on how the design for shear according to current standards is made and how it compares to previous standards.

2.1 Material response

It is important to understand the behaviour of reinforced concrete, to grasp why the composite material will behave differently during different stages of its lifetime. Reinforced concrete is a composite material consisting of plain concrete and, most often, reinforcing steel bonded together. For the two materials separately, the stress-strain relationship can be seen in Figure 2.1.

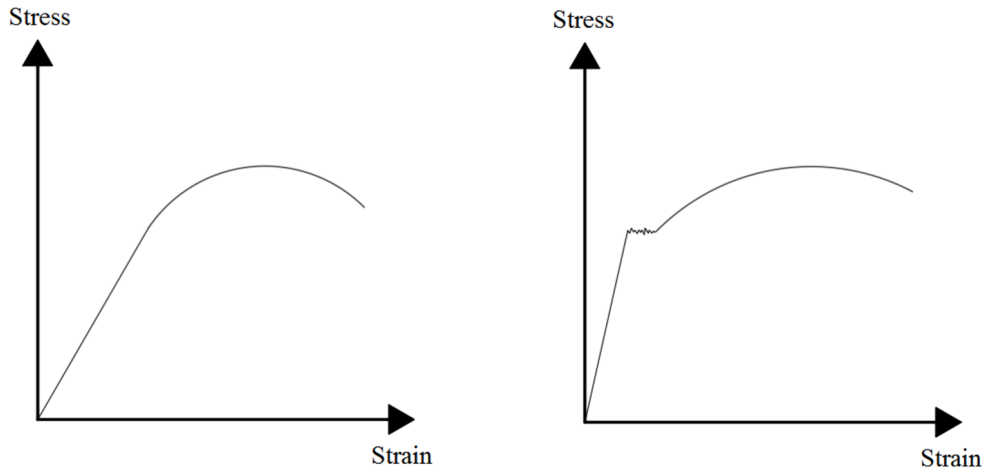

Figure 2.1 Stress-strain relationships for: (a) Plain concrete; (b) Steel.

When bonded together, the composite can be said to experience three different states. This becomes especially apparent when studying the moment-curvature relationship for a small region of reinforced concrete subjected to bending, see Figure 2.2. In the first state, the uncracked state, a linear elastic behaviour is observed up until the cracking moment, M_{cr}, is reached. The second state, the cracked state, begins as soon as the first crack appears. As the cracking propagates through the concrete, the reinforcement is engaged and a moment redistribution due to cracking takes place. When the region is fully cracked, the third state, the ultimate state, will be reached. When the capacity of one section is reached, a plastic moment redistribution takes place up until the ultimate moment, M_{ult}, is reached, whereby a collapse mechanism is formed.

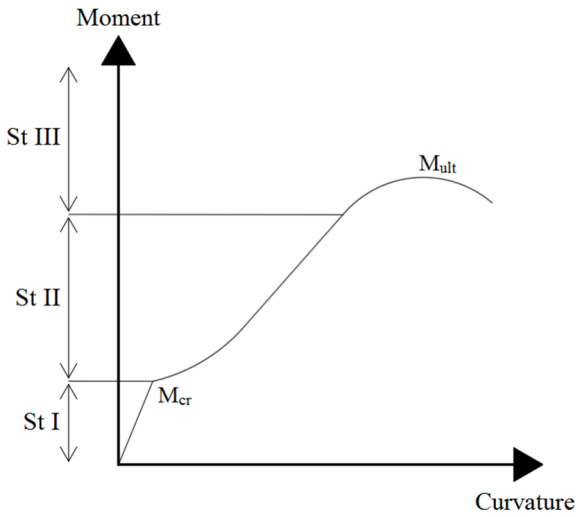

Figure 2.2 Moment-curvature relationship for reinforced concrete.

2.2 Cross-sectional forces and stresses

When a structural member is subjected to an external load, it must transfer the load to its supports in a way that fulfils equilibrium. In RC beams the load is transferred to adjacent supports via sectional forces: bending moment, M [Nm]; shear force, V [N] and normal force, N [N]. Slabs can function with both one-way and two-way behaviour, indicating whether the load is transferred to its supports in one or two directions, see Figure 2.3.

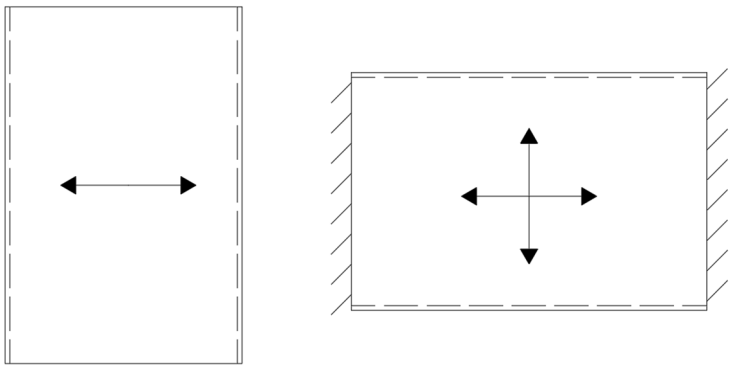

(a) (b)

Figure 2.3 Examples of different shear behaviour in a slab: (a) One-way behaviour; (b) Two-way behaviour. Dashed line indicates simply supported end, hatched line indicates fixed end, plain line indicates free end.

If the slab exhibits one-way behaviour, a simplification where the slab is considered as a beam is possible to make. This is done by dividing the slab into one-way strips, thus the sectional forces become: bending moment per unit width, m [Nm/m], shear force per unit width, v [N/m], and normal force per unit width, n [N/m].

For two-way behaviour, load is carried in more than one direction and the sectional forces should as such be divided into two main directions. Therefore, a coordinate system may be introduced for the slab, so that the sectional forces become indexed into m_x , m_y , v_x , v_y , n_x , n_y . Additionally, a torsional moment m_{xy} is introduced (Engström, 2014). A distinction should however be made that the indexes in different directions do not mean the same for moment and for shear. Moment, or bending, simultaneously work in two different principal directions and may be described by a quadratic matrix, whereas shear per definition only works in one principal direction and may be described by a vector, see Figure 2.4. Thus, moments with indexes describe the bending in those directions and shear with indexes describe the shear components in those directions. One- and two-way shear is hence a denomination which requires caution (Vaz Rodrigues, 2007).

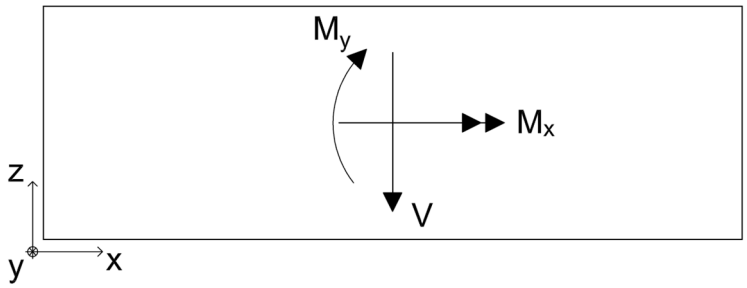

Figure 2.4 Cross-section view with moments in two directions and shear in one direction.

Almost all slabs are statically indeterminate, which gives the designer more choices of how to solve equilibrium (Engström, 2014). For design in ULS, the RC slab capacity is usually determined by the moment capacity, which is possible to vary with different reinforcement arrangements. Eurocode 2 ('SS-EN 1992-1-1', 2008) offers the possibility to design slabs with:

- Linear elastic analysis
- Linear elastic analysis with limited redistribution
- Plastic analysis
  - Lower bound approach
  - Upper bound approach
- Non-linear analysis

2.3 Uncracked state

In the uncracked state, sectional forces, due to transversal load, vary along the member and the arising stresses also vary over the cross-section, in an almost linear relation to the load in the uncracked state. The stiffness of the member depends almost entirely on the gross concrete section. For a homogenous uncracked cross-section, stresses vary according to Figure 2.5. The shear stress is then distributed in a parabolic shape with a maximum value along the gravity centre of the cross-section.

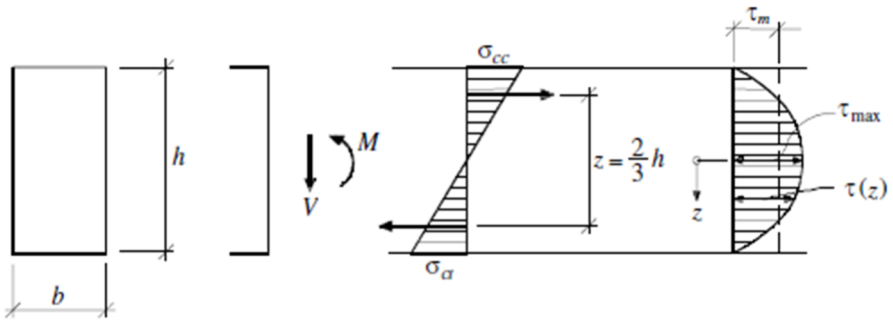

Figure 2.5 Normal stress and shear stress distribution in uncracked rectangular cross-section (Al-Emrani, Engström, Johansson, & Johansson, 2013).

For a single symmetric uncracked cross-section the shear stress at an arbitrary coordinate z can then be approximated according to equation (2.1) (Al-Emrani et al., 2013).

$$\tau(z) = \frac{S(z) \cdot V}{I \cdot b(z)} \tag{2.1}$$

where

- $S(z)$ is the first moment of area of the part of the cross-section beyond the coordinate z about the gravity centre
- V is the shear force acting in the section
- I is the second moment of area of the cross-section about the gravity centre
- $b(z)$ is the width of the cross-section at the coordinate z

For an uncracked cross-section with varying width, the maximal shear stress can be approximated on the safe side according to equation (2.2), which also holds true for cross-sections with constant width.

$$\tau_{max} = \frac{S(0) \cdot V}{I \cdot b_w} \tag{2.2}$$

where

- $S(0)$ is the first moment of area about the gravity centre with respect to the gravity centre.
- b_w is the minimum width of the cross-section

The behaviour of a slab in the uncracked state can be analysed with a linear FE analysis (Engström, 2014). This is due to the reinforcement having very little impact on the structural behaviour before cracking and the slab can therefore be assumed to be isotropic with a linear elastic response.

2.4 Cracked state

As previously mentioned, the cracked state starts as soon as the first crack appears in the concrete. Cracking lead to a loss of stiffness in comparison to the uncracked state, see Figure 2.2, and the stiffness now depends on the reinforcement amounts in different regions. Cracks form when the principal tensile stress exceeds the tensile capacity of the concrete. Since the principal stress direction varies across the structural member, different types of cracks may form. The difference between different types of cracks is the direction of propagation in the concrete. For example, in a simply supported beam, the principal stress will consist largely of bending stresses near the middle of the span and largely of shear stresses adjacent to the support, see Figure 2.6.

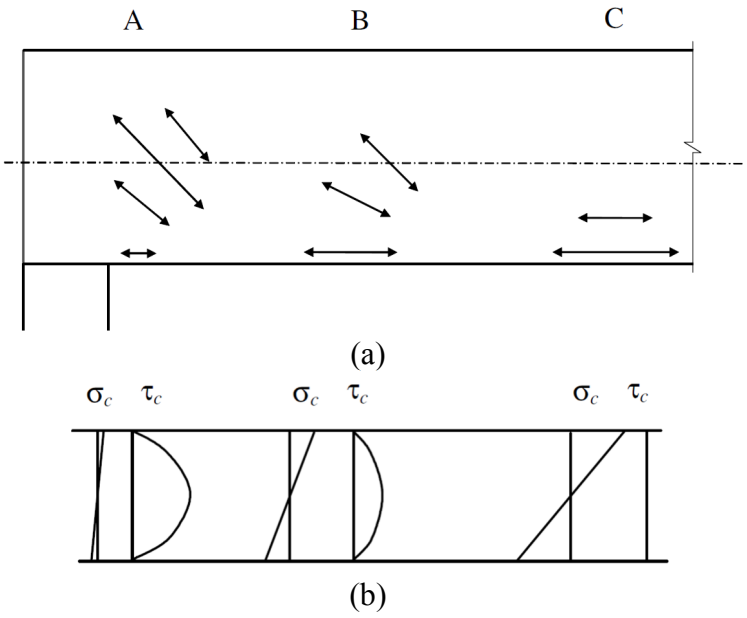

Figure 2.6 Behaviour of an uncracked structural member due to bending and shear: (a) Tensile principal stress directions; (b) Distribution of bending and shear stresses in corresponding sections (Al-Emrani et al., 2013).

The principal stress consisting mainly of bending stresses will create flexural cracks. The principal stress consisting mainly of shear stresses will create web shear cracks and the principal stresses with a mixture of bending and shear stresses will create flexural shear cracks. The different types of cracks can be seen in Figure 2.7.

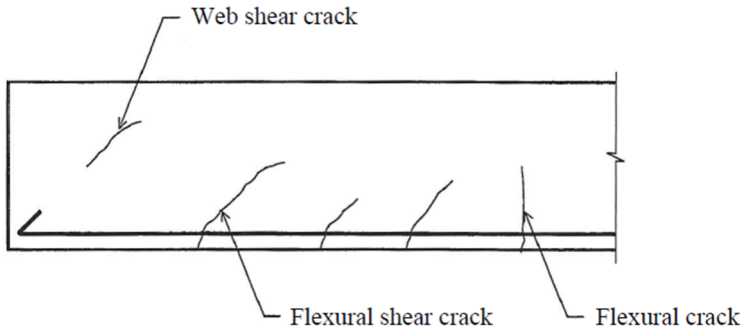

Figure 2.7 Different types of cracks in reinforced concrete (Al-Emrani et al., 2013).

When the concrete has cracked, the equilibrium conditions described in Section 2.3 are no longer valid. Many different models of interpretation exist which describes the shear behaviour in reinforced concrete to different levels of accuracy. A distinction must be made between concrete that contains shear reinforcement and concrete that does not. Concrete without shear reinforcement can only transfer small shear forces, by interlocking of aggregates and dowel action from the longitudinal reinforcement (Broo, 2008). If the concrete does contain shear reinforcement, a common way to represent the force pattern is by a truss model (Al-Emrani et al., 2013). The structural member is divided into compressive struts and tensile ties such that:

- concrete in-between cracks and the top chord (above the cracked part of the concrete) are regarded as compressive struts.
- reinforcement (both longitudinal and transversal) is regarded as tensile ties.

Thus, compression from external loads transfer through the inclined concrete compression chords where the reinforcement can transfer the loads past the cracks to a new compressive strut, see Figure 2.8.

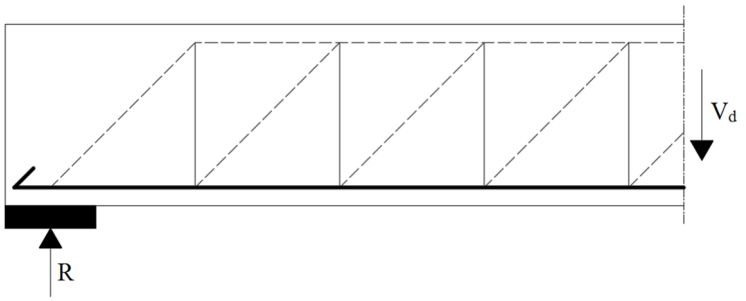

Figure 2.8 Truss model for RC beam with shear reinforcement. Dashed lines indicate compressive struts and full lines indicate tensile ties.

For an arbitrary section somewhere along an RC beam with shear reinforcement, see Figure 2.9, equilibrium conditions will yield that the inclined compressive force, F_{cw}, in that section can be calculated with equation (2.3).

$$F_{cw} = \frac{\sigma_{cw} \cdot b_w \cdot 0.9d}{\sqrt{2}} \tag{2.3}$$

where

σ_{cw} is the incline compressive stress in the web
b_w is the minimum thickness of the web
d is the internal lever arm between the longitudinal compressive and tensile chords

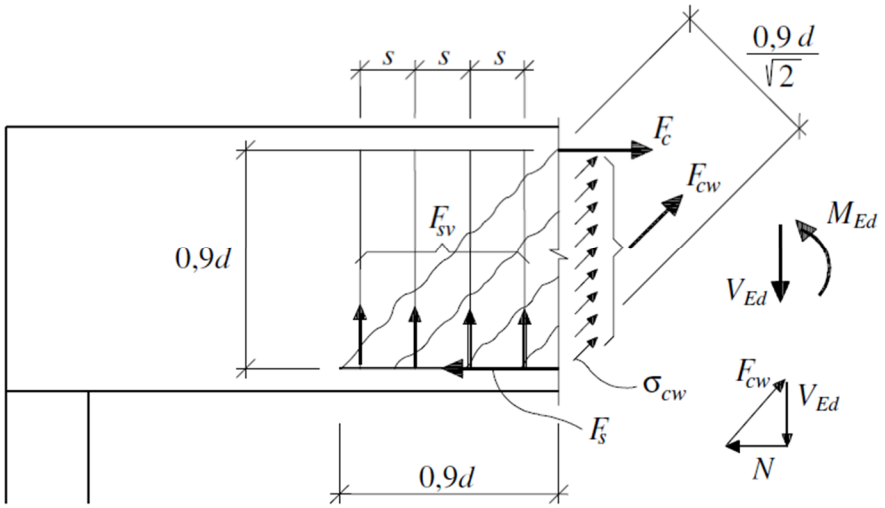

Figure 2.9 Truss model for RC beam section with shear reinforcement after cracking (Al-Emrani et al., 2013).

The behaviour of a slab in the cracked state is not easy to predict, as the cracking and moment redistribution are non-linear processes. A non-linear FE analysis may describe the behaviour of the cracked state assuming all information regarding materials, reinforcement arrangements and boundary conditions are given and correctly implemented (Engström, 2014).

2.5 Ultimate state

When the concrete is fully cracked, an increase in load will lead to yielding in the reinforcement. When the first bar has started to yield, the ultimate state starts (Engström, 2014), see Figure 2.2. As the load increases, more bars will yield until a failure mechanism is developed. Yielding will start in the stiffer regions, which attracts load, and a plastic moment redistribution will take place, provided that the member is ductile enough, to spread load towards weaker regions. The ultimate state exhibits non-linear behaviour.

2.5.1 Ultimate limit state

The end of the ultimate state is denoted as the ultimate limit state (ULS), which is when failure is defined. If the shear capacity of a slab is not sufficient, the ductile failure in bending may be shifted to a brittle failure in shear, which can be categorized into either one-way or two-way shear failure (Vaz Rodrigues, 2007), see Figure 2.10 and Figure 2.11. The two-way shear failure is commonly referred to as punching shear failure and one-way shear failure in RC slabs is analogous to the shear failure in beams. If the shear component in one of the slab's strips causes it to fail, it will fail in a beam-like behaviour. One-way shear failure may be divided into two main failure modes, shear sliding failure and web shear compression failure, which are described in the following sections.

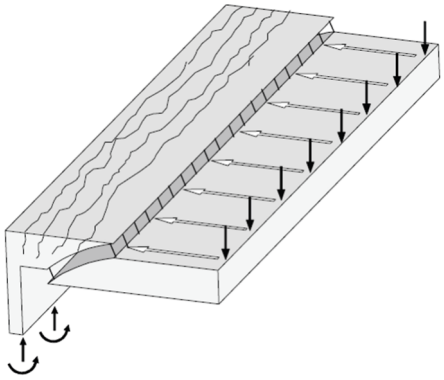

Figure 2.10 One-way shear failure of RC slab (Vaz Rodrigues, 2007).

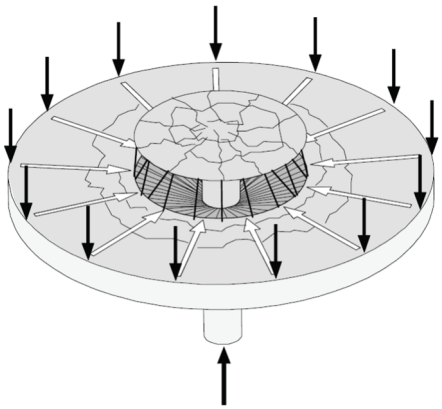

Figure 2.11 Two-way shear failure of RC slab (Vaz Rodrigues, 2007).

2.5.1.1 Shear sliding failure

Shear sliding failure is a one-way shear failure which can happen in members both with and without shear reinforcement. In a sliding failure, the concrete along both sides of a shear crack slide in relation to each other, see Figure 2.12. The capacity for this type of failure depends on the interlocking effects of aggregates in the crack surface as well as the longitudinal reinforcement in the crack (Al-Emrani et al., 2013).

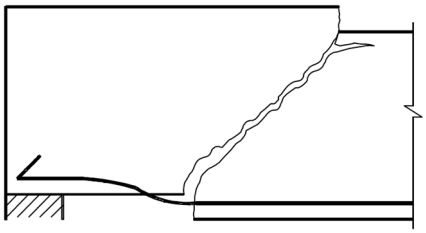

Figure 2.12 Shear sliding failure of RC beam without shear reinforcement (Al-Emrani et al., 2013).

If the member contains shear reinforcement, see Figure 2.13, the capacity increases drastically due to the fact that the transversal reinforcement must yield before shear sliding may take place (Al-Emrani et al., 2013).

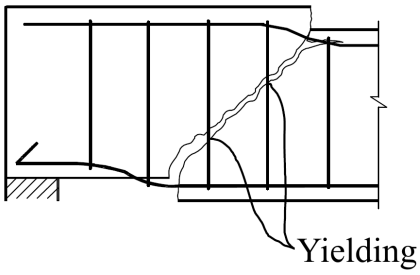

Figure 2.13 Shear sliding failure of RC beam with shear reinforcement (Al-Emrani et al., 2013).

2.5.1.2 Web shear compression failure

If too much transversal reinforcement is provided, the concrete in between cracks may instead crush before sliding, see Figure 2.14. Hence, an RC beam or slab have a maximum shear capacity determined by the web shear compression failure (Al-Emrani et al., 2013). This failure mode is also categorized as a one-way shear failure.

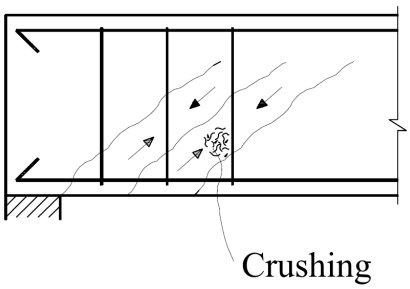

Figure 2.14 Web shear compression failure of RC beam with shear reinforcement (Al-Emrani et al., 2013).

2.5.1.3 Punching shear failure

Punching shear failure is a two-way shear failure specific for RC slabs which are supported by columns or subjected to point loads. In case of a punching shear failure, a cylindrical cone around the concentration of stresses is sheared off, see Figure 2.11. Seen from a section in the middle of a column, as in Figure 2.15, the punching failure resembles the one-way shear failure. What differs is the crack propagation up until failure, as shown by Vaz Rodrigues (2007), where an annular crack forms for the cracking load, see Figure 2.16(a). For increasing load, a redistribution from radial towards tangential load carrying leads to cracking as in Figure 2.16(b). After these cracks have occurred no new cracks form, but rather the crack width increases up to failure and a pattern as in Figure 2.16(c) can be seen.

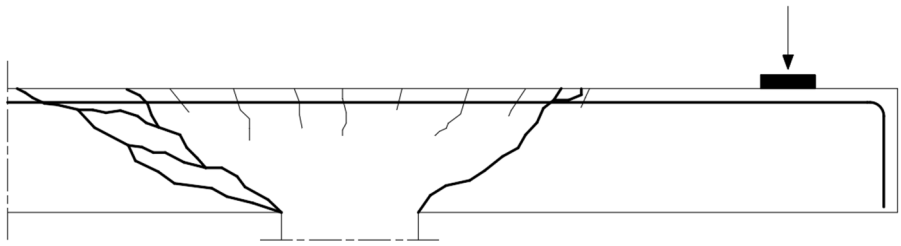

Figure 2.15 Crack pattern in a section of a slab with punching shear failure.

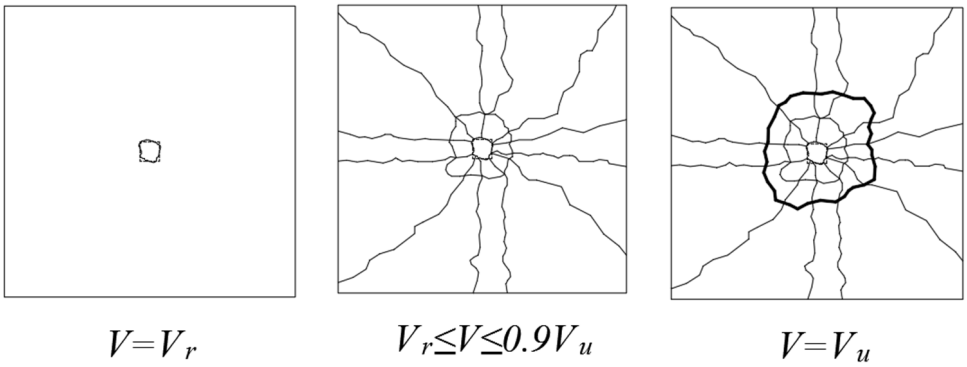

Figure 2.16 Crack pattern for: (a) Cracking load; (b) Load between cracking load and 90% of ultimate load; (c) Ultimate load.

2.6 Design codes

When designing structures, laws that affect the process must be considered. In Sweden, the hierarchy consists of four/five different levels ('Regelhierarki – från lag till allmänt råd', 2014):

- Constitution
- Law
- Regulation
- General advice
- The European Union (EU) regulations and directives, which acts on the level of the Swedish law

Boverket is the current name of the Swedish government authority that publishes regulations which help to interpret the law for house buildings. Trafikverket is the corresponding authority for infrastructure. The EU has published technical standards, Eurocodes, regarding how structural design should be carried out in its member countries. In addition, the Eurocodes are completed with national annexes, for which each country is responsible, to adapt the code more specifically. In Sweden, Boverket and Trafikverket are responsible for these national annexes called *EKS* and *EBS* respectively.

Historically, different regulations have existed.

- 2011 – present: Eurocodes and its national annexes, EKS and EBS, is the acting regulation ('EKS från 2008', 2014).

- 1994 – 2010: *Boverkets Konstruktionsregler* (BKR) (Boverket, 2003) was the acting regulation ('BKR från 1994 till 2010', 2014) which in turn gives reference to *Boverkets Handbok om Betongkonstruktioner* (BBK) (Boverket, 2004) specifically for concrete structures. BBK specifies calculation methods and demands in a similar fashion as Eurocode does.
- 1989 – 1994: *Boverkets Nybyggnadsregler* (NR) (Boverket, 1989) was the acting regulation, which also referred to BBK (Boverket, 2004) for concrete structures.
- 1968 – 1989: *Svensk Byggnorm* (SBN) (Statens planverk, 1983) was the acting regulation ('SBN från 1968 till 1989', 2014), which was published by the equivalency to the present Boverket. In SBN, further reference for design of concrete is made to *Bestämmelser för betongkonstruktioner – Allmänna konstruktionsbestämmelser* (Statens Betongkommitté, 1969) and to *Förslag till bestämmelser för dimensionering av betongplattor på pelare jämte utdrag ur kommentarer* (Statens Betongkommitté, 1964).

To strengthen existing structures, it is important to consider how they were designed when built. This section describes differences in the design codes previously mentioned, except NR since reference to BBK was given and as such, the design procedure would be the same as for BKR. Furthermore, this section aims to describe differences both in how the stresses were derived and evaluated as well as how loads were accounted for. This section should give understanding to why there may exist a need for strengthening these structures against shear failure.

2.6.1 Loads

Eurocode 1 ('SS-EN 1991-1-1', 2011), BKR (Boverket, 2003) and SBN (Statens planverk, 1983) define how loads should be treated. In this section, definitions are translated from Eurocode 1. Most assumptions regarding loads and actions are similar in the different codes, but some differences are found in the application of load combinations and characteristic values.

Loads are classified in two categories, as permanent or imposed loads. Self-weight of the structure is considered as a permanent load with exception for movable parts (e.g. movable partitions) which are treated as imposed loads. When designing for loads and actions the most unfavourable case, during construction and service life, should be governing.

Actions are further divided into different categories depending on certain variations (e.g. time or distribution in space). They are as follows:

- Three types of actions are considered with regard to time; permanent actions, variable actions and accidental actions.
- Actions can be fixed or free depending on spatial distribution.
- Actions that vary in a way that they could cause fatigue failure are considered fatigue actions.
- Depending on how an action is applied it is regarded as static or dynamic.

A fixed action is an action that has a single clear distribution over the structure. A free action is an action that, within reason, is assumed to have an arbitrary distribution over the structure. Values of loads are obtained, to the extent possible, from statistical

methods and results from studies. Actions that could occur at the same time should be combined, unless there is a small chance of this happening, if so, the combination may be neglected. However, concentrated loads and distributed imposed loads are usually not combined. Unless anything else is specified, loads are assumed to produce static action.

2.6.1.1 Permanent loads

When designing for permanent loads, the total self-weight of bearing and non-bearing structural parts should, in load combinations, be treated as one single action. In situations where they are to be moved, added or removed the most critical load case should be used. Self-weight should be stated with a single value calculated from the geometry and characteristic values of density. Mean values are to be used when doing these calculations.

2.6.1.2 Imposed loads

Imposed loads are treated as free variable loads, with exception of specific cases. They should be regarded as quasi-static actions. Floor areas are divided into different categories with regard to their specific use. When designing floor slabs, the values of imposed loads are decided based on which category the area belongs to. For situations where a floor slab will be subjected to different load categories, the most critical load case should be used. In case of an imposed load acting simultaneously as other variable loads, the total imposed load should be regarded as a single load. Table 2.1 presents a comparison of suggested values in Eurocode, BKR and SBN for distributed imposed loads for two examples of load categories. It is noteworthy that the values correspond well between the different codes.

Loads from people, furniture, movable objects or vehicles should be described as uniformly distributed, line loads, concentrated loads, live loads or combinations of all of them. The effect of self-weight of movable partitions can be taken into account by adding an equivalent uniformly distributed load to the imposed load.

When designing floor slabs, the imposed load should be treated as a free load applied to the most unfavourable part of the area of influence, with regard to the studied effect. To determine the minimum load bearing capacity of the slab locally, a separate verification of a concentrated load should be carried out.

Eurocode also allows an imposed load from a single category to be reduced due to a probability reduction with a factor, α_A, which is related to the affected area, whereas BKR and SBN does not.

Table 2.1 Comparison between values for distributed imposed loads [kN/m^2] in Eurocode, BKR and SBN. Values from SBN are presented with "normal occurrence".

Specific Use	Eurocode	BKR		SBN	
		Free*	Fixed*	Free*	Fixed*
Areas for domestic and residential activities	1.5 – 2.0	1.5	0.5	1.5	0.5
Office areas	2.0 – 3.0	1.5	1.0	1.5	1.0

*Generally, a fixed action will affect the structure at the same place in the same way, whereas a free action could be moved or altered. Most actions will, however, consist of two parts, one fixed and one free.

2.6.1.3 Characteristic values

The characteristic values of the imposed loads are given by categories with regard to specific use. These values can be found in tables in the relevant code. If a value is not to be found, it should be determined for each individual case. Depending on what code that is studied these values may vary, Eurocode tend to give intervals whereas BKR gives set values, see Table 2.1. It is also notable that the classification of the categories differs to some extent.

2.6.1.4 Load combinations

The most notable difference, with regard to loads, between Eurocode, BKR and SBN is the partial factors for combining loads. The codes use different multiplication factors for both permanent and variable loads in ULS, see Table 2.2. SBN does not utilise partial factors in the same way as Eurocode 1 and BKR do. Thus, the load will not be treated with the same safety approach when designing according to SBN. In addition, Eurocode and BKR, treat three safety classes, with regard to the extent of personal injury that could occur in case of collapse of a structural part; where safety class 1 is the lowest, with small risk of personal injury, and safety class 3 is the highest. A multiplication factor is then used depending on the given safety class, see Table 2.3.

Table 2.2 Examples of partial factors for load combination in ultimate limit state according to Eurocode and BKR.

Type of load	Eurocode	BKR
Permanent load	1.35	1.0
Variable load	1.5	1.3

Table 2.3 Different safety classes and their corresponding partial factors.

Category	Eurocode	BKR
Safety class 1	0.83	1.0
Safety class 2	0.91	1.1
Safety class 3	1.0	1.2

All partial factors for unfavourable actions in Eurocode 1 are higher than their corresponding values in BKR. However, regarding the partial factors for the safety

classes, the opposite can be observed, i.e. all partial factors for safety classes in Eurocode 1 are lower than their corresponding values in BKR. The result of this, as illustrated by Table 2.4, is that when combining the partial factors for the type of load and safety class the combined factor ends up being close for Eurocode and BKR.

Table 2.4 Combined partial factors for load combinations and safety classes for Eurocode and BKR.

Category	Eurocode	BKR	Eurocode	BKR
	Permanent	Permanent	Variable	Variable
Safety class 1	1.12	1.0	1.25	1.3
Safety class 2	1.22	1.1	1.36	1.43
Safety class 3	1.35	1.2	1.5	1.56

2.6.2 Shear design

When designing for shear in RC slabs, both types of failure, shear and punching, should be included, if relevant. RC slabs are in all design codes, investigated in this thesis, designed for shear as beams. When designing a slab for beam-like shear it is assumed to act like a thin, wide beam, as mentioned in Section 2.2. This assumption is considered valid, as research has shown that the width of a member has no significant impact on its one-way shear resistance (Sherwood, Lubell, Bentz, & P Collins, 2006).

2.6.2.1 Shear

BBK and Eurocode 2 present roughly the same methods for design against shear failure whereas SBN differs. In this section the notations used in Eurocode 2 have been adopted to the expressions in BBK. According to Eurocode 2, a general expression according to equation (2.4) can be used to determine the resistance of a shear reinforced concrete member. The determination of resistance utilises the truss model described in Section 2.4.

$$V_{Rd} = V_{Rd,s} + V_{ccd} + V_{td} \tag{2.4}$$

where

- $V_{Rd,s}$ is the design value of the shear force which can be sustained by the yielding shear reinforcement
- V_{ccd} is the design value of the shear component of the force in the compression area, in the case of an inclined compression chord (i.e. if the member has an inclination)
- V_{td} is the design value of the shear component of the force in the tensile reinforcement, in the case of an inclined tensile chord (i.e. if the member has an inclination)

$V_{Rd,s}$ can be determined from equation (2.5), where the inclination of the truss model can be assumed to any value such that $21.8° \leq \theta \leq 45°$.

$$V_{Rd,s} = \frac{A_{sw}}{s} z\, f_{ywd} \cot\theta \tag{2.5}$$

where

A_{sw}	is the cross-sectional area of the shear reinforcement
s	is the spacing of shear reinforcement
f_{ywd}	is the design yield strength of the shear reinforcement
z	is the internal lever arm
θ	is the angle between the concrete compressive strut and member axis perpendicular to the shear force

If no shear reinforcement is included, which is not a demand for slabs according to Eurocode 2, the capacity is determined only from the contribution of the plain concrete shear capacity, which is calculated with equation (2.6a).

$$V_{Rd,c} = \left[C_{Rd,c} k (100 \rho_l f_{ck})^{\frac{1}{3}} + k_1 \sigma_{cp}\right] b_w d \tag{2.6a}$$

with a minimum value determined by equation (2.6b)

$$V_{Rd,c} = \left(v_{min} + k_1 \sigma_{cp}\right) b_w d \tag{2.6b}$$

where

$C_{Rd,c}$	is a material specific constant, national value
k	is a geometric variable, in [mm]
ρ_l	is a ratio between the cross-sectional reinforcement area and the concrete area
f_{ck}	is the concrete compressive strength, in [MPa]
k_1	is a constant, national value
σ_{cp}	is the stress in the concrete due to normal forces
v_{min}	is $0{,}035 k^{3/2} f_{ck}^{1/2}$

The capacity for crushing of concrete is checked by setting a limiting maximum value of the shear resistance according to equation (2.7).

$$V_{Rd,max} = 0.5\, b_w\, d\, \nu\, f_{cd} \tag{2.7}$$

where

ν	is a strength reduction factor for concrete cracked in shear

BBK utilises the same expressions for calculating the resistance contributions, but also allows for summing of concrete and shear reinforcement contributions, $V_{Rd,c}$ and $V_{Rd,s}$ respectively. Eurocode on the other hand, does not allow for the summation of concrete and shear reinforcement contribution. For instance, if an element is provided with shear reinforcement the total shear capacity of the element is equal to only the contribution from the shear reinforcement, $V_{Rd,s}$. However, SBN does not utilise the truss model

described in Section 2.4. Statens Betongkommitté (1969) suggests a method where the shear stress in a non-shear reinforced concrete beam is controlled against a resistance, calculated from a base value of shear strength tabulated for different values of concrete strength classes with standard geometries. Table 2.5 presents the tabulated values, with concrete strength classes of that time.

Table 2.5 Base values of shear strength for different concrete classes with standard geometries, adapted from (Statens Betongkommitté, 1969).

Strength class	Base value for shear strength [MPa]
K600	0.59
K550	0.57
K500	0.55
K450	0.52
K400	0.49
K350	0.46
K300	0.42
K250	0.39
K200	0.34
K150	0.29

If shear reinforcement is needed, it may be assumed either that the shear reinforcement solely carries the shear stresses or that concrete also contributes to the capacity. A control is then made with equation (2.8).

$$R \leq h \sum A \, \sigma_a (\sin \alpha + \cos \alpha) \tag{2.8}$$

where

- R is the support reaction (giving rise to shear)
- h is the cross-section height
- A is the shear reinforcement area per unit length with a certain inclination and tensile stress
- σ_A is the allowed tensile stress for the shear reinforcement
- α is the angle between the shear reinforcement and the member's centroidal axis

Suggestions are also given regarding the layout of shear reinforcement. For slabs specifically, stresses may be determined according to the theory of elasticity where it must be proven that the bending capacity is enough in all directions of the slab and that torsional moment is accounted for. Otherwise, the theory of plasticity using the yield line method may be used, where it must be proven that the risk of failure due to bending is greater than the risks of other failure modes. Specific attention to shear in slabs is not given to a greater extent than that it should be avoided. Thus, a conclusion can be made that specific shear design in RC slabs before BBK became the acting regulation was a rare occurrence.

2.6.2.2 Punching

Eurocode 2, BBK and SBN all differ with regard to the extent of which punching shear failure should be designed for. SBN refers to Statens Betongkommitté (1964) for punching resistance where it is stated that around a column, a circular area with diameter c should be controlled for punching. c is double the distance from the centre of the column to the zero-moment perimeter around the column. The shear stresses, τ_{nom}, within a perimeter B/d can then be calculated according to equation (2.9) and be compared with the resistance, τ_1, calculated according to (2.10).

$$\tau_{nom} = \frac{P}{\pi\, h^2 \left(\frac{B}{d} + 1\right)} \tag{2.9}$$

where

P is the punching load (support load)
B is a diameter
d is the effective depth

$$\tau_1 = \tau_0 \frac{15}{10 + \frac{c}{2d}} \tag{2.10}$$

where

τ_0 is a tabulated value for different concrete strength classes

If equation (2.11) is fulfilled, no further check of the punching is required. If equation (2.12) is fulfilled, a further check is needed but no shear reinforcement is required. If equation (2.13) is fulfilled, shear reinforcement is needed and recommendations for layout are given. If none of equations (2.11) to (2.13) are fulfilled, the design is not acceptable.

$$\tau_{nom} \leq 0.65\tau_1 \tag{2.11}$$

$$0.65\tau_1 < \tau_{nom} \leq \tau_1 \tag{2.12}$$

$$\tau_1 < \tau_{nom} \leq 1.5\tau_1 \tag{2.13}$$

BBK refers to AB Svensk Byggtjänst (1990) for punching design which expands on the same procedure used in SBN, in such way that similar equations are used for determining the capacity. Methods for calculating the capacity for general cases are however provided, instead of as in SBN, where a standard geometry had a tabulated value. BBK had as such given the possibility to determine the capacity for more complex structures.

With the introduction of Eurocode 2 came an even more general approach to consider punching. The calculation model is, in principle, the same as before, illustrated in Figure 2.17 and Figure 2.18, where the capacity should be checked along a perimeter at a given distance from the column face. Additionally in Eurocode 2, should shear

reinforcement be needed, another perimeter beyond which shear reinforcement is no longer needed should be checked. Methods for determining the loaded area for different columns than circular ones are also given.

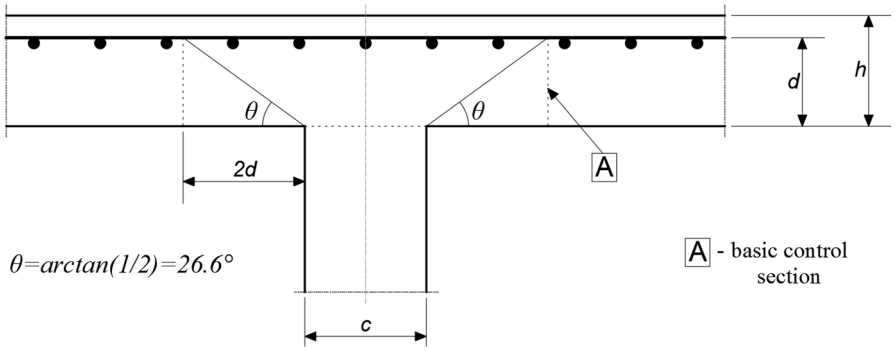

Figure 2.17 Cross-sectional view of calculation model adapted from ('SS-EN 1992-1-1', 2008).

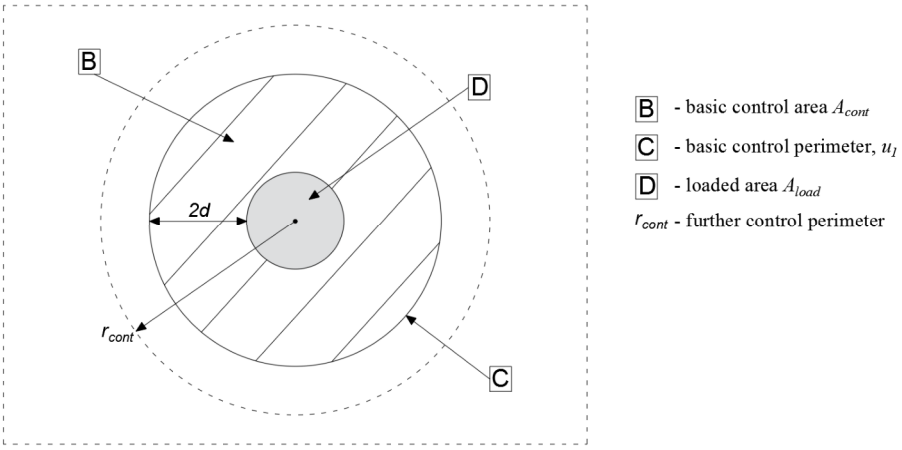

Figure 2.18 Plan view of calculation model adapted from ('SS-EN 1992-1-1', 2008).

As for determining the punching shear capacity, punching shear reinforcement is not needed in cases where equation (2.14) is fulfilled.

$$v_{Ed} < v_{Rd,c} \tag{2.14}$$

where $v_{Rd,c}$ can be determined from equation (2.15).

$$v_{Rd,c} = \left[C_{Rd,c} k (100 \rho_l f_{ck})^{\frac{1}{3}} + k_1 \sigma_{cp}\right] \geq v_{min} + k_1 \sigma_{cp} \tag{2.15}$$

where

ρ_l is the ratio between reinforcement and concrete cross-sectional areas in both x- and y-directions
σ_{cp} is the average normal stress in the concrete from both x- and y-directions
v_{min} is a variable depending on functions of f_{ck} and k

Should punching shear reinforcement be needed, a new resistance consisting of contributing parts from both the compressed concrete and shear reinforcement can be determined from equation (2.16).

$$v_{Rd,cs} = 0.75 v_{Rd,c} + 1.5 \frac{d}{s_r} A_{sw} f_{ywd,ef} \frac{1}{u_1 d} \sin \alpha \qquad (2.16)$$

where

s_r is the radial spacing of perimeters of shear reinforcement around the loaded support
$f_{ywd,ef}$ is the effective design strength of the punching shear reinforcement
u_1 is the perimeter length of a punching subjected area

In conclusion, Eurocode 2 offers a more general approach which, compared to older design codes, may be applied to many different cases and more complex load situations. SBN offers very limited design methods other than a simple method for checking the shear resistance and providing general advice to avoid situations where shear becomes the designing failure mode.

2.6.3 Example of capacities according to different codes

To illustrate how the actual shear capacities differ between the different design codes, the resistance of an example beam has been calculated with methods provided in the different design codes, see Appendix A. In the example, a simply supported beam with dimensions as shown in Figure 2.19 was controlled with regard to its shear capacity according to Eurocode 2. The beam was assumed to be subjected to an arbitrary distributed load, q_d, see Figure 2.19(a). As suspected, the beam required shear reinforcement which was then designed according to Eurocode 2.

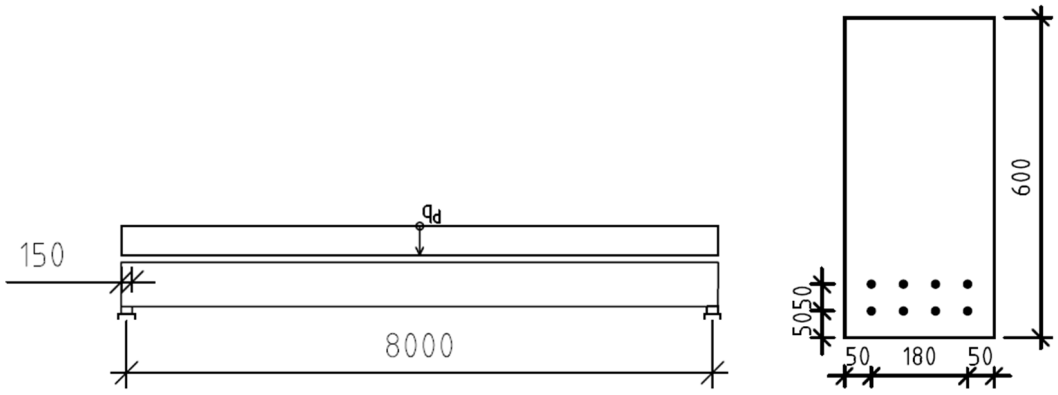

Figure 2.19 Views of the studied beam: (a) Elevation view; (b) Cross-sectional view.

The calculated shear reinforcement layout, which consisted of 8 mm diameter steel bars with an even spacing of 140 mm, was then treated as input for the remaining methods. The capacity was then determined according to both BBK and SBN for the same input values as for the Eurocode. The resulting capacities are presented in Table 2.6.

Table 2.6 Determined capacities for the illustrated example.

Design code	Shear capacity [kN]
Eurocode 2	184
BBK	263
SBN	265

The resistance according to Eurocode 2 is well below that of BBK and SBN, around 30% lower. A reason for this lies in the fact that Eurocode does not add the concrete and shear reinforcement contributions together. It is assumed that when shear reinforcement is needed, all capacity is determined by the shear reinforcement. BBK and SBN, on the other hand, include the contributions of both. If the concrete shear capacity, determined according to Eurocode 2, had been added to the shear reinforcement capacity it would have yielded a total shear capacity of 286 kN. This value would have corresponded better to the capacities determined according to BBK and SBN. The fact that Eurocode underestimates the shear capacity of reinforced concrete is further confirmed by research. Walraven, Belletti, & Esposito (2013) also shed light upon the fact that the underestimation of shear capacity varies with different shear reinforcement amounts and in their study a trend of greater underestimation in beams with a higher shear reinforcement ratio could be observed. Mari & Cladera (2007), on the other hand, argues that the shear resistance is underestimated more for lower amounts of shear reinforcement according to Eurocode 2, due to the concrete contribution not being taken into account when following this code. Both studies do, however, agree on the discrepancy between the calculated capacity and the one derived from testing. Particularly for RC slabs Lantsoght, de Boer, & van der Veen (2017) and Rombach & Kohl (2013) state that the shear capacity of slabs is underestimated since the load distribution in slabs is conservatively considered, and that the concrete contribution to the shear capacity does not reflect reality in a true enough manner. Mari & Cladera (2007) state that the shear resistance determined by Eurocode serves the purpose of easily determining if enough shear capacity is provided for a structure, which otherwise would not be assumed to fail in shear. However, if a more precise prediction is needed, other methods for determining the shear capacity may be utilised. Particularly, Mari & Cladera (2007) proposes corresponding methods of determining shear capacity produced by the American Concrete Institute or the Canadian Standards Association as alternatives.

In the example presented, an arbitrary load was assumed and consisted only of one single part. In a real design situation, a permanent load part would have had to be combined with an imposed load part with corresponding partial safety factors. Although, as brought up in Section 2.6.1.4, the load combinations would still end up close to each other and it can be said that the choice of design code will have a small impact on the load effect. However, the capacity will, if there is a need for shear reinforcement, be determined in a more conservative way when using Eurocode. Thus, existing concrete structures dating back to before the implementation of the Eurocodes may need shear strengthening if analysed according to these current design codes.

3 Shear Strengthening Methods

There are a few distinct methods to increase the shear capacity of existing concrete elements. Shear strengthening is commonly done with steel materials or, more recently, fibre reinforced polymer (FRP) (Täljsten, 2002). This section describes methods available today, which in research have been proven effective in increasing the shear capacity. Fernández Ruiz, Muttoni, & Kunz (2011); Koppitz, Kenel, & Keller (2013) and Nováček & Zich (2016) state that there exist, in principle, four distinct ways of increasing the shear capacity of slabs subjected to punching shear failure. One is to enlarge the support region susceptible to shear failure, i.e. making the column wider, this can be done by casting additional concrete or by adding a capital, see Figure 3.1(a). A second method is to add flexural strengthening as shown in Figure 3.1(b). The third method is to introduce post-installed shear reinforcement with internal or external bonding, see Figure 3.1(c). The fourth method is the use of post-installed prestressed members, see Figure 3.1(d). In addition, there are more methods applicable to beams available, e.g. wrapping of the beams as described by Monti (2006). As previously explained in Section 2.2, the one-way shear behaviour of a slab can be regarded as that of a wide beam. Therefore, shear strengthening methods for beams that have been found in the literature are described in this section and possible applicability of these methods to slabs is discussed in Section 3.5.

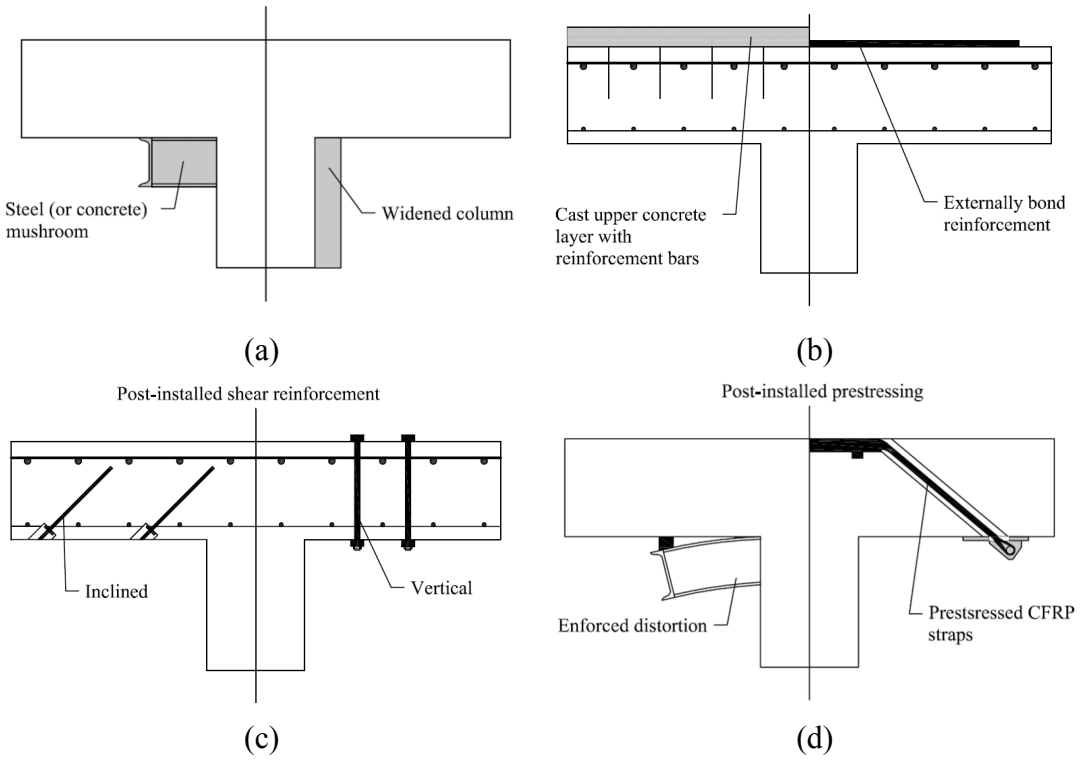

Figure 3.1 Overview of shear strengthening methods for RC slabs, adapted from (Koppitz et al., 2013).

3.1 Methods using steel

Different shear strengthening methods using steel exist. Fiset, Bastien, & Mitchell (2017) compare two methods of drilling steel bars into the shear critical zone, one

method which drills the bars into the concrete from the top and one method which drills bars into the concrete from both the top and the bottom. Another method is proposed by Fernández Ruiz et al. (2011) where steel bars are only drilled from the soffit and Breveglieri, Aprile, & Barros (2014) describe a method with embedded through section (ETS) steel bars. The following subsection describes the mentioned strengthening methods in further detail. In general, methods with steel function so that shear reinforcement is added.

3.1.1 Drilled-in steel bars

Perhaps the most intuitive method to reproduce the effect of shear reinforcement, or steel stirrups, is to add similarly working steel to the concrete. In principle, this method includes three steps:

- Drilling a hole through the thickness of the slab (through the beam height in case of beams).
- Filling the hole with adhesive (in most cases epoxy).
- Inserting the steel bars inclined or straight and letting the adhesive cure.

The steel bars can be inserted from the top or the bottom of the hole depending on the existing reinforcement layouts and other possible hinders. Caution must be taken while drilling holes in the concrete, so that existing flexural reinforcement is not destroyed.

Fiset et al. (2017) tested two different steel shear strengthening methods for thick concrete slabs, >450 mm. The thickness of the slab has an impact on the embedment length, but the method should principally be applicable to thinner slabs as well. Steel bars were introduced into concrete beams either from the top side of the slab or from both the top and the bottom of the beam. Holes were bored in the concrete, which were cleaned and subsequently filled with epoxy resin into which the steel bars were placed. The top-sided drilled-in steel bars were inserted into the concrete so that no disturbance would be caused on the bottom longitudinal reinforcement, see Figure 3.2(a). The double-sided drilled-in steel bars had an overlap in the middle of the concrete section and otherwise penetrated the whole concrete section, see Figure 3.2(a) and Figure 3.2(b).

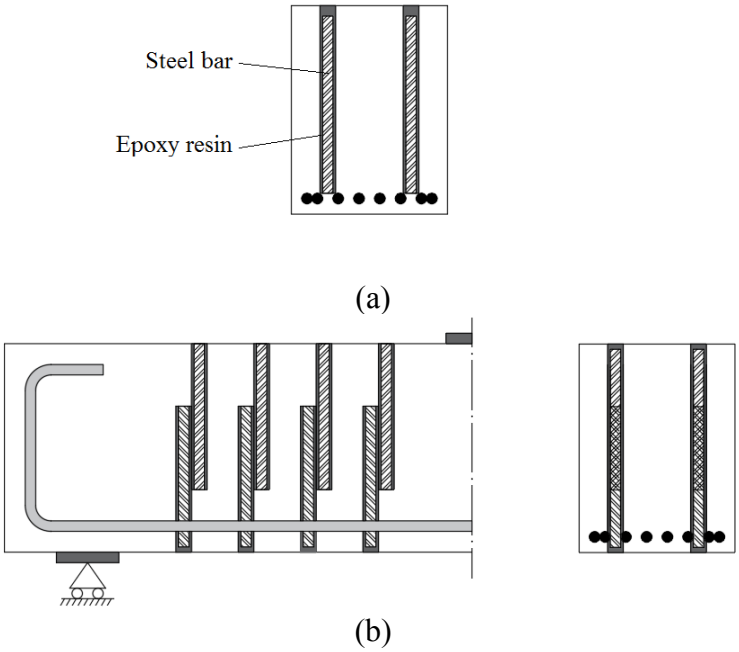

Figure 3.2 Overview of the two methods studied: (a) Cross-section of top-sided drilled in steel bars; (b) Section and cross-section view of double-sided drilled in steel bars, adapted from (Fiset et al., 2017).

Since the double-sided method, see Figure 3.2(b), provided a longer embedment length as well as a larger shear reinforcing area in the overlapping region, it proved more efficient in increasing the shear capacity than the single-sided strengthening shown in Figure 3.2(a). Both methods tended to fail in debonding between the steel and the adhesive, though the double-sided method could utilise more of the steel capacity before debonding occurred. However, both methods provided a substantial distinction, with an increase in shear capacity of around 45%.

If the top of the slab would be difficult to reach, e.g. due to cladding, Fernández Ruiz et al. (2011) presents a method with drilled-in steel bars from the soffit of the slab. In their study, the steel bars are inserted in a similar fashion as previously described, with an epoxy-filled hole bored in the concrete into which inclined steel bars are placed. This method proved efficient as well, increasing the shear capacity with 13% to 60% due to different configurations. However, the governing failure mode was not stated and therefore it is difficult to comment on its effect on the debonding problem.

In order to increase the embedment length of the steel bars to the maximum and avoid debonding failure, a method called the ETS method exits. In this method the hole is drilled inclined or straight through the entire thickness of the structure. A complete through section embedment method is described by Barros & Dalfré (2013), in Section 3.2.3.

Breveglieri et al. (2014) used the principle of the ETS method for examining T-slabs. Holes were bored from the bottom of the concrete beam and were filled with an epoxy resin in which steel bars were inserted, see Figure 3.3. Bars could either be inserted vertically or with an inclination. Since the web, in this case, is assumed to transfer the

shear forces, the section which is embedded through is the web. This explains why the steel bar is not embedded all the way through the flange.

The study concluded that the inclined ETS strengthening is more effective for increasing the shear capacity than the vertical strengthening, compare the largest increase in capacity from vertical bars of 68% with 135% which was the largest increase using inclined bars. This is explained by the fact that the inclined bars have a longer embedment length than the vertical bars. Still, the failure mode perceived was debonding between steel bar and epoxy resin.

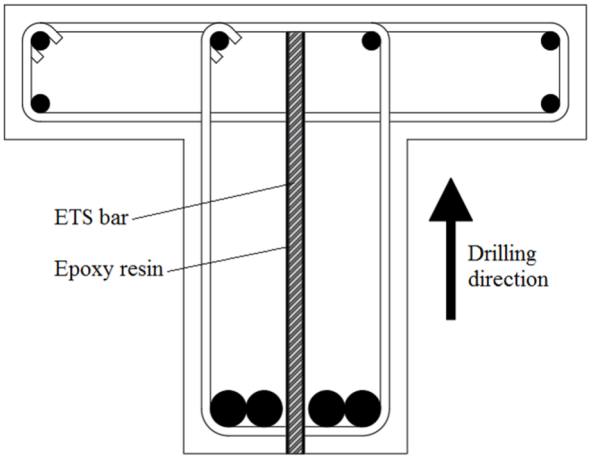

Figure 3.3 Cross-sectional view of ETS method applied on T-beam, based on (Breveglieri et al., 2014).

3.1.2 Vertical bolts

Askar (2015) investigated the effect of post-installed shear reinforcement through vertical post-tensioned steel bolts, drilled through the slab on the punching shear capacity. Noteworthy for this study is that the slabs first were loaded until failure and then repaired with new concrete and strengthened with the vertical bolts. Vertical holes were drilled through the concrete in the shear critical area where steel bolts were inserted together with an adhesive, and fastened with nuts in a circular pattern around the column, see Figure 3.4. Two different arrangements of bolts were compared, the first with one row of bolts, as in Figure 3.4, and the second with two rows of bolts. It was concluded that the repair with prestressed bolts increased the shear capacity beyond its original capacity by 4% up to 22%.

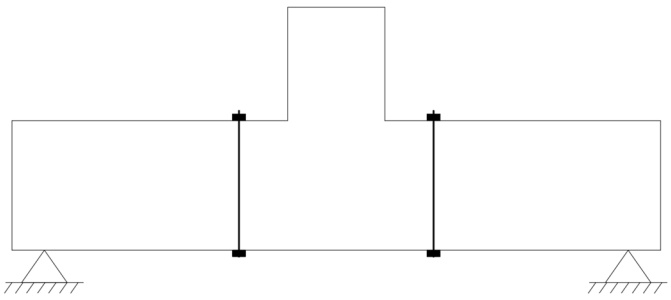

Figure 3.4 Vertical steel bolt strengthening of slab, adapted from (Askar, 2015).

Adetifa & Polak (2005) also performed a study on the shear resistance of RC slabs subjected to punching strengthened with vertical steel bolts. The difference being that:

- The slab was not pre-loaded to failure before testing.
- The bolts were placed in rows of two main directions instead of a circular pattern, see Figure 3.5.

Four similar slab specimens were tested, where one control specimen was compared to three specimen with two, three and four rows of bolts respectively.

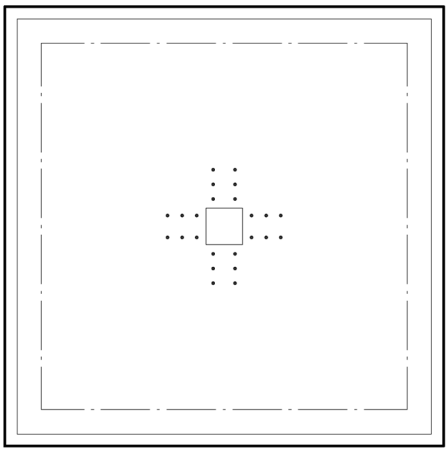

Figure 3.5 Test setup for specimen with three rows of vertical bolts, adapted from (Adetifa & Polak, 2005). Thick line indicating edge of slab, thin line indicating the reinforced area of the slab and dash dotted line indicating simply supported edge.

Results showed that the ultimate capacity was increased and the strengthening could shift the failure mode from punching to flexural. The ultimate capacity was increased approximately 45% regardless of applying two, three or four rows of bolts. No difference of capacity increase was observed since all the specimens failed in flexure.

3.1.3 External steel plates

Elbakry & Allam (2015) tested a method, which does not categorize as introducing shear reinforcement to the concrete, consisting of rectangular steel plates fastened on the top of a support subjected to shear, i.e. punching shear specifically. The fastening of the plate to the concrete was done by means of vertical steel studs welded to the steel plate and glued-in with an adhesive to the concrete. Different planar dimensions and thicknesses of the plate were tested as well as different stud sizes and arrangements. As for previous cases, debonding was concluded as the governing failure mode, making the stud size and arrangement the most important aspect of this strengthening method. In the study, the shear capacities of the examined slabs were increased by 14 to 39%.

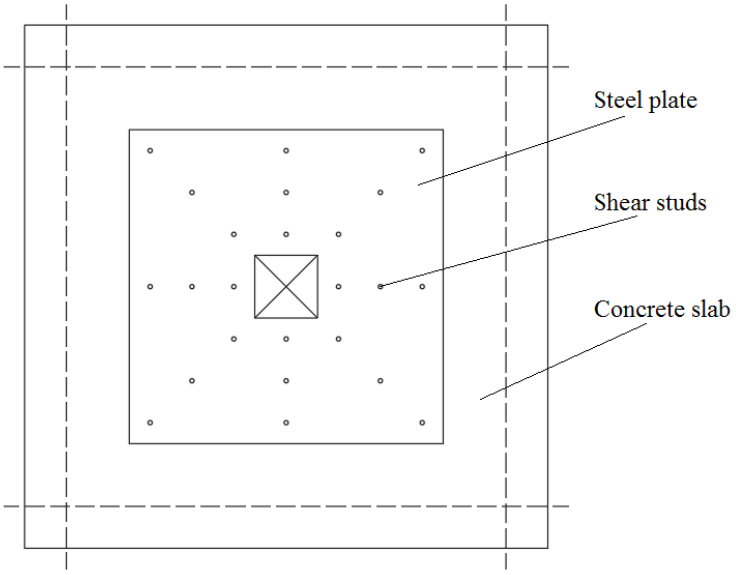

Figure 3.6 Example of arrangement for external steel plate and studs, adapted from (Elbakry & Allam, 2015).

3.2 Methods using FRP

The fibre reinforced polymer (FRP) composite material has proved in many studies to be an efficient material when strengthening existing concrete members (Meisami, Mostofinejad, & Nakamura, 2013). This is mainly due to it being a lightweight and non-corrosive material with a high tensile strength. However, FRP experiences a more brittle failure than steel, see Figure 3.7, which causes a sudden collapse if the member would go to failure.

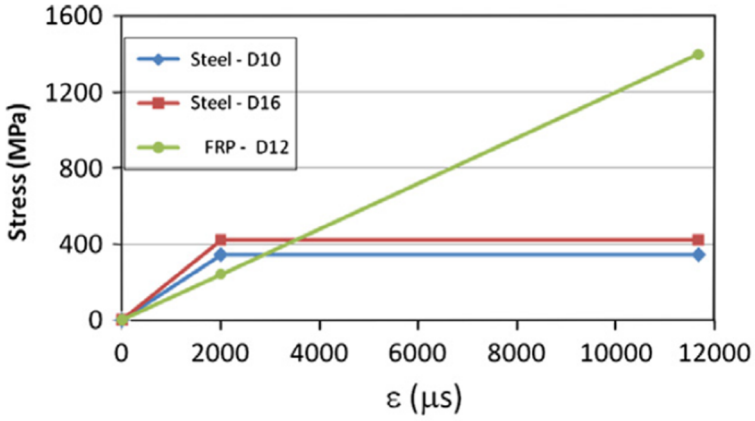

Figure 3.7 Comparison of material behaviour, stress-strain relationship, of Carbon FRP (CFRP) and steel (Meisami et al. 2013).

There are several shear strengthening methods utilising the properties of FRP. One is the externally bonded reinforcement (EBR) technique, see Figure 3.8(a), where FRP sheets or laminates are applied to the surface of the concrete member. Another method is the near surface mounted reinforcement (NSMR) technique, see Figure 3.8(b). In this method, slits are cut open on the surface of the member to be reinforced in which FRP

rods or bars are then glued with an epoxy adhesive, thus increasing the shear capacity. A third method is the previously mentioned ETS technique, see Figure 3.8(c), which consists of inserting FRP rods into predrilled holes and bonding them with an epoxy adhesive, also described for steel in Section 3.1.1 (Chaallal, Mofidi, Benmokrane, & Neale, 2011).

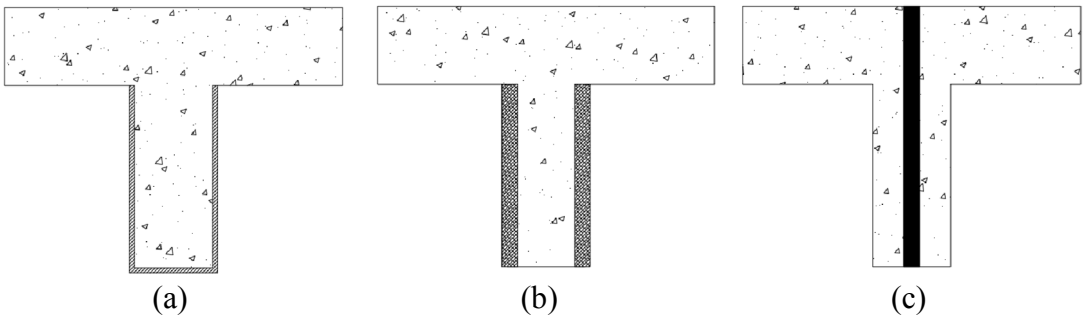

Figure 3.8 Example of shear strengthening methods using FRP: (a) EBR; (b) NSMR; (c) ETS.

3.2.1 Externally bonded reinforcement

Different arrangements of EBR exist, both when studying a beam from the side as well as studying a cross-section of a beam, see Figure 3.9 & Figure 3.10. Depending on the circumstances, a situation may not always allow for a specific arrangement of the FRP strips, e.g. wrapping according to Figure 3.10 would be hard to implement on a slab on its own. However, if possible, wrapping is an efficient method as the FRP will be able to reach its ultimate capacity, which may not always be the case for the other methods (Ferreira, Oller, Marí, & Bairán, 2016). The other methods, side bonding and U-jacketing presented in Figure 3.10, usually fail in debonding when a critical shear crack is formed. A solution to completely avoid, or at least to postpone, such behaviour would be to anchor the FRP with rods or steel profiles. Out of the two methods, side bonding and U-jacketing, another study performed by Jung, Hong, Han, Park, & Kim (2015) proved U-jacketing to provide more shear capacity than side bonding.

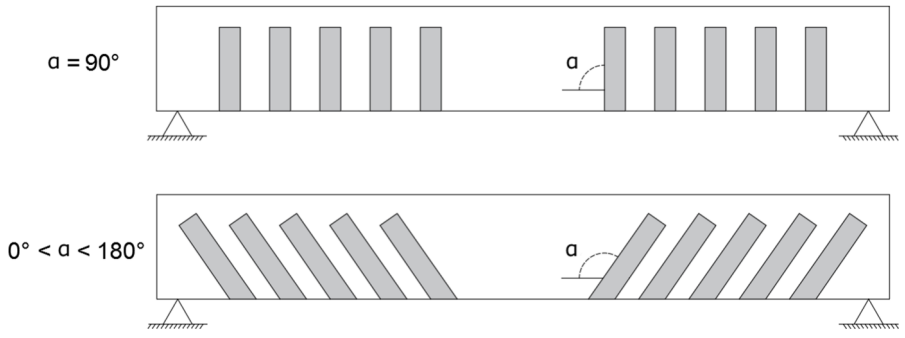

Figure 3.9 Different arrangements of external FRP shear strengthening, seen from an elevation view adapted from (Monti, 2006).

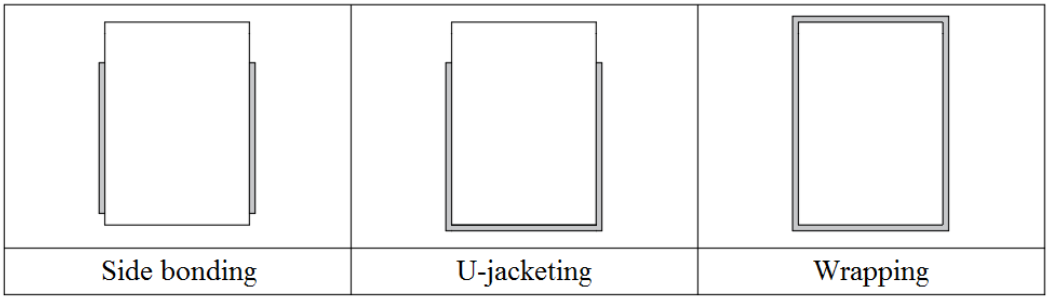

Figure 3.10 Different arrangements of external FRP shear strengthening, seen from a cross-sectional view adapted from (Monti, 2006).

It is worth noting that these three methods have been examined for beams and that they might not be as effective on slabs. This would be due to the fact that added stiffness on the external sides would have less influence on the shear capacity of the beam, the wider it becomes.

There are, however, circumstances under which some the methods can become applicable to slabs. If holes are drilled in the slab, CFRP strips could be threaded through and wrapped around the holes as Binici & Bayrak (2006) suggest in their study, see Figure 3.11. Different layout patterns of FRP strips were investigated, resulting in an increase in shear capacity between 20% and 58%. It is pointed out that the drilling could affect the existing longitudinal reinforcement and the risk of bending failure should be evaluated. If risk of damage to the longitudinal reinforcement is suspected, additional strengthening of the flexural capacity will be required. Furthermore, the importance of treating the sharp edges of the drilled holes is mentioned as these could damage the FRP strips when applied.

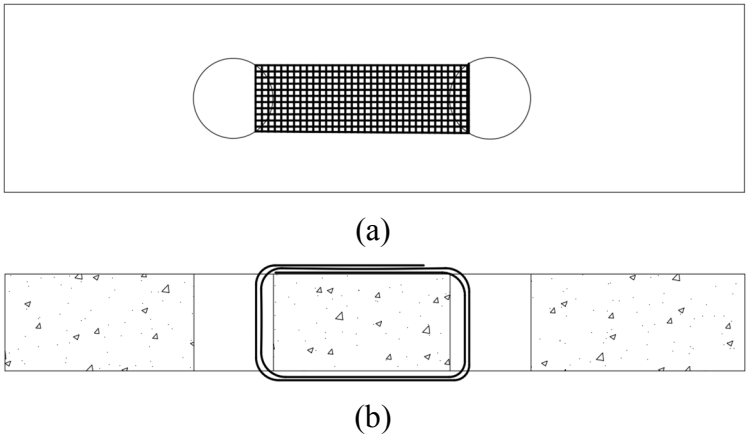

Figure 3.11 Wrapping of FRP strips applied on a concrete slab: (a) Top view; (b) Side view.

In a study conducted by Esfahani, Kianoush, & Moradi (2009) an EBR method which was implemented as flexural strengthening was evaluated with regard to its impact on the punching shear capacity of an RC slab. The study examined a quadratic slab containing two different dimensions of flexural steel reinforcement, two different concrete grades and was strengthened with CFRP strips, see Figure 3.12. The slab was loaded by a column in the centre and three different widths of CFRP strips were

compared against a non-strengthened control specimen. It was concluded that all specimen, regardless of reinforcement size and concrete grade, experienced an increase in punching shear capacity due to the CFRP strengthening in the ranges of 14% to 98%. The increase was particularly more prominent for specimens with a higher concrete grade, smaller flexural reinforcement size and wider CFRP strips.

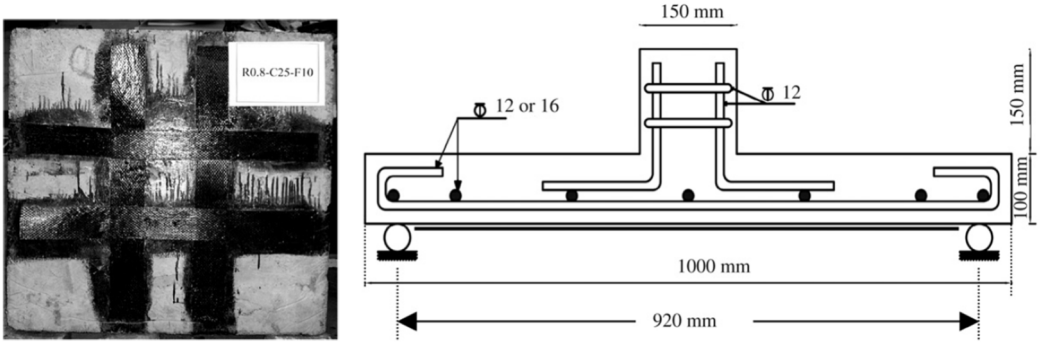

Figure 3.12 Setup of test specimen (Esfahani et al., 2009).

3.2.2 Near surface mounted reinforcement

NSMR has been used for a long time, although in its early stages steel bars were used rather than FRP (Täljsten, 2002). Some concerns when using steel was the bonding between the concrete and the steel bars, as well as covering the steel once in place in order to protect it against corrosion. The introduction of adhesives, rather than casting the bars into the concrete, made the bonding of the reinforcement better and easier. However, the concern regarding corrosion still existed. By replacing the steel with FRP, a lot of these issues were dealt with. The characteristics of FRP, described in Section 3.2, are very well suited for NSMR (Täljsten, 2002).

Unlike EBR, which requires little altering of the concrete member, NSMR requires some preparation of the concrete surface before it can be applied. The method consists of using FRP bars that are bonded in pre-cut slits on the surface of the concrete element with an epoxy adhesive, see Figure 3.13 for comparison of cross-section using EBR and NSMR.

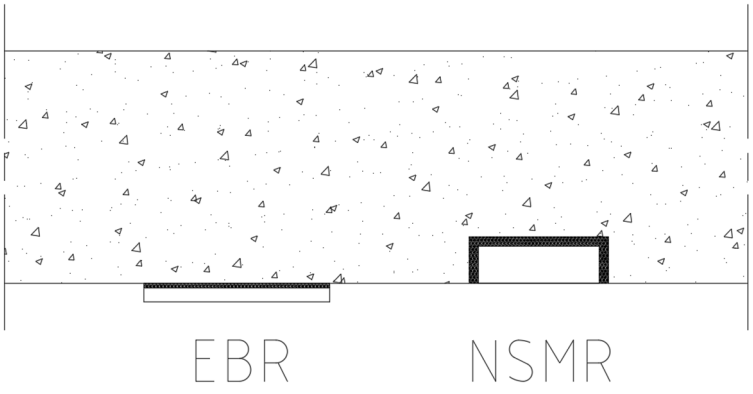

Figure 3.13 Comparison between EBR and NSMR.

In a study carried out by De Lorenzis & Nanni (2001), the efficiency of using NSMR consisting of FRP rods were evaluated. RC beams, with a T-shaped cross-section, were examined using two different setups of FRP rods, vertically installed, see Figure 3.14(a), and with a 45-degree inclination, see Figure 3.14(b).

(a) (b)

Figure 3.14 Two of the beams, after failure, studied by De Lorenzis & Nanni (2001): (a) Vertically installed FRP rods; (b) FRP rods installed with an inclination (De Lorenzis & Nanni, 2001).

The study concluded NSM FRP to be an efficient way of strengthening RC beams with regard to shear, and the shear capacity was increased with 35% up to 106% compared to the reference beams used in the study (De Lorenzis & Nanni, 2001). Usage of the inclined installation of FRP rods, shown in Figure 3.14(b), improved the shear capacity even further, however, with the disadvantage of an increased quantity of material used. This could be derived from debonding of the FRP rods being the main failure mechanism, as the inclined rods provide a longer embedment length. The conclusion of NSMR being an effective strengthening method can be backed up by Täljsten (2002), who also concludes NSMR to be an effective method with numerous benefits over EBR such as a higher fracture energy at failure and a better protection against e.g. vandalism or fire.

3.2.3 Embedded through section

Unlike EBR and NSMR, ETS-techniques penetrates through the cross-section of the concrete beam or slab, rather than working on its outside. The technique is carried out by drilling holes through the cross-section, with a chosen inclination. Bars of FRP or steel, described in Section 3.1.1, are inserted and bonded with adhesives into the pre-drilled holes, see Figure 3.15 for an example of the method (Barros & Dalfré, 2013).

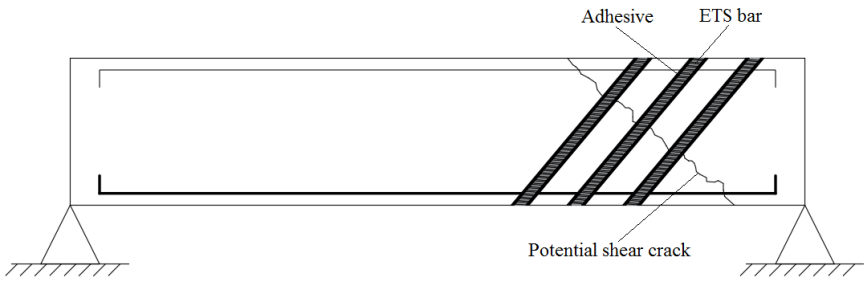

Figure 3.15 Example of the ETS technique carried out on an RC beam, based on (Barros & Dalfré, 2013).

One of the benefits of the ETS technique is that the bars that are acting inside the strengthened member are a lot more protected against outside influences, such as corrosion or vandalism, compared to EBR and NSMR. In a study carried out by Chaallal et al. (2011) it was also shown that the RC beams strengthened by FRP rods using the ETS technique failed in flexure or yielding in the regular shear reinforcement steel, compared with EBR and NSMR which both failed in debonding of the FRP. This means that the reinforcing material of the other two methods might not be utilised to its full potential. However, this observation should not be taken as general since it only holds true for their specific studied parameters. As for the increase in capacity, the study proved the method to increase the shear capacity with 60%.

3.3 Methods using alternative materials

As mentioned in the introduction of this chapter, steel and FRP are the two most commonly used materials for strengthening existing RC beams and slabs. However, these are not the only materials used, as several others exist. In many cases, the methods used for these materials resemble the ones applied for steel and FRP, but they are for various reasons not as commonly used. This section brings up a few examples of such alternative strengthening materials and methods.

3.3.1 Textile reinforced mortar

Although strengthening with FRP has many advantages over steel, it still has some drawbacks such as high cost, sensitivity to high temperatures and inapplicability in wet or cold conditions (Tetta, Koutas, & Bournas, 2018). Therefore, other materials have been introduced in order to deal with these disadvantages, one of them being textile reinforced mortar (TRM). TRM consists of textile fibre reinforcement, arranged in varying open-mesh configurations, see Figure 3.16. These are then bonded using non-organic, cement-based mortars (Triantafillou & Papanicolaou, 2006).

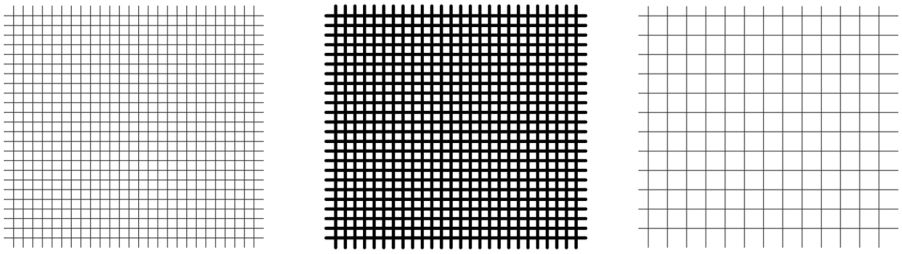

Figure 3.16 Example of different fibre-mesh configurations used in TRM.

Tetta et al. (2018) suggests that using TRM is as effective as FRP, when used as externally bonded reinforcement (EBR) and applied using the U-jacketing method. They investigate the use of different textile materials, different textile-fibre amount and different mesh configurations. The study was able to conclude that an increase in number of textile layers, meaning an increase of external reinforcement, increased the shear capacity proportionally, for the examined ratios. Further, it was shown how the use of different fibres, at lower reinforcement ratios, led to different failure modes. The specimens using glass-fibre and basalt-fibre both experienced fracture of the jacket as the governing failure mode, whereas the specimen with heavy carbon-fibre experienced slippage of the vertical fibres in the mortar and the specimen with light carbon-fibres failed due to debonding. The use of carbon TRM performed equally well as a reinforcement consisting of carbon FRP. Textiles with a denser pattern resulted in an improved bonding behaviour, leading to a better performance of the reinforcement.

The applications of the methods presented in Figure 3.17 were studied when Triantafillou & Papanicolaou (2006) evaluated the use of TRM. In this evaluation, it was concluded that the method is able to increase the shear capacity with 70%. Although TRM shows good properties with regard to shear reinforcement, it is further suggested that, for design, additional coefficients regarding the performance would need to be produced through additional studies.

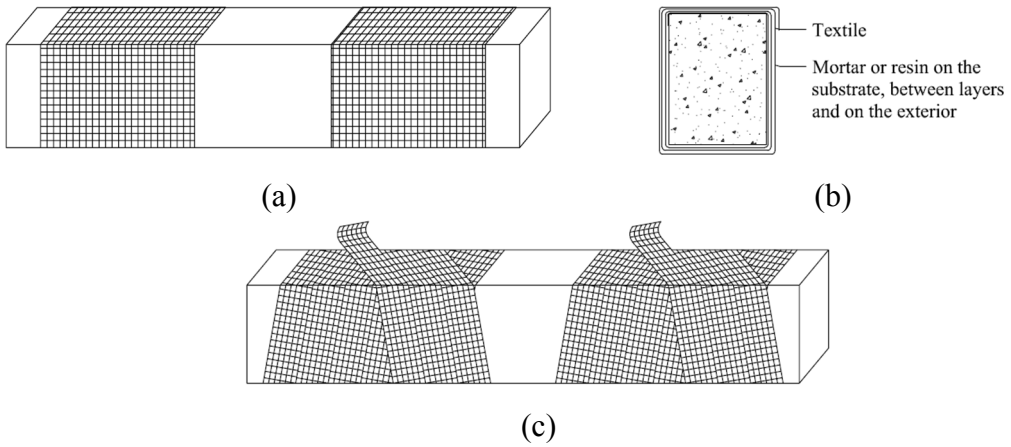

Figure 3.17 Different applications of TRM laminates used in the study carried out by (Triantafillou & Papanicolaou, 2006): (a) Single sheet wrapping; (b) Layers of wrapping; (c) Strips wrapped with an inclination, adapted from (Triantafillou & Papanicolaou, 2006).

3.3.2 Steel fibre reinforced concrete

Another material used to reinforce structures for shear, is steel fibre reinforced concrete (FRC) (Ruano, Isla, Pedraza, Sfer, & Luccioni, 2014). The material consists of plain concrete mixed with an addition of fibres in order to enhance its characteristics. Ruano et al. (2014) explains further that different types of fibres can be used e.g. steel, glass or carbon. Depending on what fibres are used, the behaviour of the failure may differ, e.g. glass fibres tend to give a more brittle failure whereas steel fibres generally will produce a more ductile failure. The benefit of the added fibres is that they change the cracking behaviour. So rather than the concrete producing a few large cracks, the fibres help tie the material together, resulting in more evenly distributed small cracks. Fibres used in combination with self-compacting concrete, creates an easy-to-cast material, suitable for post-strengthening purposes. Figure 3.18 explains how a jacket of self-compacting FRC is cast around a concrete member in order to reinforce it.

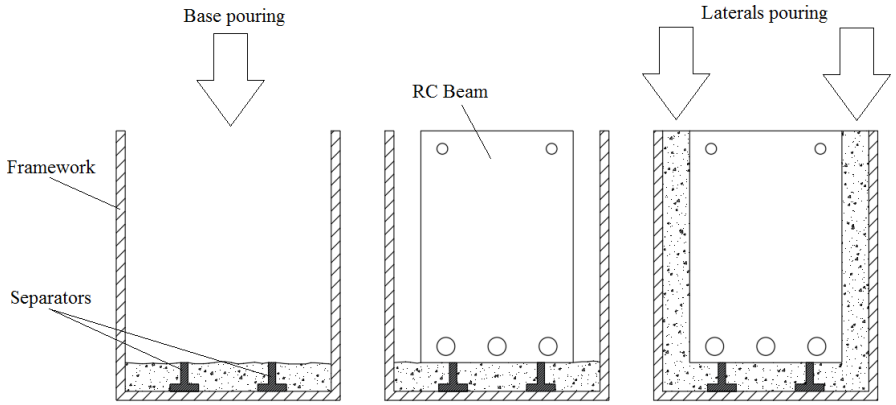

Figure 3.18 Procedure of reinforcing a RC beam by casting a jacket of self-compacting FRC adapted from (Ruano et al., 2014).

Ruano et al. (2014) also performed a comparison of the jacket-casting method using regular self-compacting concrete and self-compacting steel FRC. In their study, they were able to conclude that the specimen reinforced with FRC performed a lot better with regard to shear capacity, increasing the shear capacity with up to 117%.

3.3.3 Shape memory alloys

Rius, Cladera, Ribas, & Mas (2017) propose the usage of shape memory alloys (SMA) as a new strengthening method. The major characteristic of SMA, making the material appropriate for strengthening purposes, is the shape memory effect. This effect means that when the material is subjected to heat it is able to change back into a predefined shape. By restraining the material from changing shape when heated, recovery stresses will appear in the material, effectively prestressing the member it is applied on. A negative aspect that is mentioned with this strengthening method is its high price. However, as it is a new material and research is ongoing, cheaper SMA with similar properties are to be expected. It is also pointed out in the paper that the amount of material needed is small and that it should only be used in critical regions, rather than for complete members.

In order to evaluate the usage of the material as a potential strengthening method, experiments were carried out by Rius et al. (2017) on reinforced concrete beams. Two different applications were evaluated, one by applying the material by spiralling it around the beam, see Figure 3.19(a), the other in a U-configuration, similar to U-jacketing, see Figure 3.19(b). The spiral application was further evaluated by making two identical setups, but only activating (i.e. heating) the reinforcement in one of them.

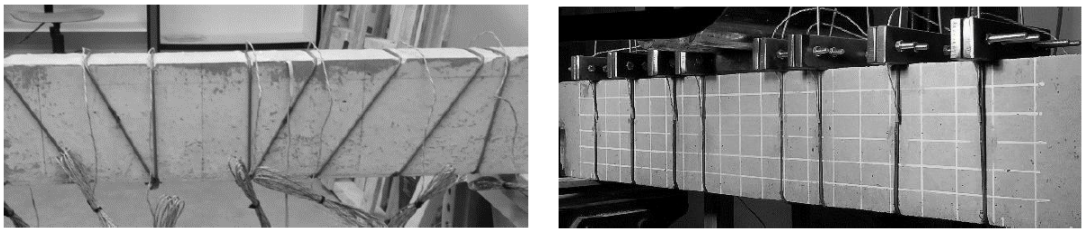

(a) (b)

Figure 3.19 The two different SMA applications: (a) Spiralling; (b) U-shape (Rius et al., 2017).

The experiment showed that the shear capacity was increased with 89% to 106% in the members with the activated reinforcement. However, the member with the non-activated SMA, experienced only a negligible increase in capacity. Rius et al. (2017) concludes the strengthening technique to show a promising potential but point out that more research is needed.

3.4 Summary of presented methods

To create a clear view of the efficiency of the mentioned methods, a summary of their increase in capacity with regard to respective technique is presented in Table 3.1. The increase of capacity is taken from reference specimens used in the different studies. It should, however, be regarded that as the evaluation of the methods are performed in laboratories on differently shaped members and under different circumstances, this summary cannot be used to determine the most efficient method. It will rather give the reader an appreciation of the order of magnitudes of the presented methods.

It should further be noted that the table does not present the ratio of reinforcement material used for each method and that within each method an increase of material would generally generate a higher capacity. In some evaluations of the methods, alterations have been made with regard to the execution, e.g. inclined or vertically installed bars in the drilled in steel bars method, this, in combination with reinforcement ratios explains the larger capacity intervals seen for some of the methods.

Table 3.1 Summary of capacity increase using the different methods.

Reinforcement method	Increase of capacity [%]	Failure mode	Shear action	Reference
Drilled in steel bars	43-45 13-60 65-135	Debonding	One-way	Fiset et al. (2017) Fernández Ruiz et al. (2011) Breveglieri et al. (2014)
Vertical steel bolts	4-22 45	Punching Flexure	Two-way	Askar (2015) Adetifa & Polak (2005)
External steel plates	14-39	Debonding	Two-way	Elbakry & Allam (2015)
Externally bonded FRP	11-54 23 20-58 14-98	Debonding	One-way Two-way	Jung et al. (2015) Chaallal et al. (2011) Binici & Bayrak (2006) Esfahani et al. (2009)
Near surface mounted FRP	35-106 31	Debonding	One-way	De Lorenzis & Nanni (2001) Chaallal et al. (2011)
Embedded through section FRP	27-41 60	Yielding of reinforcement	One-way	Barros & Dalfré (2013) Chaallal et al. (2011)
Textile reinforced mortar	50-160 70	Debonding	One-way	Tetta et al. (2018) Triantafillou & Papanicolaou (2006)
Steel fibre reinforced concrete	32-117	Shear failure in beam	One-way	Ruano et al. (2014)
Shape memory alloys	89-106	Shear failure in beam	One-way	Rius et al. (2017)

3.5 State-of-practice today

The state-of-practice refers to how shear strengthening is most commonly performed today. According to senior consultant at ÅF I. Larsson (personal interview, 2018-02-23) the most intuitive strengthening method is to provide some sort of post-installed shear reinforcement, with an inclination to provide sufficient anchorage length. Larsson further states that the fixation of the shear reinforcement to the concrete preferably is done with bolting, but adhesives may be used if it is of importance to "hide" the strengthening as much as possible, or if it hinders a flat surface. If the ease of production is important, vertical shear reinforcement may be used instead of the inclined. Methods that agree with these statements are the drilled-in steel bars, see Section 3.1.1, vertical steel bolts, see Section 3.1.2 and FRP ETS, see Section 3.2.3.

Nováček & Zich (2016) reports on methods commonly used for strengthening flat slabs against punching. In accordance with Larsson, post-installing shear reinforcement is mentioned as a common method, as well as increasing the effective depth of the slab, which to an extent is utilised in the external steel plate method, see Section 3.1.3. The effective depth of the critical section can also be increased by a concrete topping, i.e. a layer of concrete cast on top of the slab, which can be reinforced with e.g. textile reinforcement. Furthermore, it is stated that enlargement of the perimeter of the support and adding additional flexural reinforcement are methods considered more unusual. The method of adding flexural reinforcement is comparable to the NSMR method described in Section 3.2.2.

Fernández Ruiz et al. (2011) also reasons around which strengthening methods that are customary. Contrary to Nováček & Zich (2016), the enlargement of supporting concrete region and adding flexural reinforcement are mentioned as common solutions. Nováček & Zich (2016) argues that support enlargement method is mostly used by specific actors who already possess the knowledge of how this is done. Otherwise, Fernández Ruiz et al. (2011) confirm that installing shear reinforcement is a common method.

Larsson (2018) also mentioned that shear strengthening of slabs has not been a common problem and because of this the state-of-practice is difficult to estimate. Steel has been available for a longer period of time than FRP and hence attributes, such as durability, which is an important parameter in civil engineering, are less established for FRP. However, the literature review conducted in this study has indicated that more research is being produced for shear strengthening with FRP, in the recent years, more often for beams than slabs. This may indicate that FRP methods will be more commonly used in the future, even though pros and cons must be evaluated for each case individually. Some methods described in this report are still on an experimental state and more applicable to beams than slabs, such as the fibre reinforced concrete jacketing, see Section 3.3.2 or TRM jacketing, see Section 3.3.1. Further studies and real-life implementations are needed to evaluate the actual applicability of these methods.

In conclusion, a consensus seems to be that post-installed shear reinforcement, both in steel or FRP, is the method of choice today. Soft values such as e.g. investment cost and ease of production must be weighed against each other to determine which of the methods should be used. Additionally, as previously stated, caution must be taken so that the flexural reinforcement will not be compromised while drilling holes in the concrete.

4 Literature Review regarding FE Modelling

FE modelling is a powerful tool when evaluating new and existing structures (Broo, 2008). By taking adequate constitutive models for the material, the behaviour of a structure or a part of a structure, can be studied with regard to e.g. stress distribution, capacities or failure modes. It is advised to always verify the model and compare the numerical results with results obtained from testing to make sure that the model is properly and accurately describing the structural behaviour, hence that the results are to be trusted. However, if this is done, the model can be used to evaluate several parameters, such as different load combinations or reinforcement amounts, that would be too costly and time consuming to test in a lab. In design situations the numerical results are verified with hand calculations.

When modelling for bending moment and normal forces, well-recognized and verified methods exist but that is not the case when modelling shear and torsion (Broo, 2008). Because of this, there is an uncertainty on the modelling of shear in concrete. Depending on the level of detail in the model, different responses can be described. The detail level of the model can be altered by making different modelling choices. Some examples of choices that need to be made concern boundary conditions, element types, material models and reinforcement modelling, which will be described further in the following sections. An assessment strategy for choosing the appropriate modelling level is also described.

4.1 Boundary conditions

Depending on what choices are made when modelling the supports, the result of the analysis will vary and it is important that the boundary conditions are modelled in an accurate way in order to obtain a fully functioning model (Pacoste, Plos, & Johansson, 2012). The behaviour is governed by fixed or free translations and rotations at the supports, hence the importance of proper modelling at the support as constraining degrees of freedom will influence distribution of forces and deformation of the structure.

A problem that may occur when modelling RC slabs on columns is singularity, meaning the sectional forces and moments going towards infinity in one single point. However, there are ways to deal with this. Either the modelling of the support is refined as to avoid the singularity, or the point of singularity is disregarded and the values in the sections adjacent to the singularity are evaluated.

It is further suggested by Pacoste et al. (2012) , that in order to avoid unwanted restraints, supports should be modelled in individual points or lines with prescribed boundary conditions. Only if necessary, should supports be modelled more thoroughly. Some recommendations on how to model the support for a continuous one-way slab, by comparison to beam theory, are given in Figure 4.1.

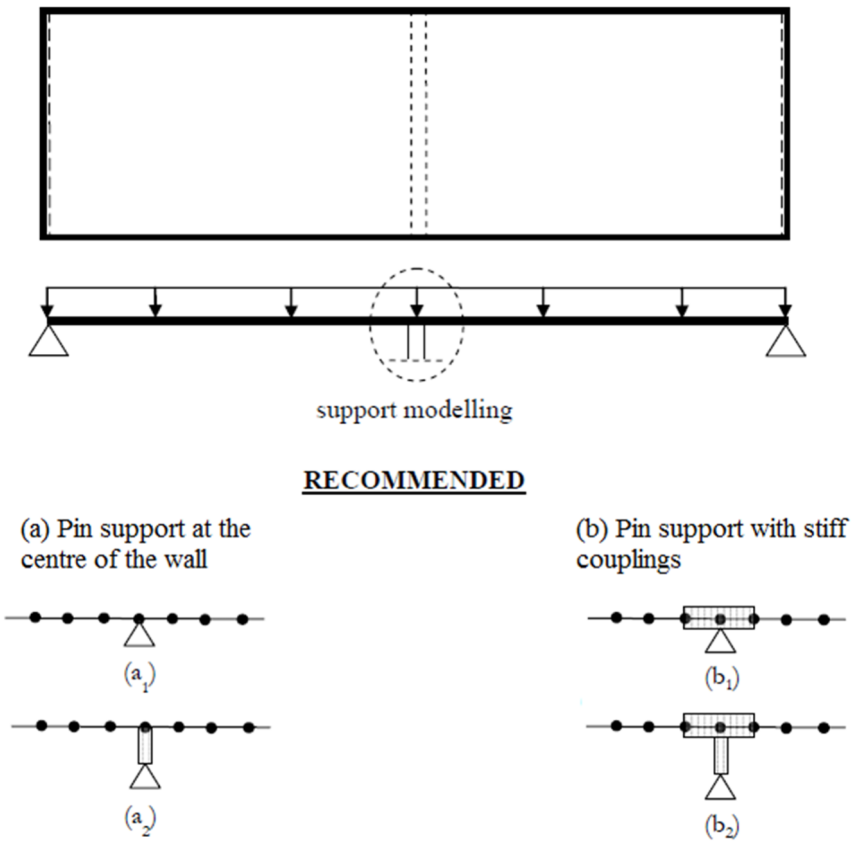

Figure 4.1 Two suggestions on how to model a hinged line support in a slab using linear shell elements, adopted from (Pacoste et al., 2012).

The two modelling suggestions have some variations. (a_1) and (b_1) are for thinner slabs, where the thickness of the slab has no significant impact, whereas (a_2) and (b_2) should be used when the slab thickness must be taken into account. In design (a), the nodes on the centre line are vertically restrained Design (b) is similar but in addition to having the centre nodes vertically restrained, they are also linked rigidly to the adjacent nodes, as shown in Figure 4.1(b).

There are some aspects that need to be taken into account when modelling slabs that have an irregular geometry. The same concepts as when modelling supports are valid, but there are some further recommendations that must be considered. If the slab is simply supported along a wall it should be modelled along the centre line of the wall, locking the nodes vertically. Some additional attention must also be paid in situations where wall supports meet, as corner lifting will appear in this area. It is also worth noting that the stiffness of the supporting wall itself might influence the slab, and it is therefore recommended to consider this when modelling the wall support. If there is a monolithic connection between the slab and the wall, it is preferred to include the wall in the model to achieve the level of restraint corresponding to reality (Pacoste et al., 2012).

By utilising the symmetry in a structure, a lot of computational time can be saved. Rather than modelling the whole structure, only a part of it needs to be studied. However, by using symmetry, an assumption is made that the structure will behave in

the exact same way on the other side of the symmetry line. It is thus important to assure that this is indeed the case (Hendriks, de Boer, & Belletti, 2017).

4.2 Element types

Davidson (2003), explains that when approached in a somewhat simplified manner, one could divide finite elements used in analysis into two categories, structural elements and continuum elements. These are then sub-divided into different types of elements, shown in Table 4.1, depending on what dimension of analysis that is performed.

Table 4.1 Division of different types of finite elements (Davidson, 2003).

Dimension	Structural element	Continuum element
1D	Bar element	Bar element
2D	2D Beam, Plate and Interface elements	Plane stress, Plane strain and Axisymmetrical elements
3D	3D Beam, Shell and Interface elements	Solids

The type of element used in the model will determine what kind of response the model will be able to describe. For example, beam elements are not the best choice to describe shear, plane stress elements can describe shear in beams or walls where load acts in the element plane and shell elements can describe out of plane bending (Broo, 2008). Therefore, it is important to choose the appropriate element type based on what kind of responses are to be studied.

The element size is also of relevance as to how accurate the results of the analysis will be in comparison to how computationally efficient it will be. Hendriks, de Boer, & Belletti (2017) suggests that the maximum size of the elements should not exceed *l/50* and *h/6,* where *l* and *h* is the span length and depth of the member respectively. It should be noted that this recommendation applies to non-linear analysis and that for a linear analysis, a coarser mesh can generally be used. There are no general recommendations regarding the minimum element size, however, the computational time will be governing for how small elements will be efficient. In order to obtain an appropriate element size for the model, a convergence study may be performed. This is done by running several analyses with an increased density of the mesh and comparing the results. The output will then be seen to converge against a true value and by considering this, a reasonable element size can be chosen.

4.3 Material models

It is important to include detailed models for the plain concrete and steel separately, as well as their interaction. Concrete can, depending on failure mode, be described in different ways. In cases where the stress state is dominantly compressive, the material can be regarded as homogeneous and isotropic, and plasticity theory is normally used to model the failure. Tensile failure in concrete, on the other hand, is described by fracture mechanics and the relation between stress and crack opening. These are,

however, not the only methods used, but they are used more frequently and are considered the important theories when modelling concrete (Plos, 2000). When performing non-linear analyses on concrete structures the non-linear stress strain relation, shown in Figure 4.2, must be accounted for.

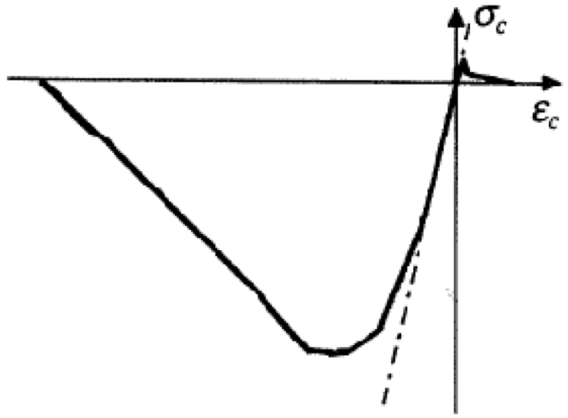

Figure 4.2 Illustration of non-linear stress-strain relation of concrete (Broo, Lundgren, & Plos, 2008).

Reinforcement steel is commonly described as elastic-plastic, as it has a reasonable linear behaviour until it starts to yield, beyond which point it starts to experience a more plastic behaviour. It can be modelled using e.g. von Mises yield criterion with isotropic hardening, obtained from testing of the bars.

In some situations, when an already existing structure is to be evaluated using FE analysis, a material deterioration may have taken place. This is the situation in the case study, which is further explained in Section 5, where extensive cracking has taken place throughout the whole structure. A way to treat this in linear elastic analysis is to reduce the Young's modulus, E, for the material. However, this method should be used with caution as the reduction is difficult to predict. There is a risk that this method is too conservative and it is important to consider the different impact the cracking may have on different parts, e.g. slabs or beams. The properties of these members should be altered accordingly. Another method of accounting for the existing cracks, in non-linear analyses, is to pre-load the model with a cracking load, de-load it and then apply the real loads.

4.4 Modelling of reinforcement

Normally, reinforcement is working one-dimensionally and carries tensile forces in one direction (Plos, 2000). Because of this, a simplification of the modelling of the reinforcement can be done and thus the usage of continuum elements can be avoided. The reinforcement can be embedded in the concrete elements instead, meaning it is not modelled as separate elements but rather strengthening the concrete elements in the direction it is applied as additional stiffness only. Any reinforcement strain would consequently have to be determined from the displacement of the concrete elements. Furthermore, as the reinforcement is fully embedded in the concrete, no bond-slip can be described by such models.

Plos (2000) further states that in order to describe the behaviour between the reinforcement steel and the concrete, the steel can be modelled using truss elements, combined with interface elements for the interaction. Another suggestion is using 3D solids for both the reinforcement and the concrete. Including this behaviour in the model would contribute to results closer to reality, although such models are significantly more complicated to implement and use. Unless the interaction between reinforcement and concrete is to be studied specifically, or there are suspicions of the reinforcement not being properly anchored, an assumption of the two materials being perfectly bonded is considered reasonable.

4.5 Assessment strategy when using FE modelling

It is important to have a clear strategy when evaluating capacities and responses of structures. Since the method for how intricate an assessment is to be done is vaguely described, or described in general terms, Plos, Shu, & Lundgren (2016) proposes an assessment strategy consisting of five levels, see Figure 4.3. Level I corresponds to simplified methods and the accuracy subsequently increases up to complex non-linear FE analysis at level V. In cases where the studied failure mode is not being represented in the FE analysis, the structural analysis needs to be combined with local resistance models. It is further suggested that an assessment on level I or II is performed initially, and that if the assessment is to be continued, it should proceed up to level V successively.

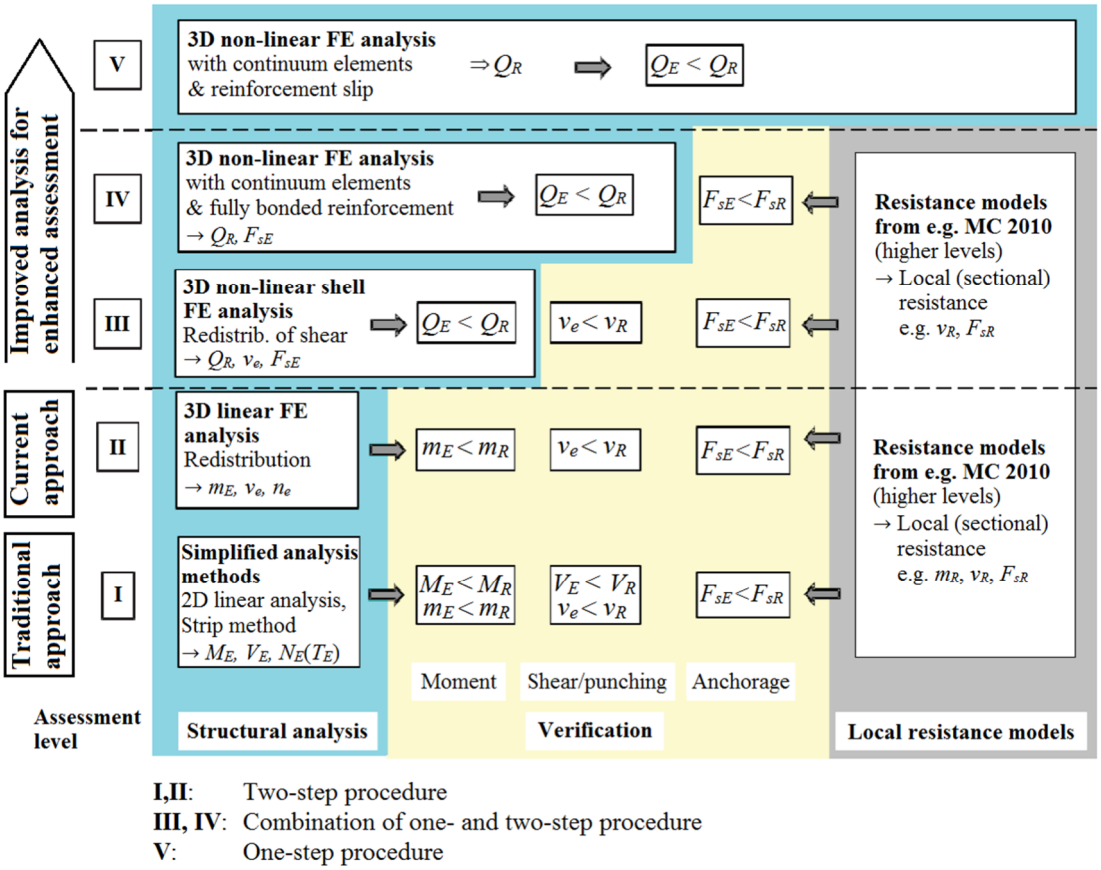

Figure 4.3 Overview of the assessment strategy scheme, adapted from (Plos et al., 2016).

It is also worth noting that the more complex an analysis becomes, the more man hours and computational time will be required. This means that a more complex model is not always the best solution, as the time and cost could be spent on other parts of the structural analysis. Also, simpler structures are less likely to benefit from a higher level analysis as their behaviour is easier to predict. The following subsections will provide a more in depth explanation of level one through five as they are described by Plos et al. (2016).

4.5.1 Level I – Simplified analysis methods

Level I studies a simplified system, often 2D beam or frame models with an assumed load distribution in the main directions. If performed on an RC slab, the strip method can be utilised. The load effects are then compared with resistances determined by local models for each effect. Design resistance models are used in accordance with codes and regulations, e.g. Eurocode 2 ('SS-EN 1992-1-1', 2008).

4.5.2 Level II – 3D linear shell FE analysis

Level II applies 3D FE models, usually based on shell or bending plate theory. Linear response and the ability to superimpose load effects is assumed, and as a consequence maximum load effects of all combinations can be evaluated. Assumptions of linear material response and geometrical simplifications will result in unrealistic stress concentrations. Combined with the reinforcement being evenly distributed, this will yield a need of redistribution of cross-sectional forces and moments. Load effects are then compared with their resistance in the same fashion as in level one.

4.5.3 Level III – 3D non-linear shell FE analysis

Level III includes a non-linear FE analysis, it involves letting the load increase successively until the structure fails. In this analysis, only the most critical load case is examined and has been determined earlier in the process. This is because performing a non-linear analysis for all combinations would take too much time. Elements used on this level are shell or bending plate elements. Reinforcement is modelled as embedded, assumed to be perfectly bonded with the concrete. Because of this, bending failures will be represented in the model. Other failure, e.g. shear or punching, needs to be checked by local resistance models. Resistance models of higher approximation are suggested to be performed in accordance with e.g. Model Code for Concrete Structures 2010 ('Model Code 2010', 2013).

4.5.4 Level IV – 3D non-linear FE analysis with continuum elements and fully bonded reinforcement

Level IV also includes a non-linear FE analysis, however, the elements used for the concrete are 3D continuum elements. Reinforcement is assumed to be fully bonded and is modelled as embedded, this is done in the same way as in level three. On this level, bending is described well, as well as one and two-way shear. Only anchorage failure has to be checked by using resistance models.

4.5.5 Level V – 3D non-linear FE analysis with continuum elements including reinforcement slip

Level V models the concrete in the same way as in level IV, but is now accompanied by modelling the reinforcement using separate elements. Bond-slip between the concrete and the reinforcement steel is hence taken into account. Individual cracks can be observed by using a fine mesh. No additional resistance models should be required to check any major failure mode as the goal is that they should all be represented by the model.

4.5.6 Summary of the assessment strategy

As a summary of the proposed assessment strategy, Plos et al. (2016) also performed an evaluation for two case studies comparing the five levels against values obtained from testing. The comparison, shown in Figure 4.4, was performed on a two-way slab designed to fail in bending and a cantilever slab designed to fail in shear. The comparison showed that for low levels of analysis, the shear capacity is underestimated to around 30% of the tested capacity and the bending is underestimated to around 65%. For increasing levels of detailing, the underestimation receded to similar values for both bending and shear, indicating that both bending and shear failure can be described better by high levels of FE modelling. The structures analysed in this example can be considered simplistic, which gives an understanding to why a level III analysis provides similar underestimation as a level V analysis. A more complex structure would probably benefit more from a higher level of modelling than what was displayed here.

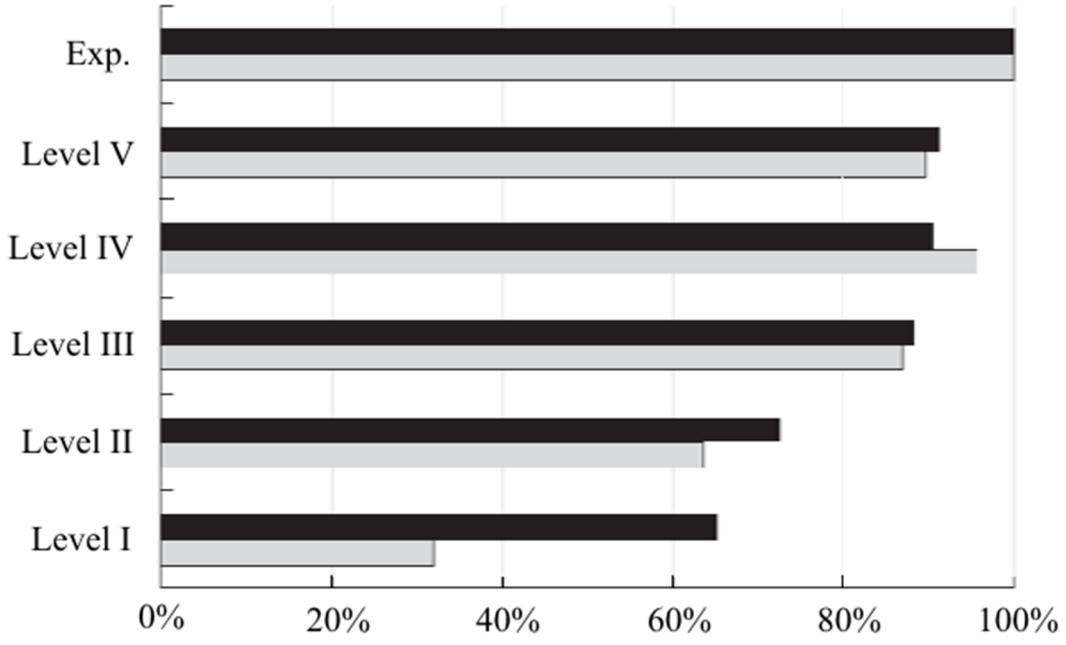

Figure 4.4 Capacity from assessment compared to values obtained from testing, grey representing two-way slab failing in bending and black represents cantilever slab failing in shear (Plos et al., 2016).

5 Case Study

An existing industrial building was selected as a case study for investigating the shear behaviour of the RC slabs and evaluating possible strengthening methods relevant to this case. The industrial building consists of RC slabs supported by beams and columns as shown in Figure 5.1. In the spans of the slab, large holes are situated in order to make room for silos, which are hanged around the perimeter of the hole. This yields large forces in the slab, which in turn raises concern for shear failure. In addition, there is a need for increasing the load of the silos.

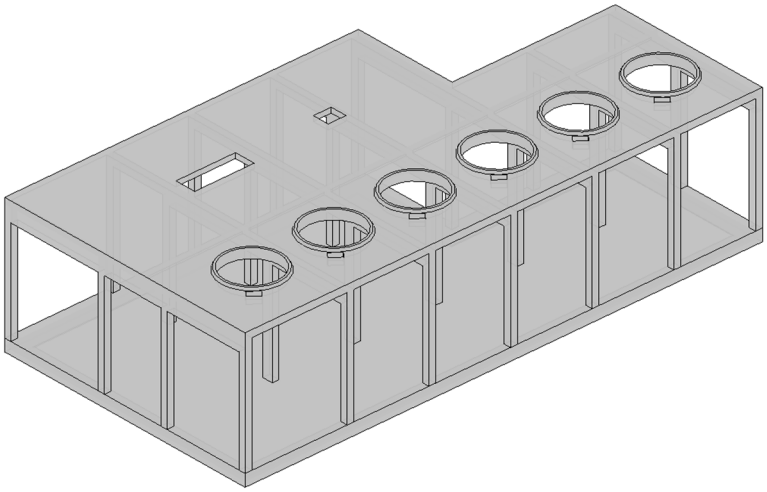

Figure 5.1 3D model of the industrial building as a case study.

The goals of investigating the case study were:

1. To assess and investigate the structural behaviour of the already cracked building by focusing on the shear behaviour of the slab in different levels of detail.
2. To investigate the need of shear strengthening due to the increase in loads and evaluate the applicable strengthening methods specific for this case study.

To achieve goal 1, which is also designated as Part 1 of this case study, the structural assessment strategy consisting of different levels proposed by Plos et al. (2016) which was presented in Chapter 4.5, was applied. The assessment was done up to level III. Finite element modelling in ABAQUS was used as a method to assess and study the structural behaviour of the building in assessment levels II and III. In level II, different FE models using beam, shell and solid elements were created and compared to each other in a linear analysis in order to examine and obtain the most reliable model to use for composite slab-beam structures. In level III, the model determined as the most reliable, while not being too computationally heavy, was developed in a non-linear analysis, which then could be compared to the previous levels as well as evaluated itself.

In Part 2 of the case study, the results from the first part were used. As a need for shear strengthening was established, the different techniques described in Section 3 were further evaluated. In an early assessment, the practical application of the methods was considered and narrowed down to those applicable for the studied slab. Furthermore, the potential increase of shear capacity due to these strengthening methods, their cost

and also applicability were analysed. In addition, the increase of shear capacity due to a flexural strengthening of the slab was evaluated.

5.1 Assessing the structural behaviour

Part 1 of the case study was conducted according to the assessment strategy proposed by Plos et al. (2016), see Section 4.5. This section is laid out so that the conditions and assumptions used in the analyses of the different levels are described, together with the following results and conclusions drawn for each level. The shear load and capacity were first determined according to 'SS-EN 1992-1-1' (2008), level I in the assessment strategy, which was subsequently set as a reference for the following assessment levels.

The structure to be analysed can be seen in Figure 5.2(a), which has been simplified to a structure as in Figure 5.2(b), in which the small openings have been neglected, as well as that the beams are assumed to be of constant height. In reality, the beam had a varying height for different spans along its length. The highlighted span in Figure 5.2(b) has been chosen for investigation in order to decrease computational demands compared to modelling the complete structure. As part of a larger structure, six spans with dimensions as shown in Figure 5.3 contain slabs with circular holes around which silos are supported. In Figure 5.4, a section view as taken from Figure 5.3 can be seen, where it is shown that the slab has a varying thickness, 0.41 m and 0.3 m. The reason for assessing the structure is that a need of increasing the variable load in the silos has arisen. The loads that the structure was going to be designed for can be seen in Table 5.1. As it is an existing structure, there are already cracks present in the structure and the need for strengthening will therefore be evaluated.

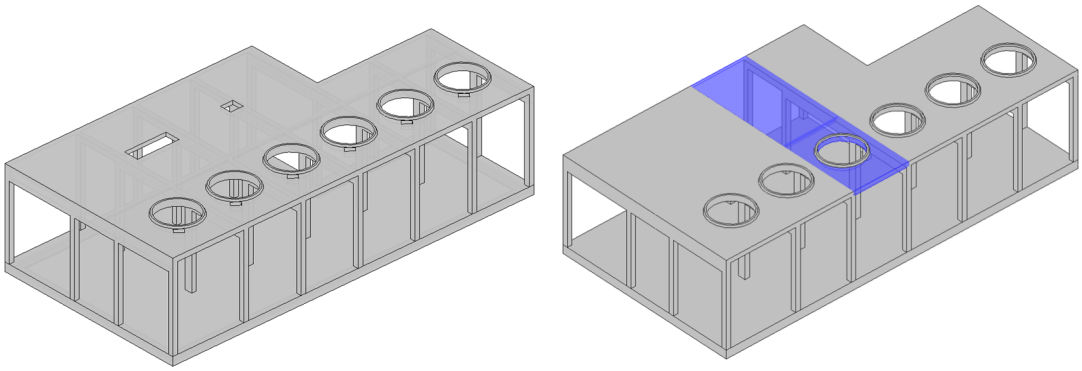

(a) (b)

Figure 5.2 3D model of the industrial building: (a) Model of structure as it is; (b) Simplified structure to be modelled.

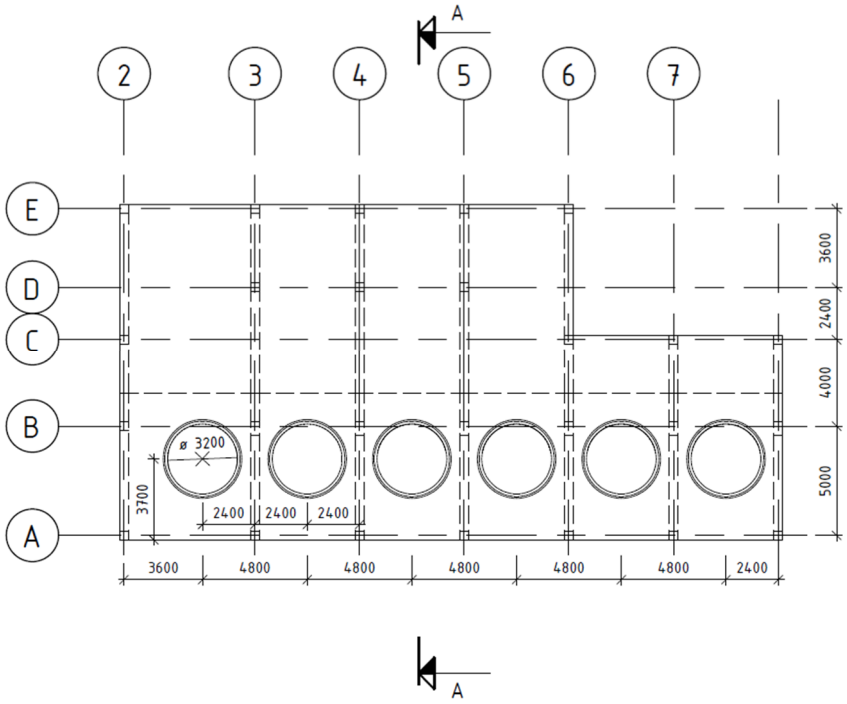

Figure 5.3 Plan view of the floor for the simplified model.

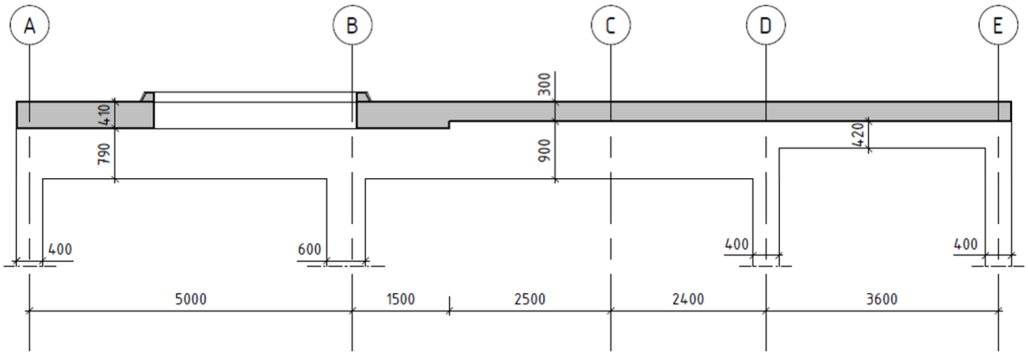

Figure 5.4 Section view of investigated spans for the non-simplified model.

Table 5.1 Loads the structure should be designed for.

Type of load	Magnitude [kN/m^2]
Self-weight	-
Distributed load on slab 0.3 m	9.81
Distributed load on slab 0.41 m	4.91
Self-weight silos	100*
Distributed load silos	350*

*This load is applied on a ring of 225 mm width around the hole

As previously stated, Part 1 of the case study aimed to investigate the structural behaviour of the structure, analytically and numerically, in terms of the shear force capacity. The case study should furthermore be able to serve as an aid for the future

work of designers dealing with similar situations. The comparison has as such been conducted in accordance with levels I to III in the assessment strategy. The reason for omitting levels IV and V is that such levels of modelling detail are too time consuming and would not fit within the designated time of this study. A summary of the assessments performed, and their used model, on the structure, in Part 1 of the case study is presented in Table 5.2.

Table 5.2 Assessment performed on the structure.

Level	Method	Model
Level I	Analytical calculations	2D Beam
Level II	Linear FE-analysis	3D Shell
		3D Shell with reduced stiffness
		3D Shell and beam model
		3D Solid
Level III	Non-linear FE-analysis	3D Shell - Load control
		3D Shell - Displacement control

It is also worth noting that level II is the level of detail most commonly used in practice. Therefore, the level III analysis will also serve as a validation of whether using level II is sufficient or if the additional time put in to a level III analysis is justifiable.

5.1.1 Level I analysis

The shear capacity of the slab was calculated in accordance with the level I analysis, that is, estimating the shear capacity of the slab analytically by following Eurocode 2 guidelines. As the slab does not contain any shear reinforcement, the calculated shear resistance is derived from the concrete's capacity of resisting shear alone. When performing calculations on the slab, a strip with a width of 1 m was studied. Furthermore, some simplifications were made for the calculations, an even distribution of 0.2 m between tensile reinforcement as well as a constant diameter of the bars, 12 mm, was assumed, see Appendix B for the full reinforcement distribution in the slab. According to a previous assessment, made by ÅF, the concrete quality in the building, i.e. the compressive strength of the slab, was measured to 33 MPa. This corresponds to concrete class C25/30, which was then used for the calculations.

In the FE analyses, the slab was modelled as two span halves with the beam situated in the middle using symmetry as boundary conditions, further described in Section 5.1.2, see also Figure 5.10. Therefore, the level I analysis was performed with the same geometry.

The shear effect in the slab was calculated using the simplified calculation model shown in Figure 5.5, with three different loads applied. The calculation model was applied along two paths, further referred to as path A and path B, in the 0.41 m thick part of the slab, see Figure 5.6. Out of the two paths studied, path A yielded the higher shear value. The slab was assumed to distribute the load with one way-action in these hand calculations. All assumptions and calculations made for the level one assessment are shown in Appendix C.

The loads acting on the structure are presented in Table 5.1. These values were assumed in accordance with previously assumed values from the project at ÅF for the level I analysis. The self-weight and a distributed load were applied along the length of the beam model, and point loads were applied on both ends corresponding to loads from the silos on the collars around the slab openings.

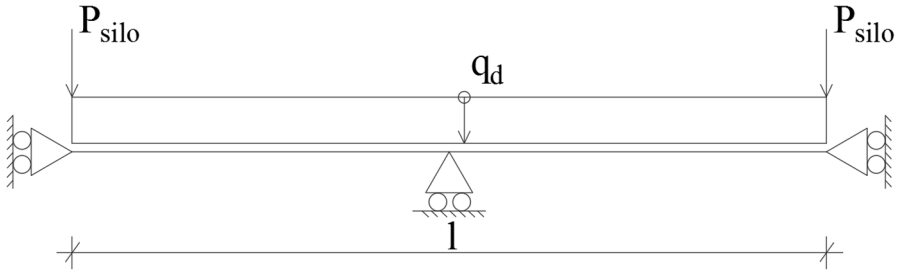

Figure 5.5 Calculation model used for the level I analysis.

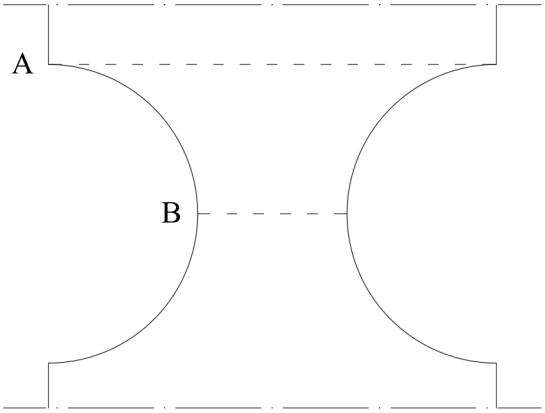

Figure 5.6 Paths studied for the level I analysis.

The shear was calculated at the design shear section which is 0.61 m from the centre of the beam, in accordance with Pacoste et al. (2012), see Figure 5.7. In the studied case the distance *d* was taken as the full thickness of the slab for simplicity.

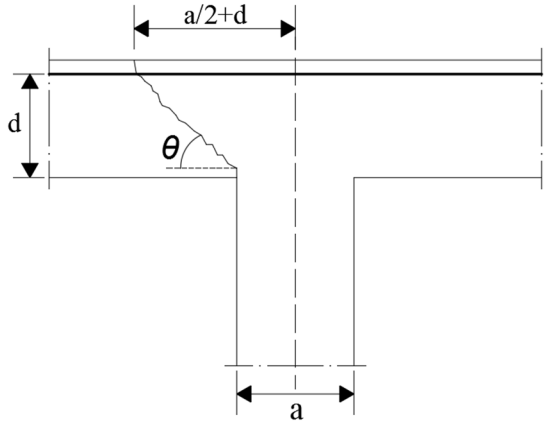

Figure 5.7 Critical section for shear force, adapted from (Pacoste et al., 2012).

5.1.1.1 Results

The shear capacity of the different thicknesses and the highest shear load in the thicker part of the slab were calculated. In addition, the shear force distribution along path A and B are shown in Figure 5.8 and Figure 5.9 respectively. The dashed line indicates the critical section for shear force and the maximum shear value was taken at this point.

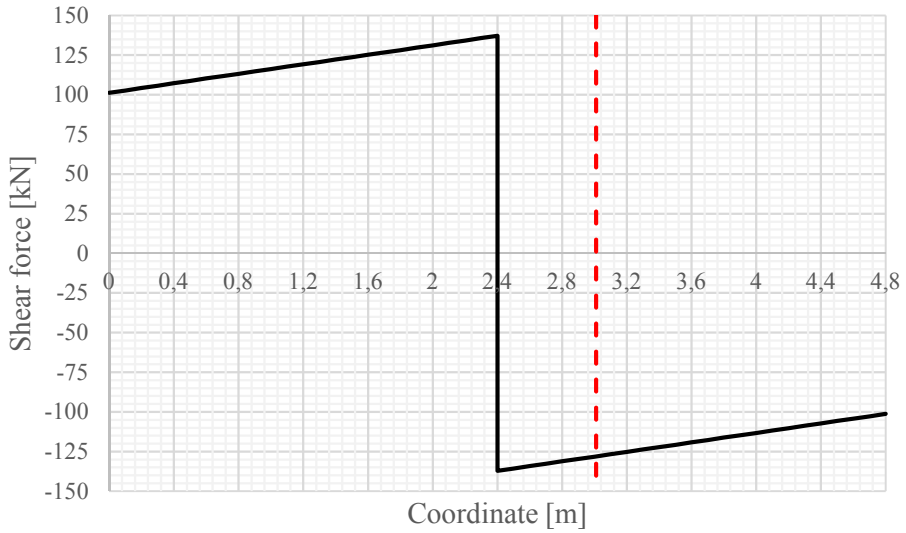

Figure 5.8 Shear force distribution along path A.

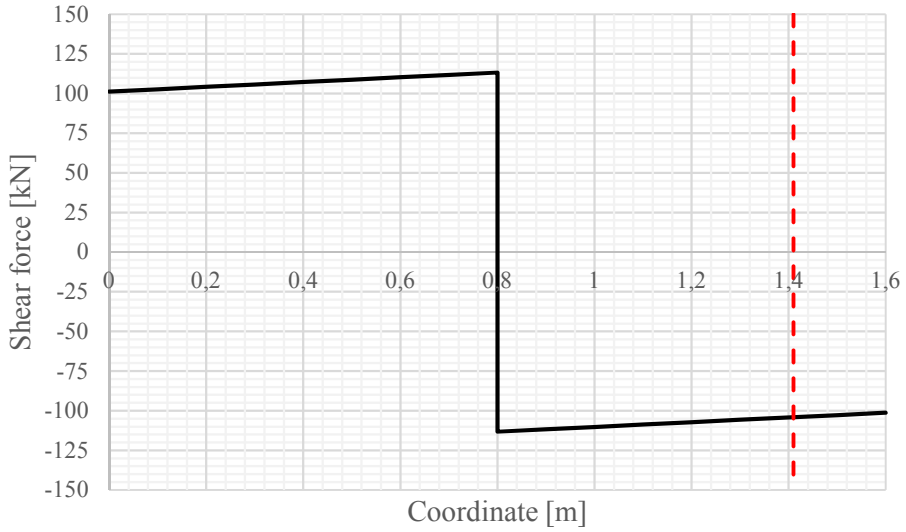

Figure 5.9 Shear force distribution along path B.

Table 5.3 presents the shear capacity in the different thicknesses of the slab, as well as the maximum shear load in the 0.41 m thick part of the slab, this value was found along path A. In addition, the concrete capacity against crushing, which is the maximum value for the capacity, was determined.

Table 5.3 Shear load and capacities in the different slab parts.

Slab thickness [mm]	Shear in slab [kN]	Shear capacity [kN]	Crushing capacity [kN]
410	128	151	1710
300	-	120	1215

5.1.1.2 Conclusions for the level I analysis

The level I analysis showed that the shear capacity of the slab, 151 kN, was sufficient and thus, no strengthening would be needed according to this level of assessment. To confirm that no strengthening was needed, a more detailed analysis was performed, according to level II in the assessment strategy.

5.1.2 Level II analysis

As described in Section 4.5.2, level II consisted of a 3D linear elastic FE analysis. The aim for level II was to capture the shear distribution due to 3D effects and the following effects because of this. In addition, the level II analysis served as a way to provide a model as good as possible for level III, which meant that comparisons between different possible models could be made. Different models were analysed with regard to geometrical and model technical aspects. Furthermore, an aim was to provide a model which could describe slab-beam composite behaviour as good as possible.

Geometrical comparisons accounts for the extent of the structure that is modelled and how transitions between different structural members are modelled. The geometry of the structure which was modelled in ABAQUS can be seen in Figure 5.10. In addition, local directions and used notations are shown in the same figures. The models include half of two adjacent spans, as well as the supporting beam and columns.

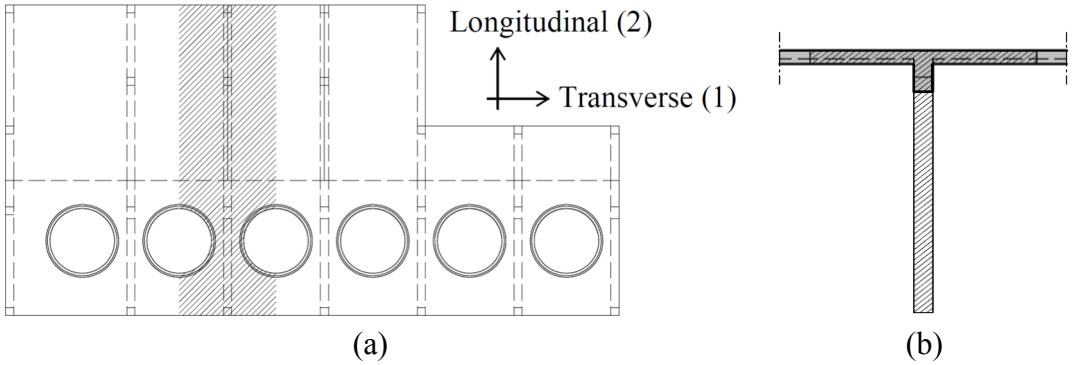

Figure 5.10 Modelled geometry of the structure, marked with diagonal hatch: (a) Top view; (b) Cross sectional view.

Different models were compared in order to estimate which modelling method is most suitable for the problem at hand. Choices made for the different models will be described as they occur in the modelling process in ABAQUS, which is made up of 9 main modules:

- Part
- Property

- Assembly
- Step
- Interaction
- Load
- Mesh
- Job
- Visualization

When modelling, the process starts from the top (Part) and continues down the list to the bottom (Visualization). ABAQUS is unitless, which means that the units used as input to the software will be the units in the output. Values and units presented in this thesis are the same as the values that were used in ABAQUS.

Part

In the Part module, geometries for the different parts of the structure are defined. Three different model alternatives were made in the Part module, see Table 5.4, where the alternatives all are sub-categories of 3D deformable types.

Table 5.4 Part module model alternatives.

Model	Element type - slab	Element type - columns & beam
Alternative 1	Shell	Shell
Alternative 2	Shell	Wire (beam)
Alternative 3	Solid	Solid

For Alternative 1, referred to as the model with shells, the slab was modelled with dimensions 4.8x15 m, with two half-circles with a diameter of 3.2 m cut-out at a mid-point offset from the slab edge of 3.7 m. Two partitions were made to represent the mid-axis of the slab in the length-direction and the transition from the slab with a thickness 0.41 m to the thinner part with a thickness of 0.3 m. Furthermore, the beam was modelled perpendicular to the plane of the slab, with a height of 0.9 m that was assumed for the full length of the slab. Columns were modelled with widths 0.4 m and 0.6 m, as shown in Figure 5.4, and heights of 7.2 m, which is the distance to the floor below. Figure 5.11(a) presents a 3D view of the model in the Part module.

For Alternative 2, referred to as the model with shells and beams, the slab was modelled in the same way as for Alternative 1. The difference being that the beam and columns were modelled as separate parts using beam elements, rather than the shell elements used in Alternative 1. Figure 5.11(b) shows the model in a 3D view after the parts had been assembled in the Assembly module.

In Alternative 3, referred to as the model with solids. The complete structure was modelled with solid elements using the same dimension as in the previous alternatives. Figure 5.11 (c) displays the model in the Part module.

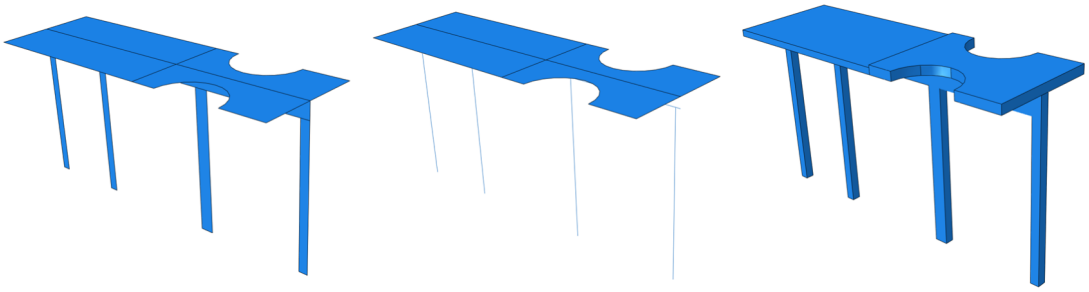

(a) (b) (c)

Figure 5.11 3D view of models in ABAQUS: (a) Shells; (b) Shells and beams; (c) Solids.

Property

In the Property module, materials and sections are assigned to the parts. For the shells model two sub-alternatives, Alternative 1(a) and Alternative 1(b), were compared. Alternative 1(b) was meant to reflect a cracked structure, as is the case in reality, referred to as the model with shells with reduced stiffness. The main reason was to investigate if any redistribution of the shear load can be captured by doing so. The model with shells and beams and the model with solids were modelled with the same material properties as the model with shells. The used material properties for concrete are presented in Table 12.

Table 5.5 Material properties used for the linear elastic analysis in Abaqus.

Property	Value
Density	2500 kg/m3
Young's modulus	31 GPa
Poisson's ratio	0.1

To represent the cracked concrete in the reduced stiffness shell model, i.e. concrete in state II, a reduction was introduced by using a lower value for Young's modulus. The reduction was determined by calculating the ratio between the bending stiffness in state I and II. However, the reduction was not constant throughout the structure and it was therefore divided into different zones depending on the magnitude of reduction. First, three main categories were observed:

- Slab over support, i.e. the area above the beam
- Slab in field, i.e. the rest of the slab
- The beam

The two slab parts were further divided, where the slab in field was divided in two parts depending on slab thickness. The slab over support was divided in five parts based upon zero-moment points along the beam. The zero-moment points were taken from the results of the analysis with shells. The five parts in the slab over support were, in the length-direction of the slab:

- 0 – 4.5 m, compression in bottom
- 4.5 – 6.8 m, compression in top
- 6.8 – 10.2 m, compression in bottom
- 10.2 – 12.2 m, compression in top
- 12.2 – 15 m, compression in bottom

By doing this, all five sections of the slab over support would correspond to having either entirely positive or negative sign of the moment curve. These five sections were then treated as T cross-sections with effective slab widths with the beam as web. By determining the position of the neutral layer in the T-section the second moment of inertia for state II could be determined for both the slab over support and the beam. When studying the slab in field, a 1 m strip of the slab was considered, for which the updated second moment of inertia could be determined. The resulting partition of the slab is shown in Figure 5.12 and the corresponding stiffness for each section is presented in Table 5.6. In addition, the beam was partitioned in the same way and its reduced stiffness is also presented in Table 5.6. The calculation procedures for the new second moment of inertias are presented in Appendix D. No other difference between the shell models with and without reduced stiffness was made.

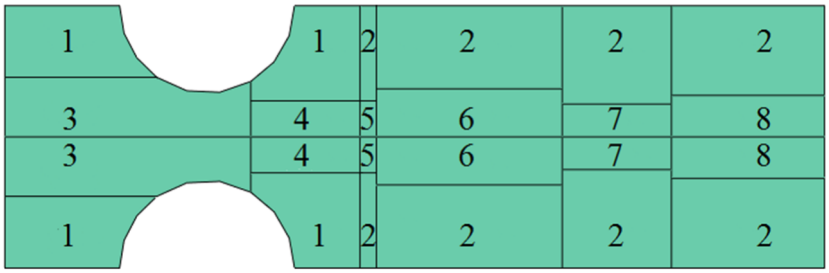

Figure 5.12 Slab partitions for reduced shell model, with numbering of different stiffness zones.

Table 5.6 Second moment of inertias in state I and II, Young's moduli for concrete in state II for the model with reduced shells in different stiffness zones.

Zone in Figure 5.12	Concrete region	I_I [m^4]	I_{II} [m^4]	Ratio (I_{II}/I_I) [%]	E_{red} [GPa]
1	Slab in field t = 0.41 m	0.00574	0.00102	17.8	5.5
2	Slab in field t = 0.3 m	0.00225	0.000313	13.9	4.3
3	Slab over support t = 0.41m [0 – 4.5 m]	0.013	0.00216	16.2	5.0
4	Slab over support t = 0.41 m [4.5 – 6.8 m]	0.029	0.00550	19.2	6.0
5	Slab over support t = 0.3m [4.5 – 6.8 m]	0.029	0.00550	19.2	6.0
6	Slab over support t = 0.3 m [6.8 – 10.2 m]	0.00415	0.00133	31.9	9.9
7	Slab over support t = 0.3 m [10.2 – 12.2 m]	0.00462	0.00202	43.7	13.5
8	Slab over support t = 0.3 m [12.2 – 15 m]	0.00362	0.00133	36.8	11.4
-	Beam [0 – 4.5 m]	0.049	0.026	52.8	16.4
-	Beam [4.5 – 6.8 m]	0.029	0.00460	15.6	4.8
-	Beam [6.8 – 10.2 m]	0.049	0.026	53.1	16.5
-	Beam [10.2 – 12.2 m]	0.025	0.00280	11	3.4
-	Beam [12.2 – 15 m]	0.048	0.025	52.4	16.2

The sections created for each of the alternatives can be seen in Table 5.7. All sections for the shells model, as well as the slab part for the shells and beams model, have been defined with Simpson's integration rule with 5 integration points, which is the default option provided in ABAQUS. The additional sections found in the other alternatives are shown in Table 5.7, but as they consisted of other types of elements they were treated differently.

Table 5.7 Sections created for the different models.

Model	Parts	Dimensions [m]
Shells	Slab 0.41 m	t = 0.41
	Slab 0.3 m	t = 0.3
	Beam and columns	t = 0.4
Shells and beams	Slab 0.41 m	t = 0.41
	Slab 0.3 m	t = 0.3
	Beam	b = 0.4, h = 0.9
	Thin column	b = 0.4, h = 0.4
	Thick column	b = 0.4, h = 0.6
Solids	Whole structure	See Figure 5.3 & Figure 5.4

Assembly

In the Assembly module, different parts are merged and aligned to each other. The parts from the models with shells and solids needed no further merging, since they were modelled as one part with the correct relations between sections. However, the model with shells and beams did require assembling of the different parts as they were modelled separately. It was done by creating instances of the different parts in the Assembly module and then arranging them in an appropriate order. At this stage the parts did not interact with each other, they were simply arranged in relation to each other, this was later treated in the Interaction module.

Step

In the Step module, different analysis steps are defined and specific output requests are created. Level II analysis was a linear elastic analysis, and no more than one step was needed. The step chosen was a general static, which is identical for all model alternatives. Default options were used for the step.

Interaction

In the Interaction module, interactions between parts are defined, e.g. couplings and constraints. For the models with shells and solids no interactions were defined. In the model with shells and beams, interactions had to be defined between the slab and the beam, and the beam and the columns. The interactions were done by using the constraint manager in the Interaction module. A tie constraint was chosen for both cases. In the beam-to-slab connection, the slab acted as a master surface and the beam as slave. For the case of the columns-to-beam connection, the beam acted as a master surface and the columns as slave. The tie had to be performed in this way because a slave surface can only be tied to one master, but the master surface can in turn be slave for an additional master surface.

Load

In the Load module, both loads and boundary conditions are defined. Five loads were defined for the structure, in accordance with previously described values: self-weight of all parts, distributed load on the 0.3 m slab part, distributed load on the 0.41 m part of the slab and self-weight as well as distributed load of the silos supported on a collar of the slab openings. Table 5.8 presents the used load values and their load type that was used in ABAQUS. The silos are in the industrial building supported on a concrete rim along the perimeter of the holes. To reflect this, silo loads were applied on a surface with width 0.225 m, see Figure 5.14(a).

Table 5.8 Load types and values.

Load	Type	Magnitude
Self-weight	Gravity	9.81 kg/s^{2}m
Distributed load slab 0.3 m	Pressure	9810 N/m^2
Distributed load slab 0.41 m	Pressure	4910 N/m^2
Self-weight silos	Pressure	100 000 N/m^2
Distributed load silos	Pressure	350 000 N/m^2

For all the alternatives, two different boundary conditions were defined. Along the longitudinal edges of the slab x-symmetry was defined, meaning displacement perpendicular to the edges (U1) is locked to zero. The rotations around the edge itself

(UR2) and around the vertical axis (UR3) were also locked as a result of the x-symmetry. The columns were casted together with the underlying floor, and were as such assumed to be fully fixed. Their translational displacements in all directions (U1, U2, U3) were locked to zero, see Figure 5.13. The used coordinate system is presented in Figure 5.13, where the slab's local 1-coordinate corresponds to the global x-coordinate and the local 2-coordinate corresponds to the global y-coordinate.

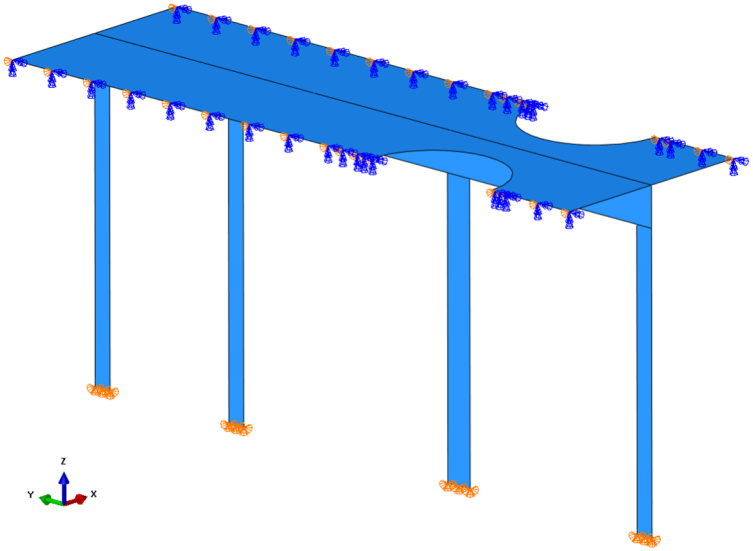

Figure 5.13 Boundary conditions used in the model. Orange arrow indicate locked displacement and blue arrow indicate locked rotation.

Mesh

In the Mesh module, all parts are meshed. To provide a good mesh around the openings, partitions were made in the slab according to Figure 5.11(b). The shortest transversal distance between the openings, 1.6 m, was divided into four equally offset vertical segments. Horizontal partitions were also made above and below the openings with an equal size as the vertical partitions to create a radial mesh pattern.

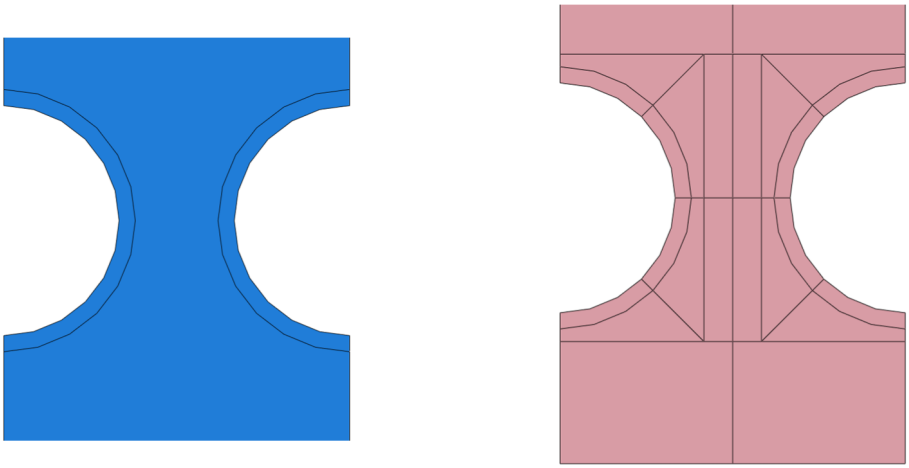

(a) (b)

Figure 5.14 Partitions around holes used in the FE-modelling: (a) Partitions for load application; (b) Partitions for meshing.

To obtain a correct enough mesh while still keeping the computational demand as low as possible, a mesh convergence study was performed for the model with shells. In the convergence study, two different outputs were compared. These were the transverse shear force in the transverse direction of the slab (SF4) and the bending moment around an axis in the longitudinal direction of the slab (SM2). The output is dependent on the local coordinate system of the slab, further explained in Figure 5.15. The directions and the local coordinate system of the slab were determined as shown in Figure 5.10.

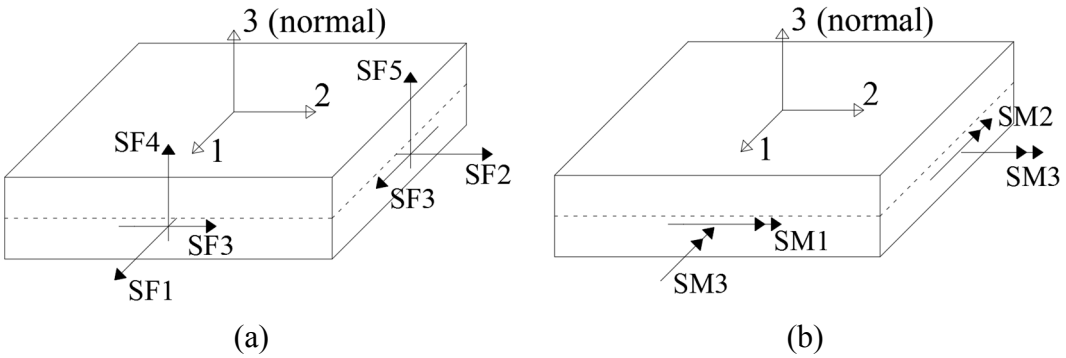

Figure 5.15 Relation of outputs to local coordinate system: (a) Section forces; (b) Section moments.

The different outputs are described in ('Abaqus/CAE User's Manual', 2016) and are as follows:

- SF1 – Direct membrane force per unit width in local 1-direction.
- SF2 – Direct membrane force per unit width in local 2-direction.
- SF3 – Shear membrane force per unit width in local 1-2 plane.
- SF4 – Transverse shear force per unit width in local 1-direction.
- SF5 – Transverse shear force per unit width in local 2-direction.
- SM1 – Bending moment force per unit width about local 2-axis.
- SM2 – Bending moment force per unit width about local 1-axis.
- SM3 – Twisting moment force per unit width in local 1-2 plane.

The SF4 output was studied along two paths. Firstly, one just above the slab openings, path A from the level I analysis, see Figure 5.16(a). Secondly, along a path as shown in Figure 5.16(c), further referred to as path C. The second path was taken at a distance 0.61 m from the centre of the beam, as per recommendations regarding shear near support from (Pacoste et al., 2012), see also Figure 5.7. Path B from the level I analysis, see Figure 5.16(b), was not utilised for the convergence study, but was used for the results when analysing the slab further.

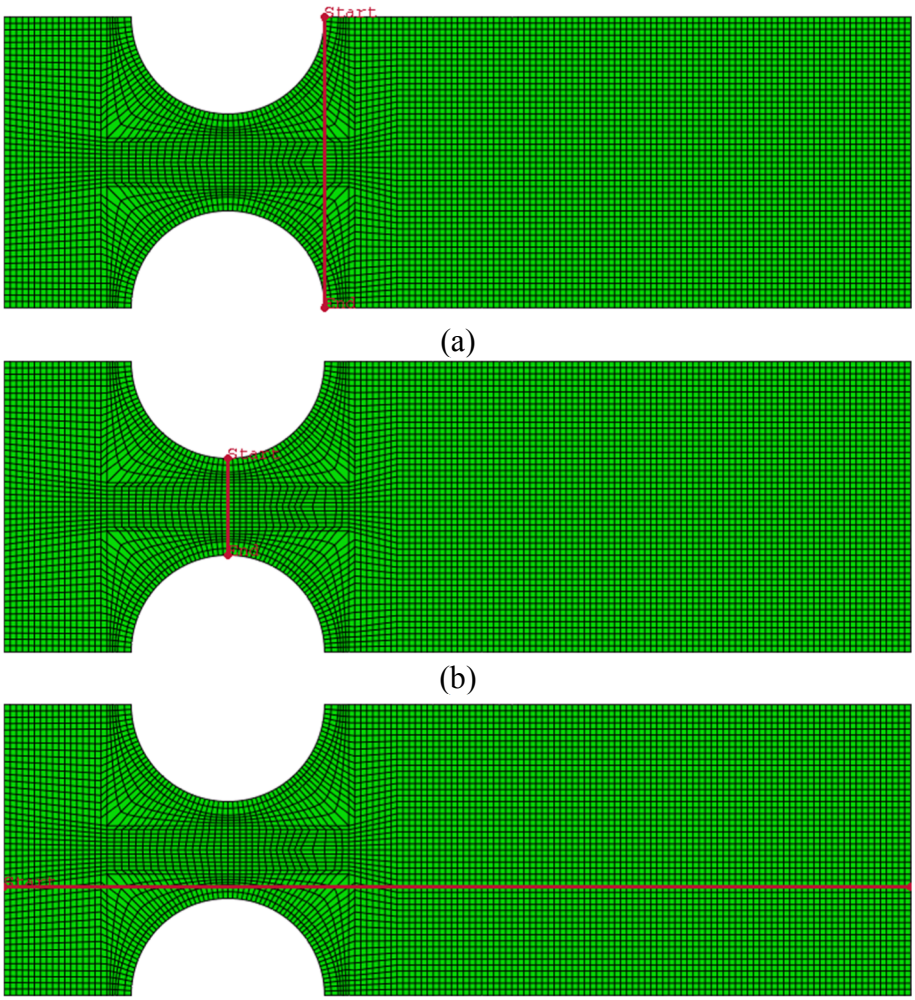

Figure 5.16 Paths used to study the slab: (a) Transversal path above the holes; (b) Transversal path between the holes; (c) Longitudinal path along beam with an offset of 0.61 m.

Six different mesh sizes were compared: 0.5 m, 0.3 m, 0.25 m, 0.1 m, 0.05 m and 0.01 m. After comparing the results shown in Figure 5.17, Figure 5.18 and Figure 5.19 it was concluded that a mesh size 0.1 m should be able to describe the problem well enough, while still keeping the computational demand fairly low. In the convergence study, the distributed load of the silo was set to 200 kN/m^2 and no self-weight of the structure was considered, this was due to previous configurations in the model. However, as only the mesh size was evaluated in this analysis the result would still be accurate.

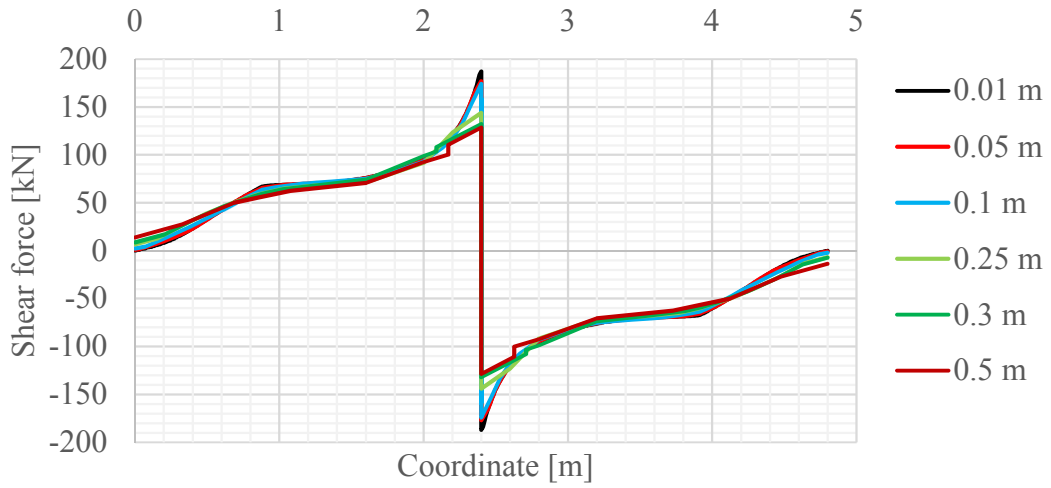

Figure 5.17 Shear force in slab (SF4) along path A.

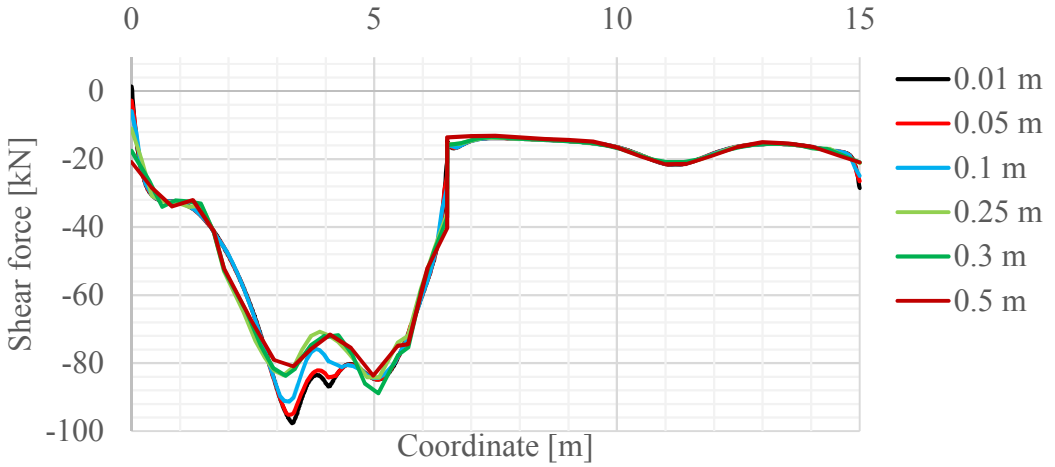

Figure 5.18 Shear force in slab (SF4) along path C.

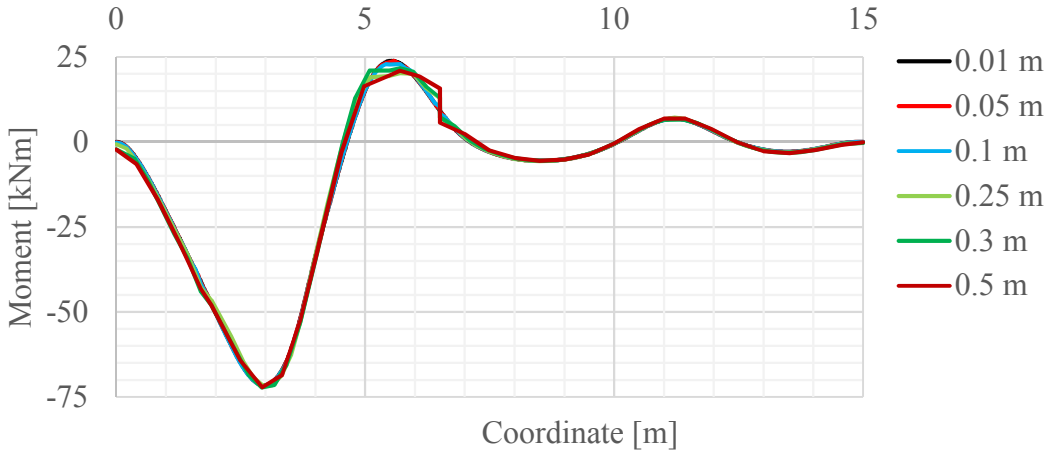

Figure 5.19 Bending moment in slab (SM2) along path C.

For the model with shells and beams, no mesh convergence study was made, since the slab still was modelled as a shell element. No mesh convergence study was conducted for the model with solids either, since this alternative served as a way of confirming the results of the other models. No further model would be used with solid elements and therefore no time was spent on optimizing the model further.

Optimization
In the Optimization module, a task may be performed so to optimize e.g. the topology or geometry of the model. No optimization was configured for any of the alternatives in the case study.

Job
In the Job module, the solution is requested and the analysis is submitted. No specific choices were made in the Job module.

Visualization
In the Visualization module, results from the job are presented.

5.1.2.1 Results and discussion

The goals of the level II analysis were:

i) Studying and comparing the different FE models for obtaining the most trustworthy results
ii) Evaluating the FE analyses of the model with reduced stiffness in an attempt to represent a cracked structure and comparing it to the original model
iii) Analysing the shear load effects in the slab and comparing it with the capacity of the slab

The results that relate to these goals are herein presented. The studied and presented results for the two first alternatives, i.e. the model with shells, with and without reduced stiffness, and the model with shells and beams are given first in this section. For the model with solid elements, which was intended as a reference model for the preceding alternatives, only the deformations were compared.

- Global deformation picture, Figure 5.20. These pictures are meant to represent any possible differences in the overall behaviour of the models. All the models show a similar pattern of deformation.
- Vertical deformation in a path along the centre of the beam, Figure 5.21. As expected, this figure shows that the deformations for the model with reduced stiffness are significantly higher compared with the other models.
- Bending moment in the slab (SM2) along a path above the centre of the beam, Figure 5.22. In this figure it is noted that the shell model represents the bending moment distribution at the supports better than the shell and beam model. The peak moments are avoided in the shells model.
- Shear membrane force along the centre of the beam, Figure 5.23. This figure indicates that the shear distribution in the shell models is higher than the one compared to the beam model.

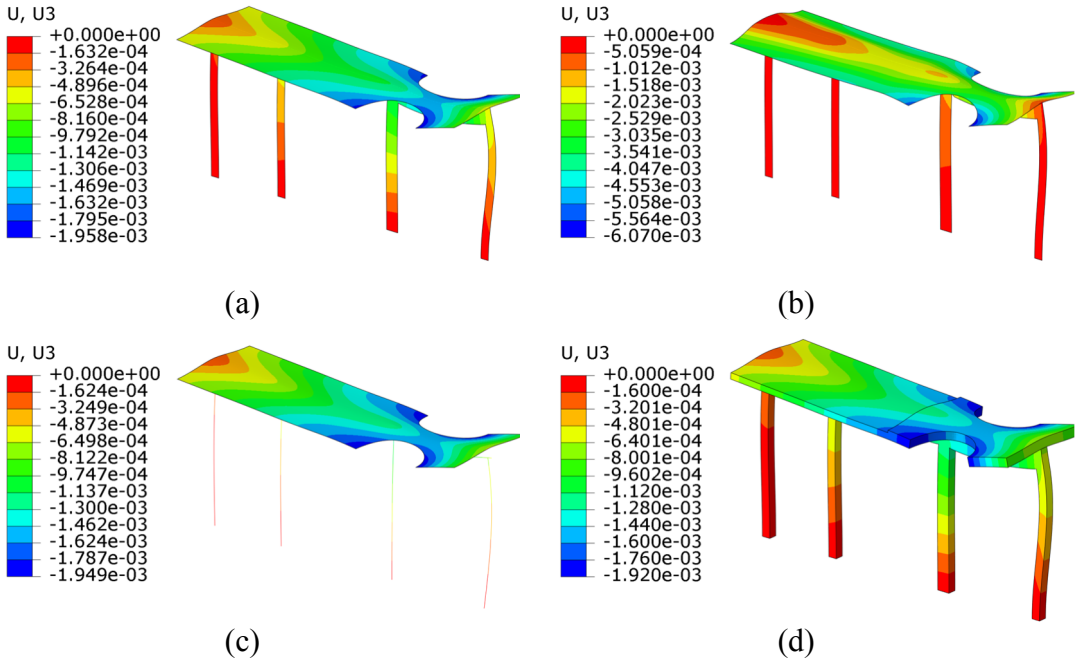

Figure 5.20 Global deformation picture [m] for: (a) Shell model; (b) Shell model with reduced stiffness; (c) Shell and beam mode; (d) Solids.

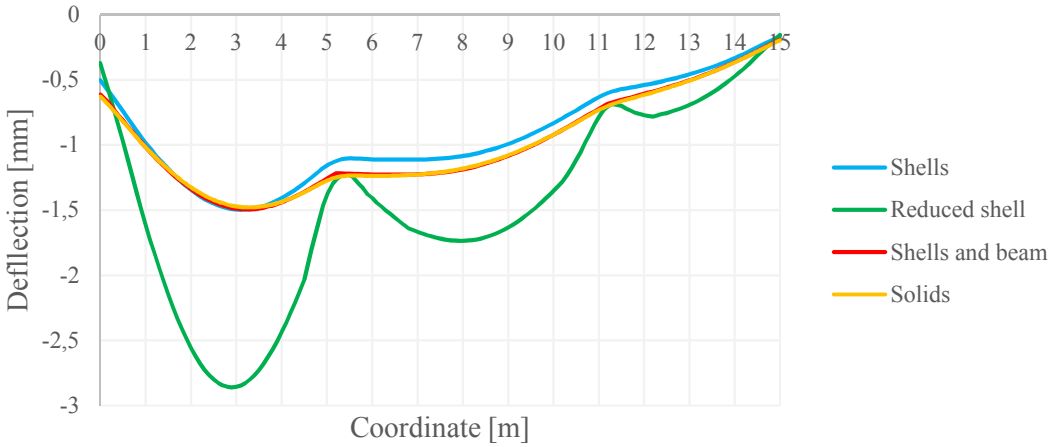

Figure 5.21 Vertical deformation along the centre of the beam.

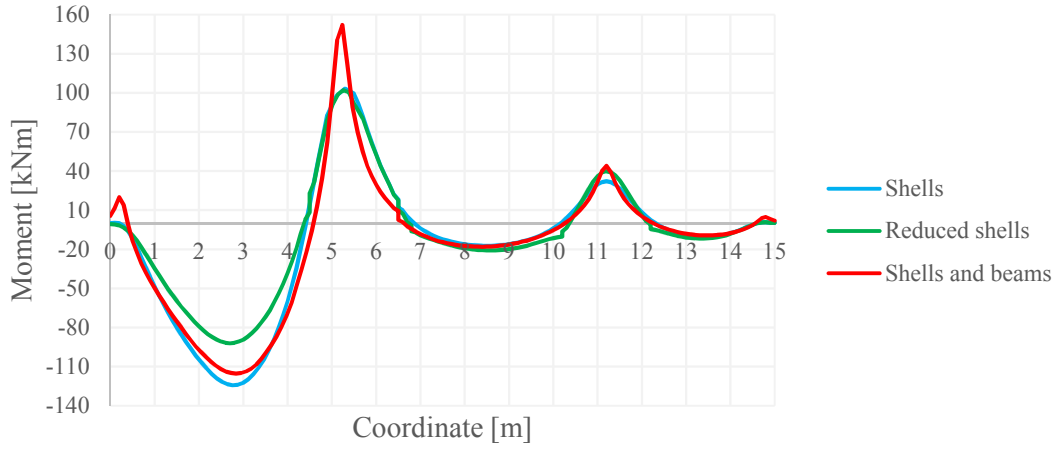

Figure 5.22 Bending moment in the slab above the beam.

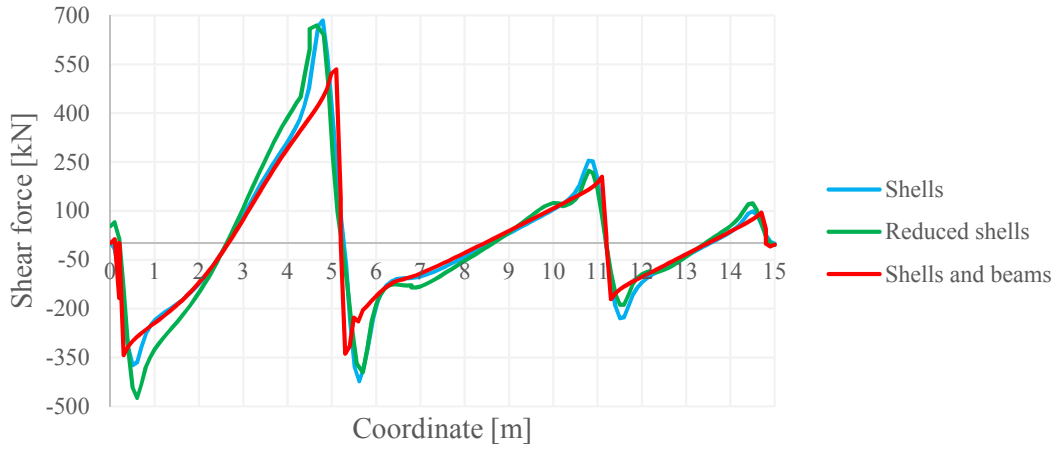

Figure 5.23 Shear membrane force in the beam.

The results and figures presenting global deformation, vertical deformation, bending moment and shear membrane force are meant to display differences and similarities between the different models. The main results of interest for the study, i.e. shear in the slab, are presented next.

Figure 5.24 presents contour plots of the shear flow in the 0.41 m thick slab for all models except the one with solid elements. The results have been limited so that the previously determined shear resistance, of 151 kN in Section 5.1.1, is the maximum value in both positive and negative magnitude. Black and grey colours indicate values exceeding the resistance. The areas that experience shear exceeding the resistance are local areas around the column, as previously mentioned. Therefore, these areas are not decisive for the shear design and can be neglected. In principle, the shear flow of all the models is similar. In order to investigate the differences between the models closer, the shear force is plotted for three paths, namely A, B and C shown in Figure 5.16, in the following figures.

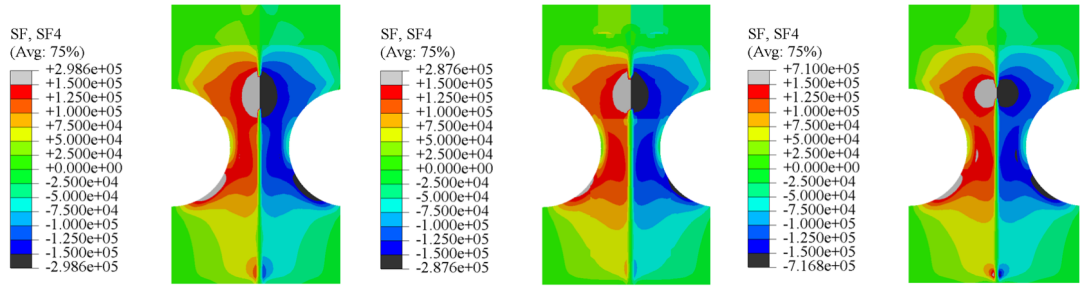

(a) (b) (c)

Figure 5.24 Transverse shear flow in slab [N] for: (a) Shell model; (b) Shell model with reduced stiffness; (c) Shell and beam model.

Transverse shear force in the slab, in the transverse direction of the slab, along path A and transverse shear force in the slab, in the transverse direction of the slab, along path B are shown in Figure 5.25 and Figure 5.26. Additionally, to assess the shear force pattern along the longitudinal direction of the slab, Figure 5.27 presents the transverse shear force in the slab along path C. The results that may be directly compared with the level I analysis are presented in Figure 5.25 and Figure 5.26.

The model of shells and beams displays a trend of higher shear forces in Figure 5.25 compared with the shell models. This can be attributed to the fact that the path is located directly above the column support. It is common that peak load effects are obtained in slabs above columns modelled with beam elements. Therefore, these peak shear forces are not to be relied upon. Figure 5.26 indicates that the shear force distribution is similar for all the models. Peak shear loads are avoided in this path for the shell and beams model, because the beam is an elastic support for the slab.

The shear flow along paths A and B show some differences between the level I and level II analyses. The governing reason for this is the simplicity of the level I calculation model. Specifically, the differences along path A, see Figure 5.25, arise due to the fact that this area is not only subjected to the load along the path itself, but also to load that is distributed from other parts of the slab. I.e. the 3D effects that are taken into account in the FE analysis are neglected in the level I analysis. Along path B, it can be further said that the difference in silo load application explains the difference in shear load pattern along the path. In the level I analysis, the silo loads were applied simply as point loads in the ends of the span, whereas in the FE model, this load was applied as a distributed load on the silo load surfaces. These surfaces had a width of 225 mm, which correspond with the difference between the load patterns. On the whole, the shear load distribution is similar with the hand calculations in path B. This comparison serves as a verification of the FE models.

The reduced shell model shows slight changes compared with the shell model in all the figures. This is due to reduced stiffness in different parts of the slab and the load is expected to be distributed differently, i.e. by finding the stiffest parts in the model. However, the changes are trivial and they can be neglected.

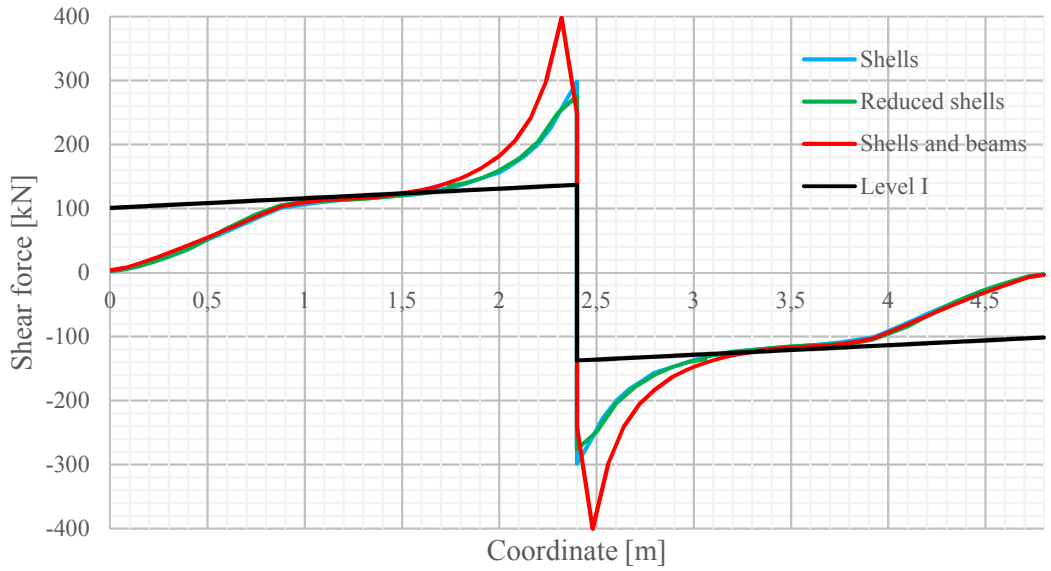

Figure 5.25 Transverse shear force in the slab along path A.

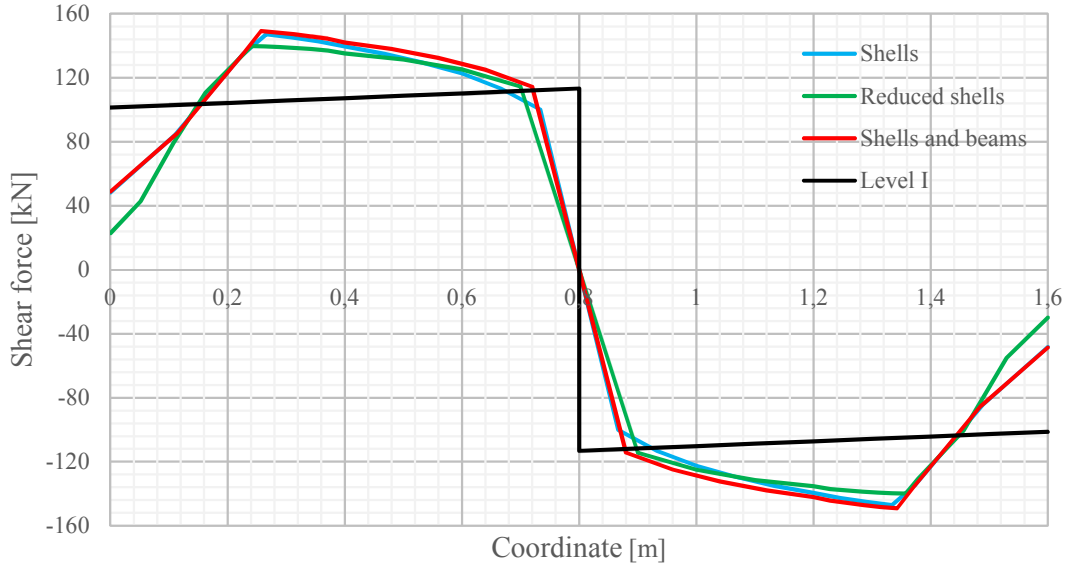

Figure 5.26 Transverse shear force in the slab along path B.

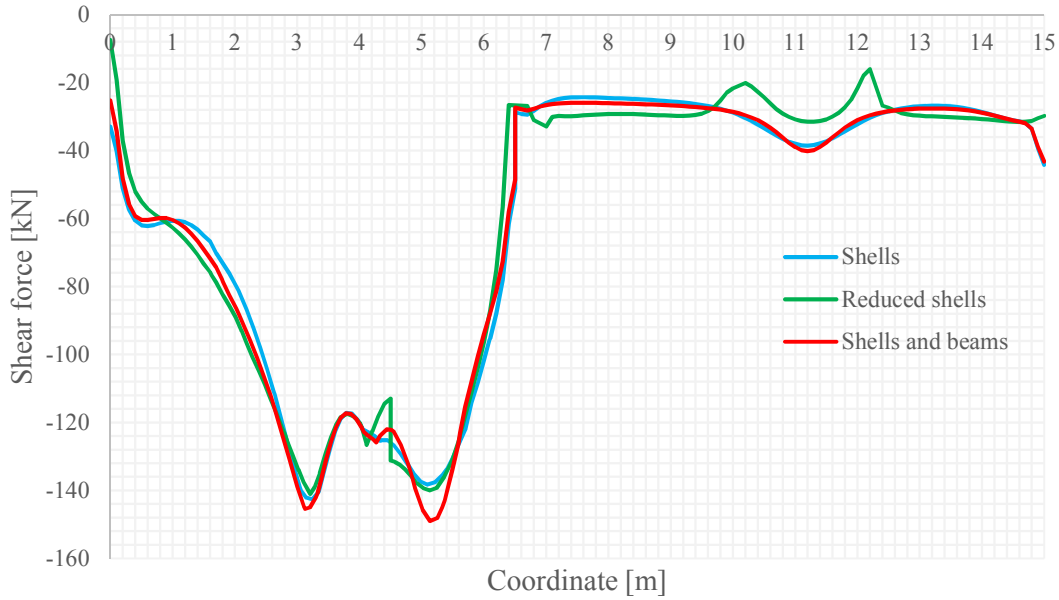

Figure 5.27 Transverse shear force in the slab along path C.

Maximum values of the shear forces in the slab along the studied paths and the vertical deflection in the beam are presented in Table 5.9. Maximum shear force values have been taken at a distance 0.61 m from support (if relevant), as per recommendations from Pacoste et al. (2012).

Table 5.9 Maximum values of shear forces in slab and vertical deflection for the different alternatives.

Alternative	Vertical deformation in beam [mm]	Shear in slab, path A [kN]	Shear in slab, path B [kN]	Shear in slab, path C [kN]
Shells	1.50	136.2	118.9	142.6
Shells with reduced stiffness	2.86	137.9	118.4	141.0
Shells and beams	1.49	146.5	118.6	149.0
Solids	1.48	-	-	-

5.1.2.2 Conclusions for the level II analysis

The overall behaviour of the models is very similar. The model with shells and beams exhibits higher values of shear force and moment in the slab in the positions of the columns, which is quite a common phenomenon. As expected, the shell model with reduced stiffness shows larger deflection but since it does not contain any discrete cracks it does not influence the shear behaviour. Assessments of existing cracked structures by the method presented in this study, i.e. applying reduced stiffness for cracked areas should, therefore, be limited to only the serviceability state as it will not capture differences in the ultimate state.

The model with only shell models shows a better representation of the load effects than the shell and beam model. The high peak load effects above column supports are avoided in the model with only shell elements. Therefore, it was decided to use the model with the same element types for the complete model, i.e. the model with shell elements only, for further analyses in level III. Additionally, the version of ABAQUS used in this study did not support embedded reinforcement for beam elements, which in principle would have made it impossible to incorporate reinforcement in the model if beam elements would have been used.

As for the main concern of the assessment, no shear strengthening is needed according to the level II analysis either. Higher shear loads can be observed in the level II analysis compared to the level I analysis. An example is the maximum shear load of 128 kN in the level I analysis which was observed along path A, see Table 5.3. The corresponding value, i.e. the maximum shear load along path A, in the level II analysis was for the shells model 136 kN, see Table 5.9. However, this was not the total maximum shear load value in the level II analysis. Instead, the maximum shear load was for the shells model 143 kN, found along path C which was not studied in the level I analysis. Still, this shear load was lower than the shear capacity of the slab, which was estimated to 151 kN.

Furthermore, an observation made when analysing the results of the level II analysis was that the parts of the slab that are not in the vicinity of the slab openings, i.e. the thin slab part, noticed only small stresses and strains. As a consequence of this, further observations, in terms of studied results and behaviour, were concentrated to the thick slab part.

As previously mentioned, a level II analysis is a common practice today and the conclusion from the level II analysis in this study agrees with the conclusion from the level I analysis, that no shear strengthening was needed. A level III analysis was performed as well, which served both as a more detailed assessment of the case study as well as an evaluating measure of the common practice that is the level II assessment.

5.1.3 Level III analysis

The level III analysis consisted of 3D non-linear FE-analyses, as described in Section 4.5.3. This model can capture only the bending failure of the slab and not the shear failure. However, the redistribution of the shear forces due to cracking is expected to be represented more accurately in this model. Therefore, the shear load effects in the slab are obtained from the analysis for the load combination of interest and are compared to calculated resistances in accordance with the analytical model defined in Section 4.5.1. The calculated capacities are presented in Section 5.1.1 and Appendix C. As stated in the conclusions for the level II analysis, the model with shell elements was used for the further analyses.

Two separate analyses were made:
1) a displacement-controlled analysis up to failure
2) a load-controlled analysis for the load of interest in order to capture the shear flow at the exact load of interest

The displacement-controlled analysis was made in order to assess the failure load and the behaviour of the structure up until failure. More specifically, the three concrete

states, previously described in Section 2.1, were searched. The load-controlled analysis was the analysis used to obtain results comparable with the previous levels of assessment, and was in that sense referred to as the main level III analysis.

For a non-linear analysis, reinforcement has to be considered in the model and non-linear material properties must be included. It is also recommended to apply the load stepwise in order to provide stability for the calculations. The direct changes compared to the linear-elastic model were made in the following modules:

- Property
    - Partitioning the model based on reinforcement layout
    - Assigning non-linear material models
- Step
    - Dividing the load process into several steps
- Interaction
    - Defining the displacement-controlled load
- Load
    - Defining the displacement-controlled load

Reinforcement

Based on the provided drawings of the industrial building, a reinforcement layout as presented in Appendix B was defined for the slab. The bottom reinforcement had four different spreadlines in the transversal direction and two in the longitudinal direction. The top reinforcement in the transversal direction of the slab was concentrated to the support regions, i.e. above the beam, and had five different spreadlines.

The beam and column reinforcement was implemented according to Appendix B. In addition to the continuous top and bottom reinforcement in the beam, bars were placed in the bottom in the spans and in the top above the columns.

In ABAQUS, reinforcement in shell elements can be included with “Rebar Layers”, when defining the slab sections in the Property module. In this setting the material, cross-sectional area per bar, spacing, orientation angle and offset from the middle of the cross-section in thickness direction are defined for each rebar layer in the section. All parts were partitioned with regard to the reinforcement layout, in order to assign the appropriate reinforcement parameters to the corresponding region. As the slab was modelled as continuous over the beam, the top beam reinforcement was included in the relevant slab regions. The slab was divided into three main regions in the longitudinal direction, see Figure 5.28:

- Field region
- Support region without beam reinforcement
- Support region with beam reinforcement

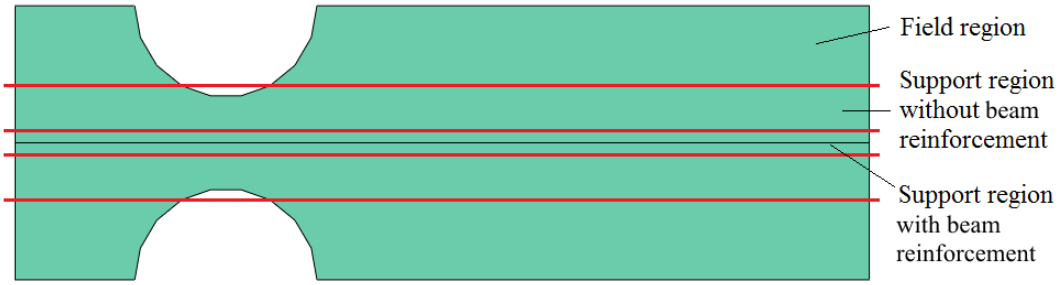

Figure 5.28 Three main regions of slab in longitudinal direction, partitions indicated by red line.

The field regions were then further partitioned into four parts in the transversal direction, corresponding to the different bottom reinforcement spreadlines. The support regions, both including and not including beam reinforcement, were partitioned into five parts in the transversal direction, corresponding to the different top reinforcement spreadlines. Furthermore, the regions including beam reinforcement were partitioned in accordance with the top beam reinforcement layout. All slab partitions corresponding to the reinforcement configurations are presented in Figure 5.29 and Table 5.10. Partitions around slab openings were moved a distance of 10 mm, corresponding to one element height, from the opening to avoid distorted elements in the mesh.

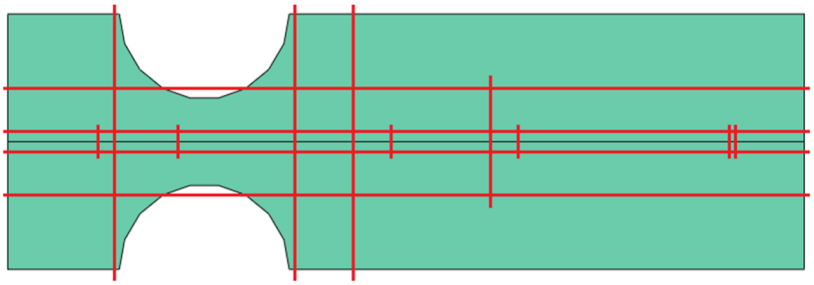

Figure 5.29 All different regions of slab with regard to reinforcement, partitions indicated by red line.

Table 5.10 Slab reinforcement configuration for different regions, positional references of sub regions refer to Figure 5.29 and are counting upwards from left to right.

Main region	Sub region		Bottom transversal	Bottom longitudinal	Top transversal	Top longitudinal
Slab 0.41 m, field	Left of openings		ø12s175	ø12s250	-	-
	Between openings		ø12s250	ø12s250	-	-
	Right of openings		ø12s200	ø12s250	-	-
Slab 0.41 m, support	Left of openings		ø12s175	ø12s250	ø16s150	-
	Between openings		ø12s250	ø12s250	ø12s250	-
	Right of openings		ø12s200	ø12s250	ø16s150	-
Slab 0.41 m, support with beam	Left of openings	1	ø12s175	ø12s250	ø16s150	4ø16
		2	ø12s175	ø12s250	ø16s150	2ø16
	Right of openings	1	ø12s250	ø12s250	ø16s250	2ø16
		2	ø12s250	ø12s250	ø16s250	6ø16+2ø20
	Between openings		ø12s200	ø12s250	ø16s150	6ø16+2ø20
Slab 0.3 m, field	-		ø12s350	ø12s350	-	-
Slab 0.3 m, support	1		ø12s350	ø12s350	ø12s350	-
	2		ø12s350	ø12s350	ø16s300	-
Slab 0.3 m, support with beam	1	1	ø12s350	ø12s350	ø12s350	6ø16+2ø20
		2	ø12s350	ø12s350	ø12s350	2ø16
	2	1	ø12s350	ø12s350	ø12s300	2ø16
		2	ø12s350	ø12s350	ø12s300	6ø16
		3	ø12s350	ø12s350	ø12s300	2ø16
		4	ø12s350	ø12s350	ø12s300	

When using shell elements to model a beam, offsets in the thickness direction will result in surface reinforcement as opposed to main reinforcement. To get around this, partitions as displayed in Figure5.30, were made. First, a partition was made corresponding to the centre line of the main bottom reinforcement, see Figure5.30(a), for which several rebar layers with different offsets were defined. The lower beam partition was then further partitioned in regions depending on amount of reinforcement, see Figure5.30(b). All beam regions were modelled to have vertical reinforcement through the middle, corresponding to stirrups.

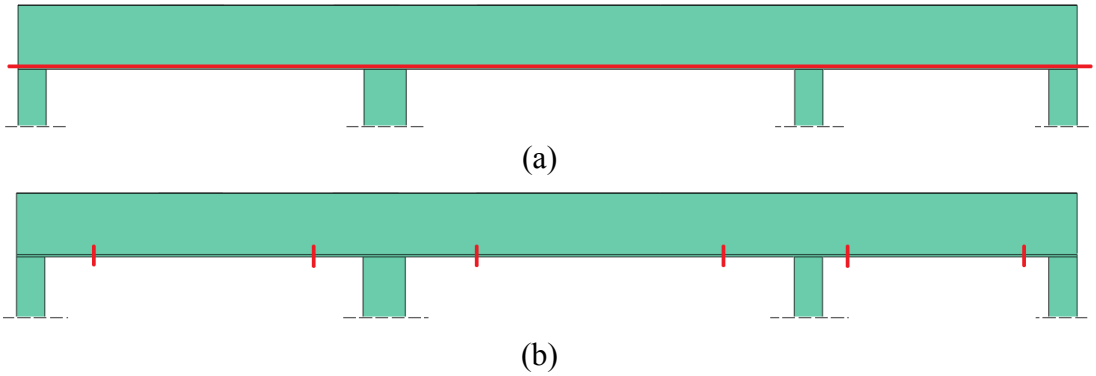

Figure5.30 Partitions of beam indicated by red line: (a) Main partition; (b) Sub-partitions.

Non-linear material models

The concrete material model was assigned to non-linear. The concrete non-linearity may be described by either a concrete damaged plasticity (CDP) model or a concrete smeared cracking (CSC) model in ABAQUS. The CDP model was chosen for the analyses, as the CSC model could not be implemented into a shell model with different material orientations, which was a necessity in this case to model the reinforcement correctly. The CDP parameters were chosen in accordance with Model Code 2010 ('Model Code 2010', 2013) and the plasticity parameters were defined with values presented in Table 5.11.

Table 5.11 CDP plasticity parameters.

Dilation angle	30
Eccentricity	0.1
f_{b0}/f_{c0}	1.16
K	0
Viscosity parameter	0.0001

All parameters were default values except the viscosity parameter, which was determined with a sensitivity analysis in the displacement controlled loading analysis. The viscosity parameter is used for visco-plastic regularization of the concrete constitutive equations in the analysis ('Abaqus/CAE User's Manual', 2016). A smaller value of this parameter provides stability to the analysis, but also results in an increased computational demand. Five different values of the parameter were compared by evaluating their influence on the load-displacement behaviour of the distributed silo load, see Figure 5.31. In this evaluation, no great differences were observed apart from how long the analyses were able to continue. As no need for stability was needed past the load value used in the real analysis, it was determined that 0.0001 would be a sufficient value.

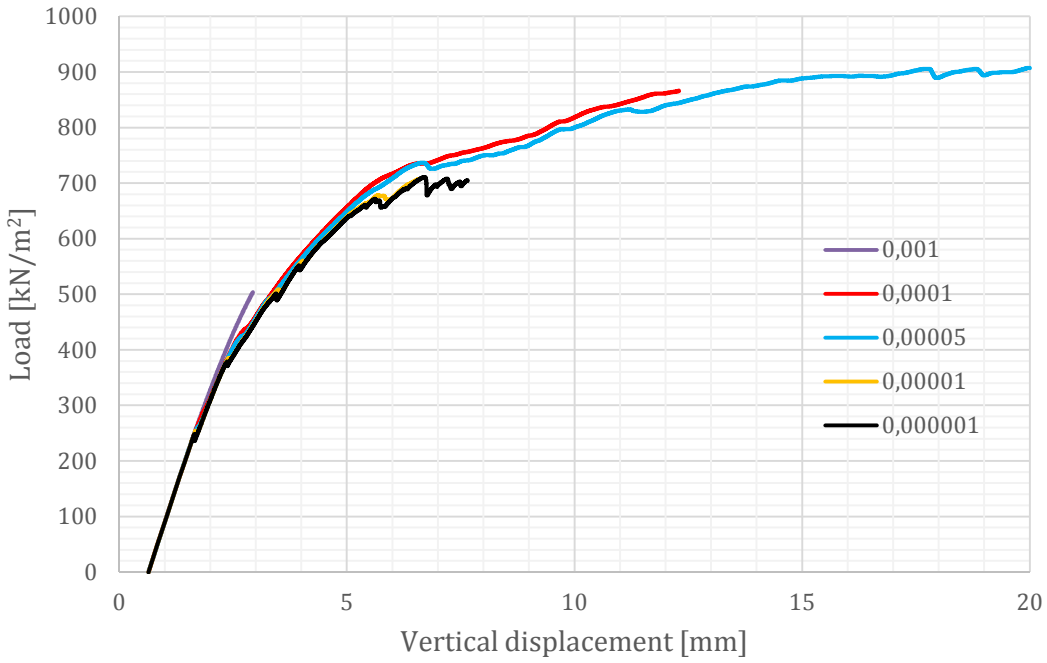

Figure 5.31 Load-displacement curves for different values of the viscosity parameter. Load values represent distributed load from the silos.

Further, the compressive behaviour was described by the stress-strain curve shown in Figure 5.32, and the tensile behaviour was defined with a yield stress of 2.6 MPa and a fracture energy of 68.5 Nm/m^2. The fracture energy was set to half the value determined from Model Code (2010), according to the standard procedure at Concrete Structures in the Division of Structural Engineering at Chalmers. Additionally, this provided more reasonable results regarding the cracking load of the structure.

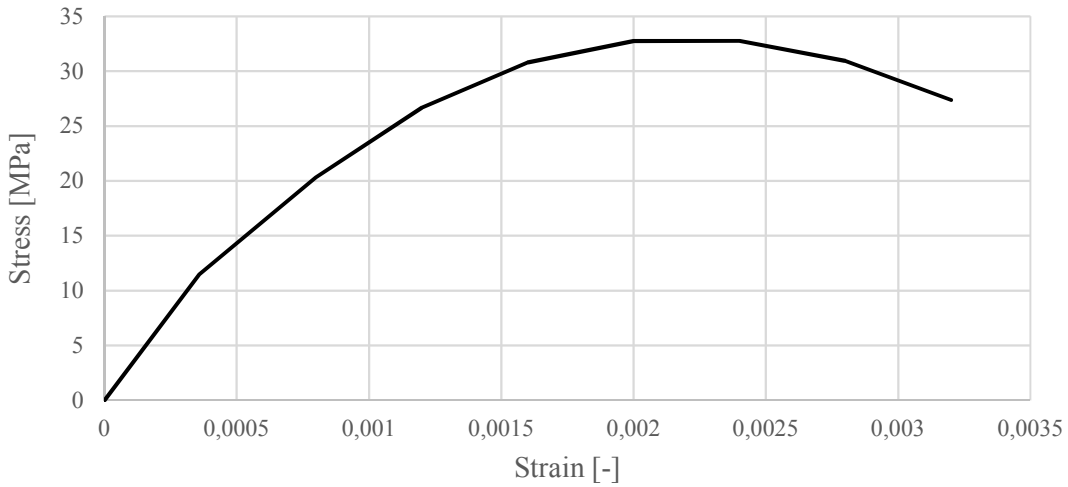

Figure 5.32 Stress-strain relationship for the concrete used in the level III analysis.

Additionaly, steel was defined with an elastic-ideally plastic behaviour with a yield stress of 500 MPa, see Figure 5.33.

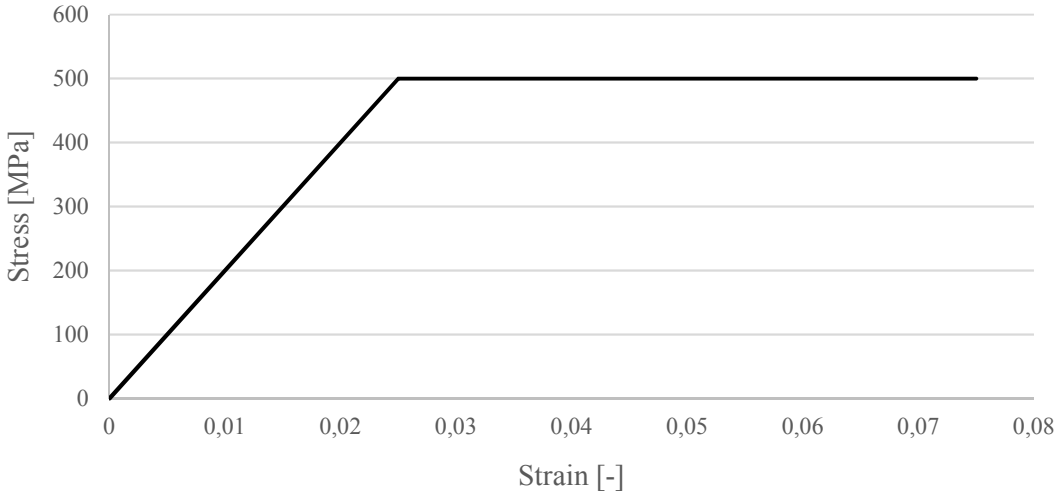

Figure 5.33 Stress-strain relationship for the steel used in the level III analysis.

Stepwise load application

To provide stability to the analysis, load applications were separated into different steps, so that the loads are applied one at a time rather than all at once. The used load application scheme can be seen in Table 5.12, which was implemented in the Step and Load modules of ABAQUS.

Table 5.12 Load application for non-linear analysis.

Load	Step 1	Step 2	Step 3	Step 4
Self-weight	Created	Propagated	Propagated	Propagated
Distributed loads slabs	-	Created	Propagated	Propagated
Self-weight silos	-	-	Created	Propagated
Distributed load silos	-	-	-	Created

Displacement-controlled loading

So far, all analyses had been load-controlled, i.e. a set load is applied and the arising effects due to this load are evaluated. However, in a displacement-controlled analysis, instead of a set load, a certain displacement is prescribed in the model, for which the effects may then be evaluated, including what load this displacement would yield. Thus, the potential of studying the behaviour of the model as it goes to failure is made possible.

For the displacement-controlled analysis, a reference point was created with a prescribed deformation of 20 mm in the negative vertical direction. It was created as a boundary condition in the Load module. Further, in the Interaction module, the reference point's deformation was tied to the outer edges of the silo load surfaces with an equation constraint. In practice, this means that 20 mm negative deformation was applied to the silo load surface's edge, which replaced the distributed silo load, see Figure 5.34. The rest of the loads were applied as they were in the previous load-controlled analysis.

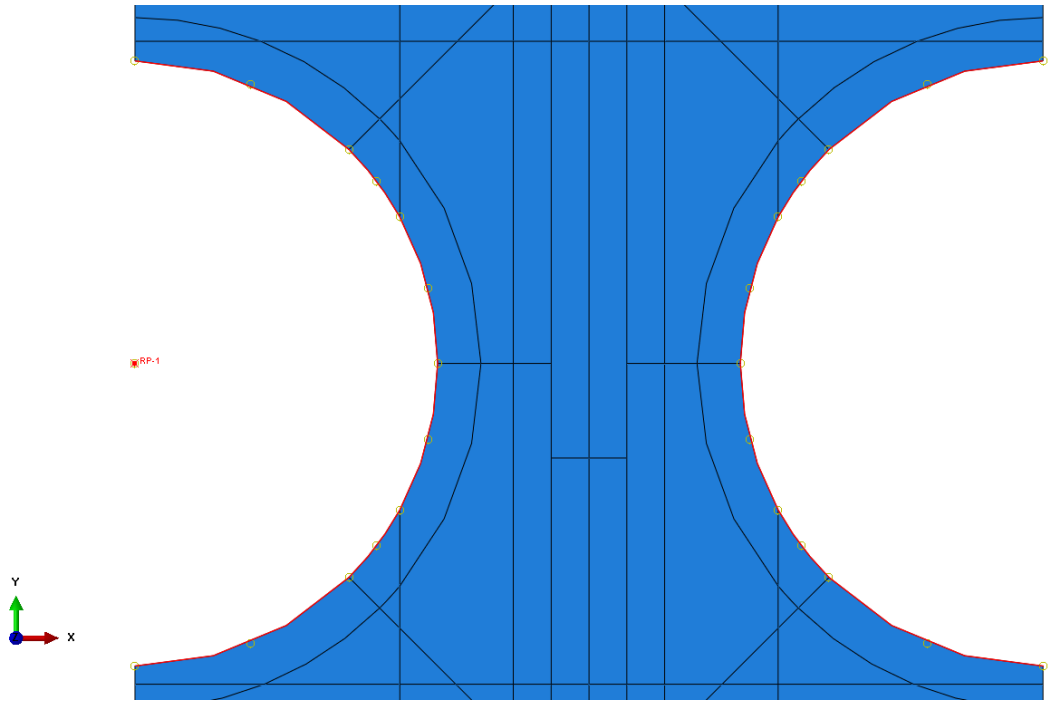

Figure 5.34 Edges (marked in red) that were prescribed a vertical deformation.

5.1.3.1 Results and discussion

Since two separate non-linear analyses were made, two separate result sections are presented. The displacement-controlled analysis served to describe the behaviour of the structure when loaded to failure. It was meant to give an understanding of how the structure behaves in different stages of its lifetime. The regular level III analysis served as a comparison against the linear elastic analysis, the level II analysis. As such, the results obtained in the level III analysis were compared against the results from the level II analysis, to identify possible differences between linear and non-linear analyses for this type of cases. The level III analysis was also compared against the hand-calculated shear capacity, determined in level I, which together with the moment capacity is presented in Table 5.13. The moment capacity of the slab in the two main directions had previously been determined, by ÅF. The moment calculated for the transversal direction of the slab in the field has been used as a general moment capacity in this study. This was chosen for simplicity reasons, as shear is the main topic of interest.

Table 5.13 Shear and moment capacity according to level I analysis.

Slab thickness [m]	Shear capacity [kN]	Moment capacity [kNm]
0.41	151	105
0.3	120	75

<u>Displacement-controlled analysis</u>
The displacement-controlled analysis was meant to give an understanding of the behaviour of the structure up until failure. An objective was to present the three different concrete states, described in Section 2.1, which are defined as:

- State I concrete, which is uncracked

- State II concrete, which starts as soon as the first crack appears
- State III concrete, which begins when the structure is fully cracked and the first reinforcement bar start to yield

This behaviour is commonly described with a load-displacement curve, which can be seen in Figure 5.35. The load has been extracted by dividing the reaction force on the reference point, which was prescribed as a displacement, by the silo loading areas. This will further be referred to as the load in this section. In Figure 5.34, the load-displacement curve of the linear elastic analysis (level II analysis) is also presented.

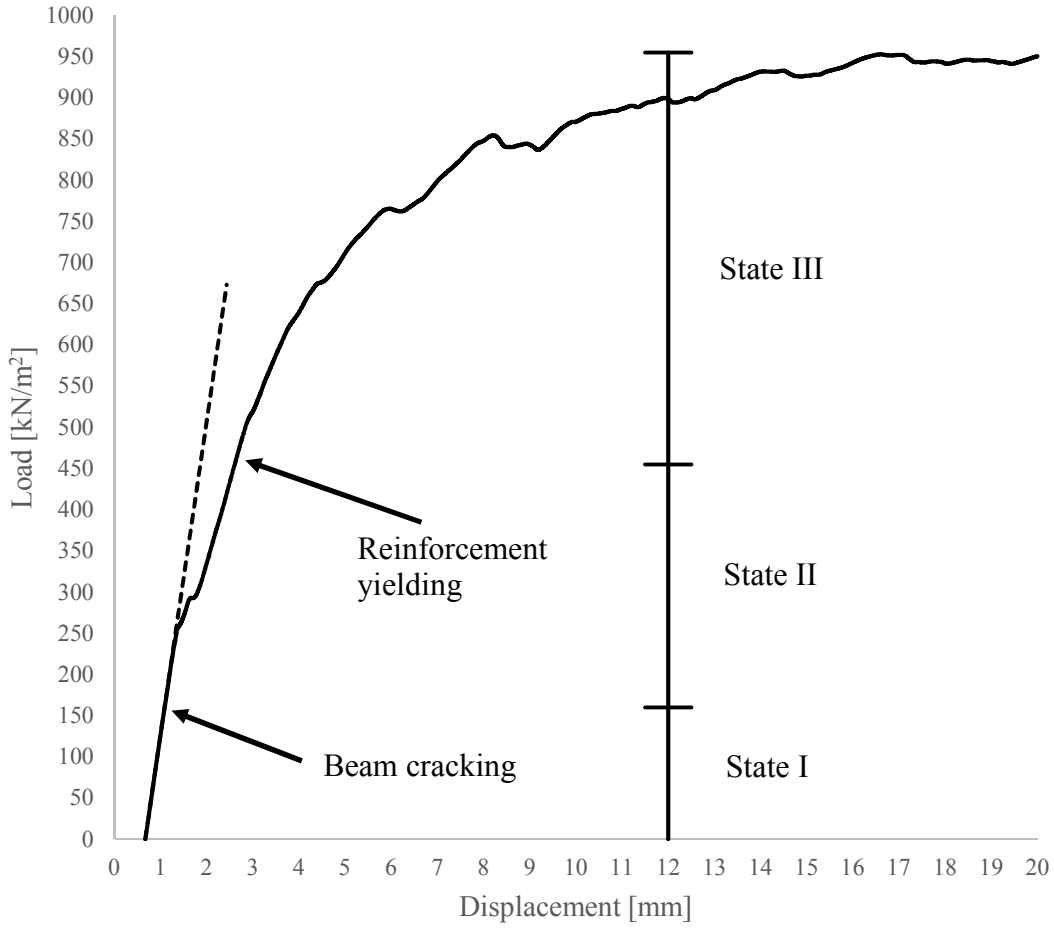

Figure 5.35 Load-displacement curve of silo load surfaces.

The reason for the load-displacement curve not starting at a displacement of 0 mm is because all the loads except the silo distributed load, which is the variable in this study, are already applied at an earlier step. When studying the load-displacement curve, presented in Figure 5.35, the structure appears to be entering state II at a load level of around 250 kN/m^2. However, when studying the strains in the beam more thoroughly, which can be seen in Figure 5.36, it can be seen that a first crack seems to appear between a load level of 150 to 170 kN/m^2. Figure 5.36 presents the tensile strains in the beam in the horizontal direction (i.e. the length direction of the beam, E22). The grey colour represents cracked concrete, as the maximum strain limit in the graphs was chosen to the tensile strain capacity of the concrete, which was determined to roughly 0.0001. The minimum strain limit in the graphs was 0, thus no compressive strains were shown, which means that black colour indicates compressive strains.

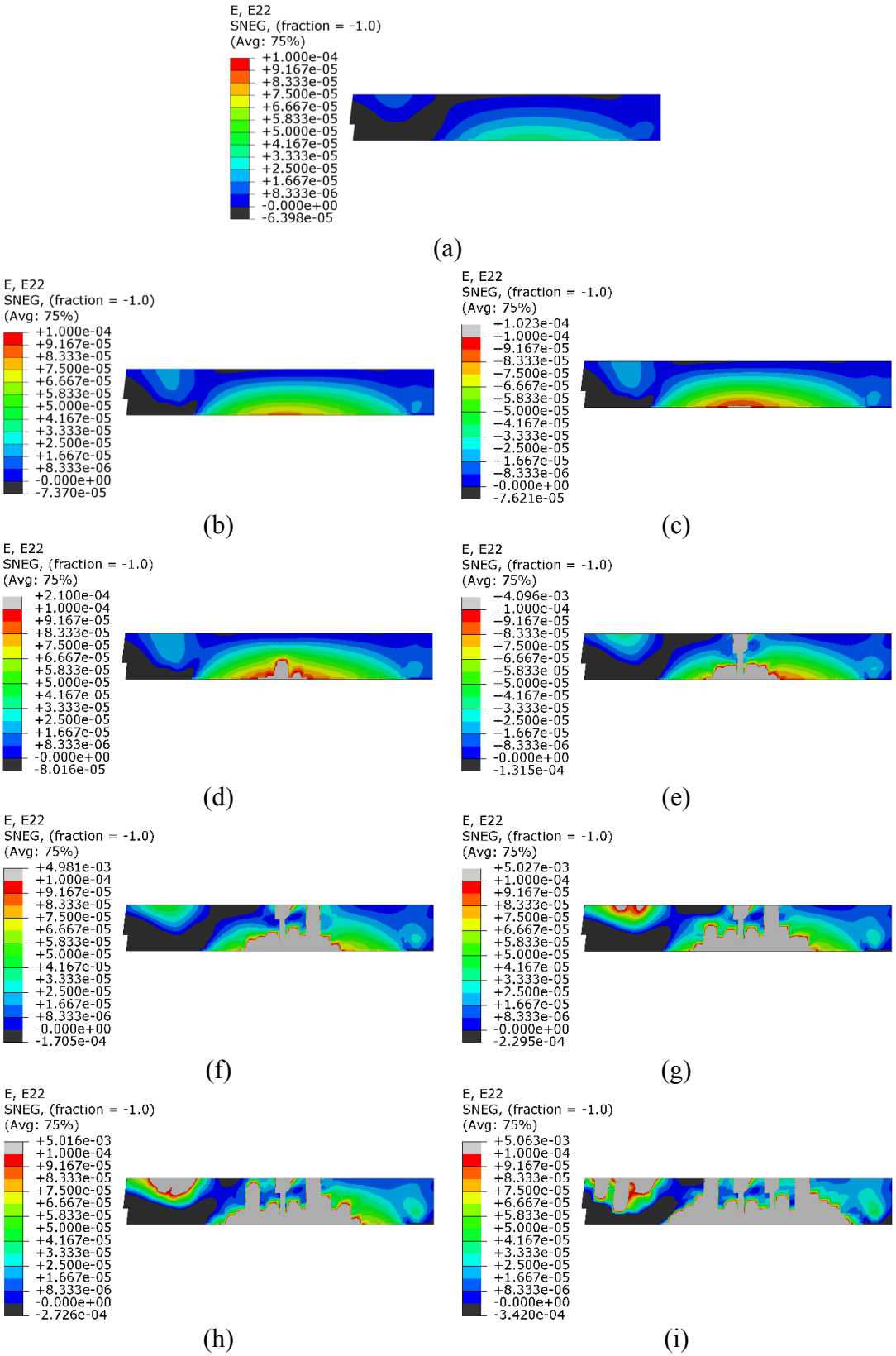

Figure 5.36 Strains in horizontal direction of the beam for load levels: (a) 0 kN/m^2; (b) 150 kN/m^2; (c) 170 kN/m^2; (d) 250 kN/m^2; (e) 400 kN/m^2; (f) 525 kN/m^2; (g) 625 kN/m; (h) 670 kN/m^2; (i) 760 kN/m^2.

In the load-displacement curve, this is only visible, when studying an enhanced part of the curve together with a comparison to the linear elastic behaviour, see Figure 5.45.

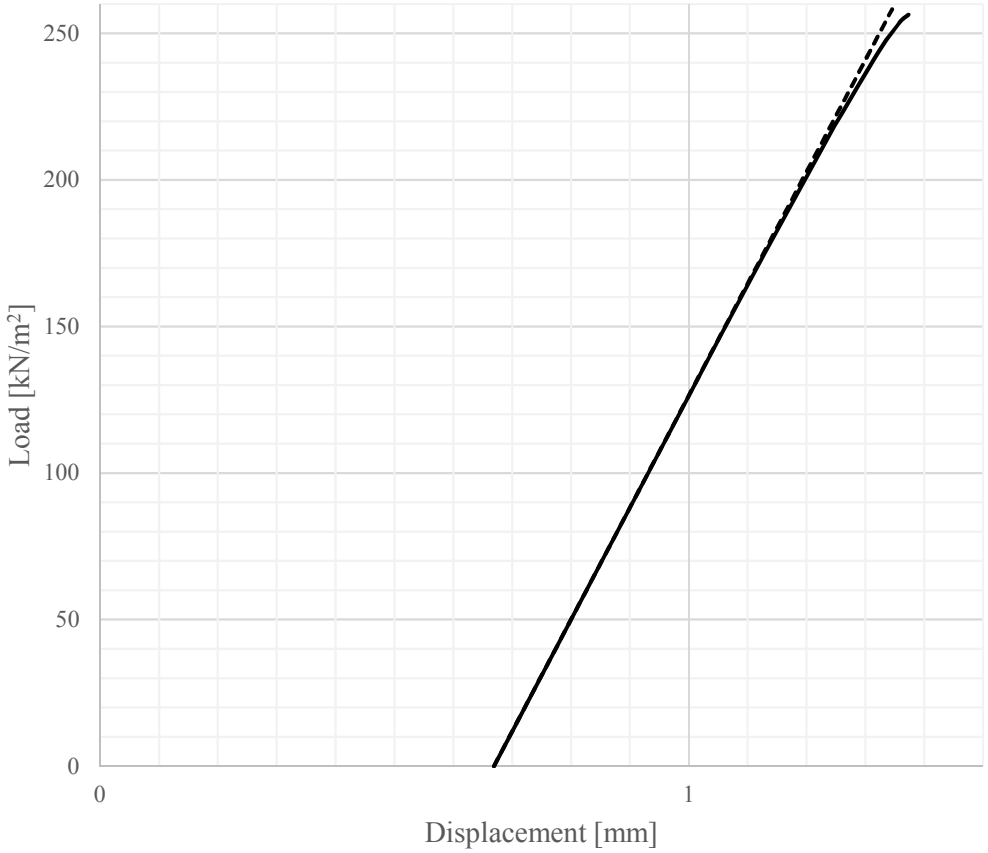

Figure 5.37 Load-displacement curve focused on the part up until 250 kN/m^2 load level with a dashed line representing the linear elastic behaviour (state I concrete).

Cracking of the beam becomes significant at a load level of 250 kN/m^2 according to Figure 5.35, this corresponds to the stiffness drops in the same figure. The moment capacity in the field of the slab appears to be reached at a load level of 400 kN/m^2. Figure 5.38 and Figure 5.39 both present contour plots of the bending moment in the 0.41 m slab for different load levels. The left column presents the bending moment around an axis in the longitudinal direction of the slab (SM1) and the right column presents bending moment around an axis in the transversal direction of the slab (SM2). The results have been limited so that the previously determined moment resistance is the maximum value in both positive and negative magnitude. Black and grey colours indicate values exceeding the resistance. However, the resistance for SM1 is not true and therefore, the left columns of Figure 5.38 and Figure 5.39 should only be used as indications of the moment distribution. The reason for this being that previous hand-calculations of the moment capacity in this direction underestimate the actual capacity due to it having simplifications of the geometry. As previously stated, bending moment failure is captured in the model.

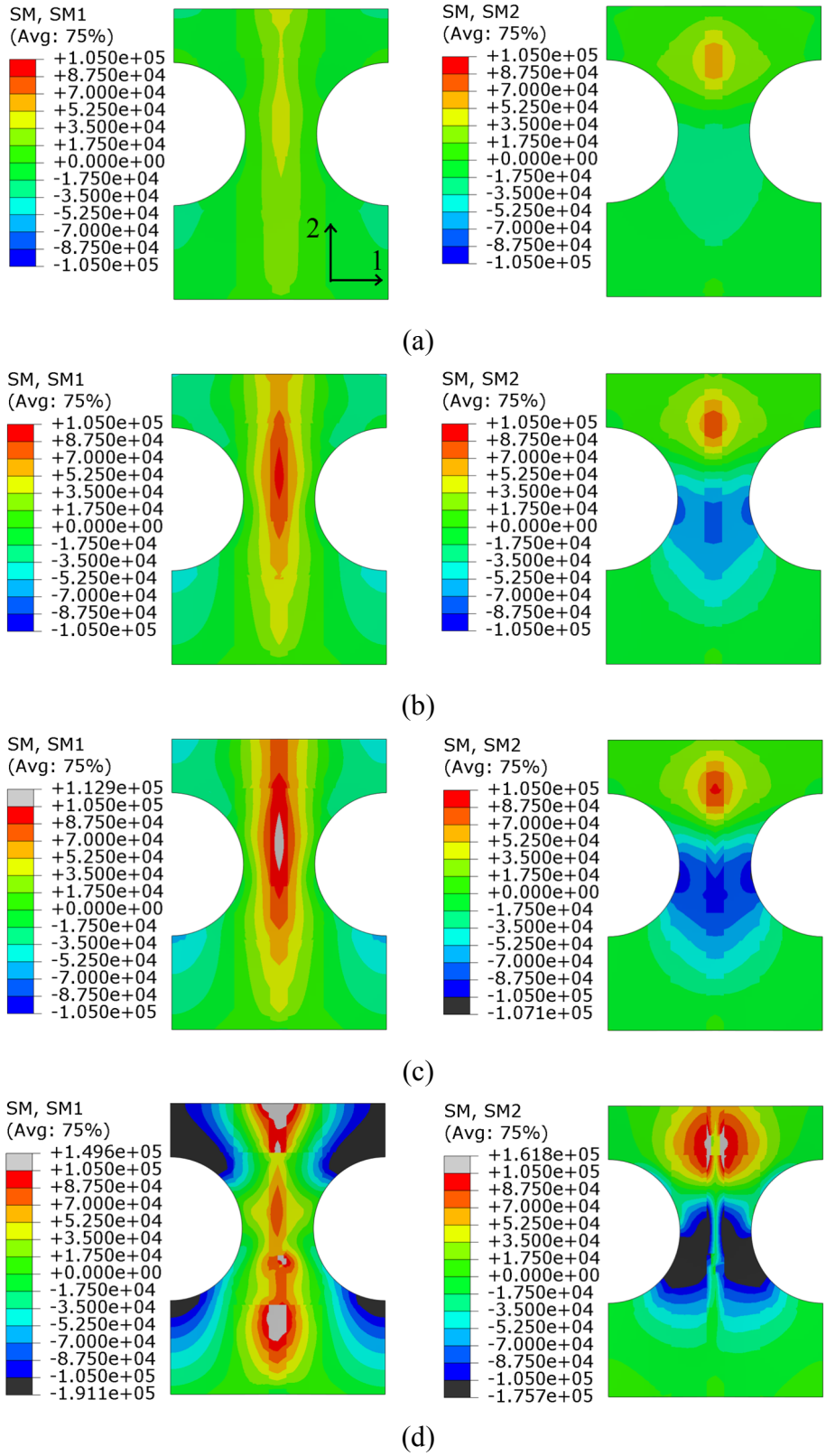

Figure 5.38 Bending moment in the thick slab [Nm] for load levels: (a) 0 kN/m^2; (b) 150 kN/m^2; (c) 250 kN/m^2; (d) 400 kN/m^2. Limits were chosen according to the previously determined resistance.

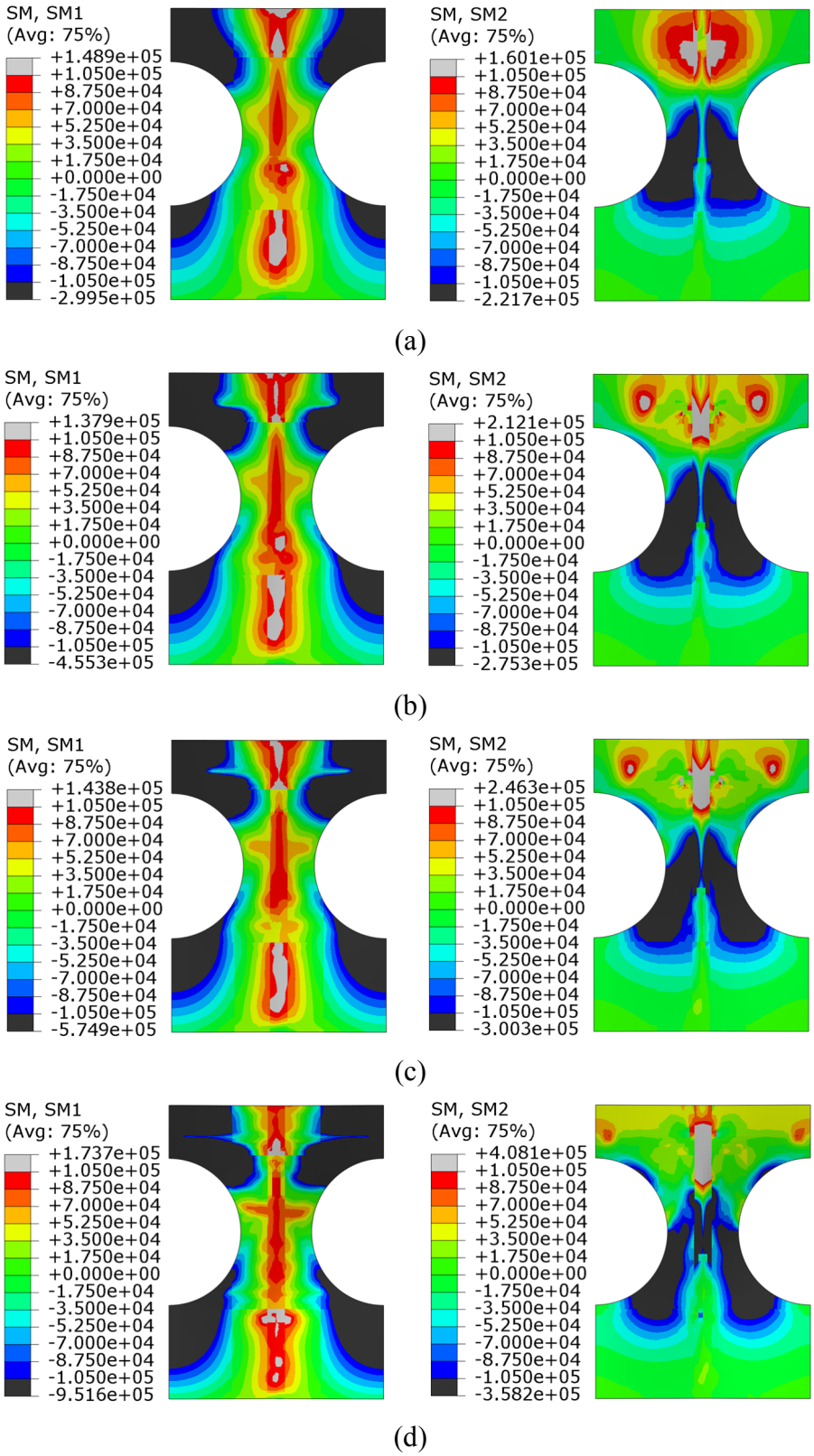

Figure 5.39 Bending moment in the thick [Nm] for load levels: (a) 525 kN/m^2; (b) 625 kN/m^2; (c) 670 kN/m^2; (d) 760 kN/m^2.

To get an indication of the cracking in the structure, the tensile strains have been studied. Figure 5.40 and Figure 5.41 present contour plots of the tensile strains in the bottom of the thick slab for different load levels. The left columns present strain in the transversal direction of the slab (E11), the middle columns present strain in the longitudinal direction of the slab (E22) and the right columns present the maximum in-plane principal strain, i.e. the combination of both E11 and E22. Figure 5.42 and Figure 5.43 show the respective strains in the top, instead of the bottom, of the thick slab. The limits were chosen so that the minimum was 0, thus no compressive strains were shown, which means that black colour indicate compressive strains. The maximum limit was chosen to the tensile strain capacity of the concrete, which was determined to roughly 0.0001. Grey colour thus indicates cracked concrete.

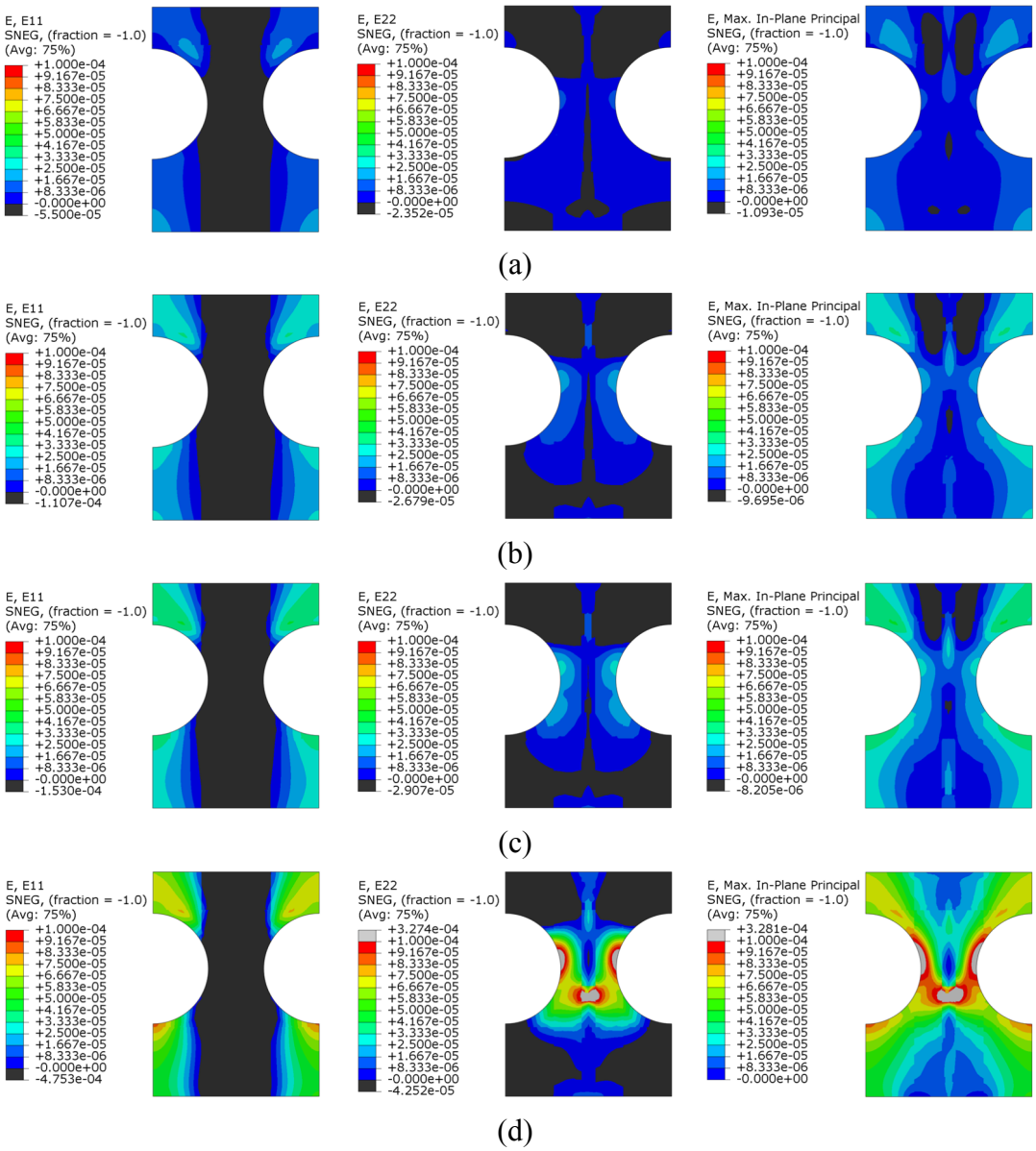

Figure 5.40 Strains in the bottom of the thick slab for load levels: (a) 0 kN/m^2; (b) 150 kN/m^2; (c) 250 kN/m^2; (d) 400 kN/m^2.

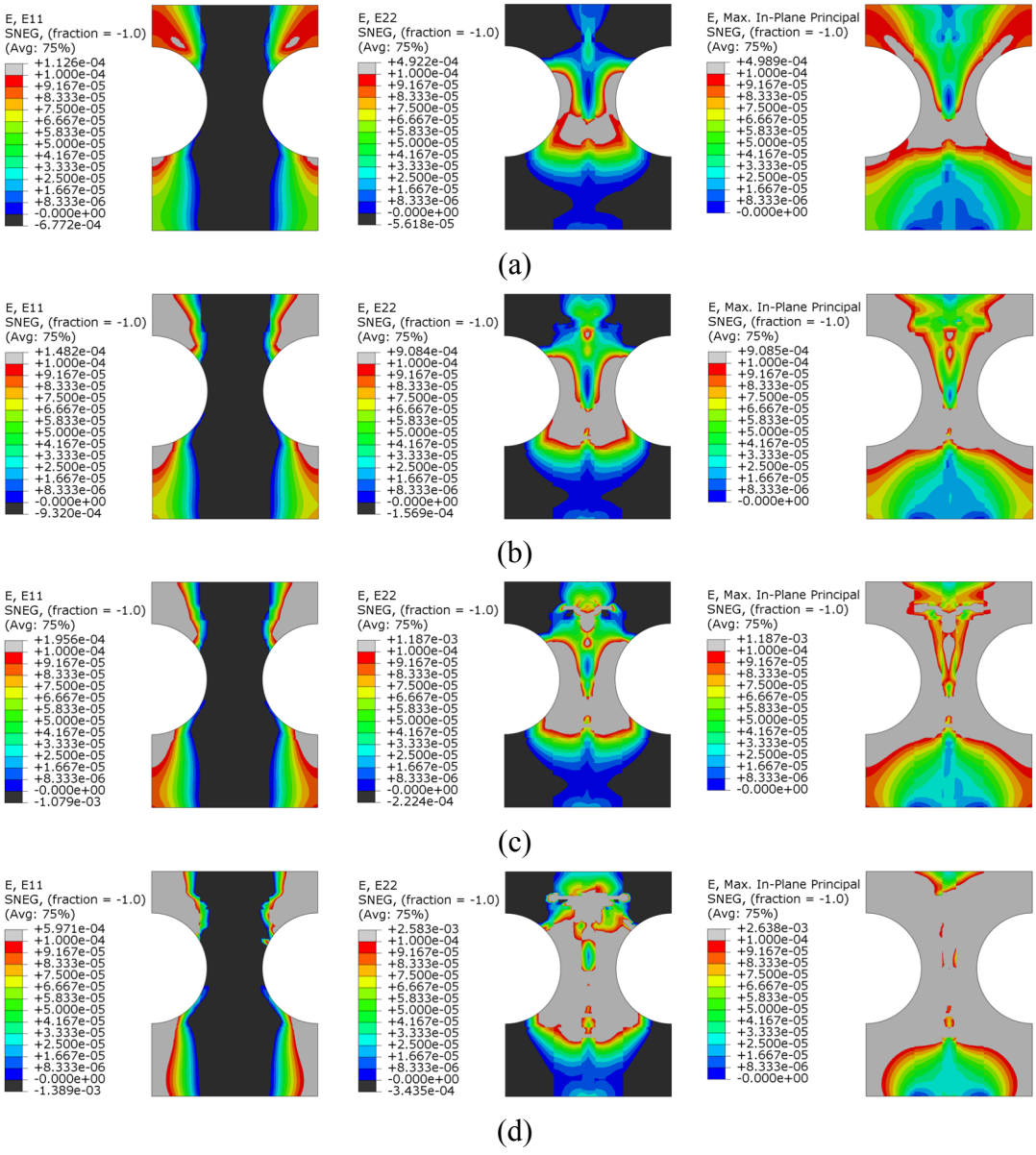

Figure 5.41 Strains in the bottom of the thick slab for load levels: (a) 525 kN/m^2; (b) 625 kN/m^2; (c) 670 kN/m^2; (d) 760 kN/m^2.

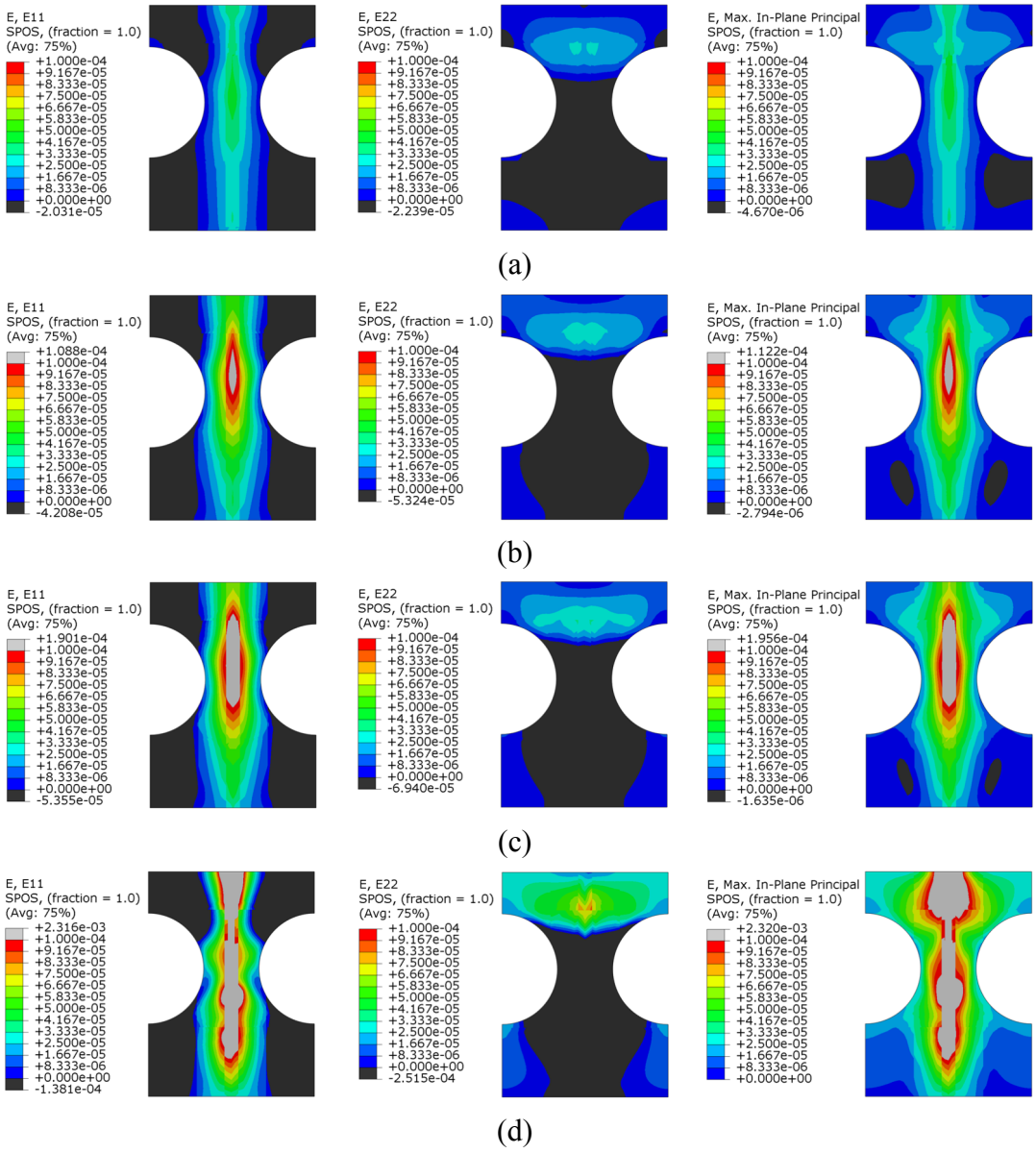

Figure 5.42 Strains in the top of the thick slab for load levels: (a) 0 kN/m^2; (b) 150 kN/m^2; (c) 250 kN/m^2; (d) 400 kN/m^2.

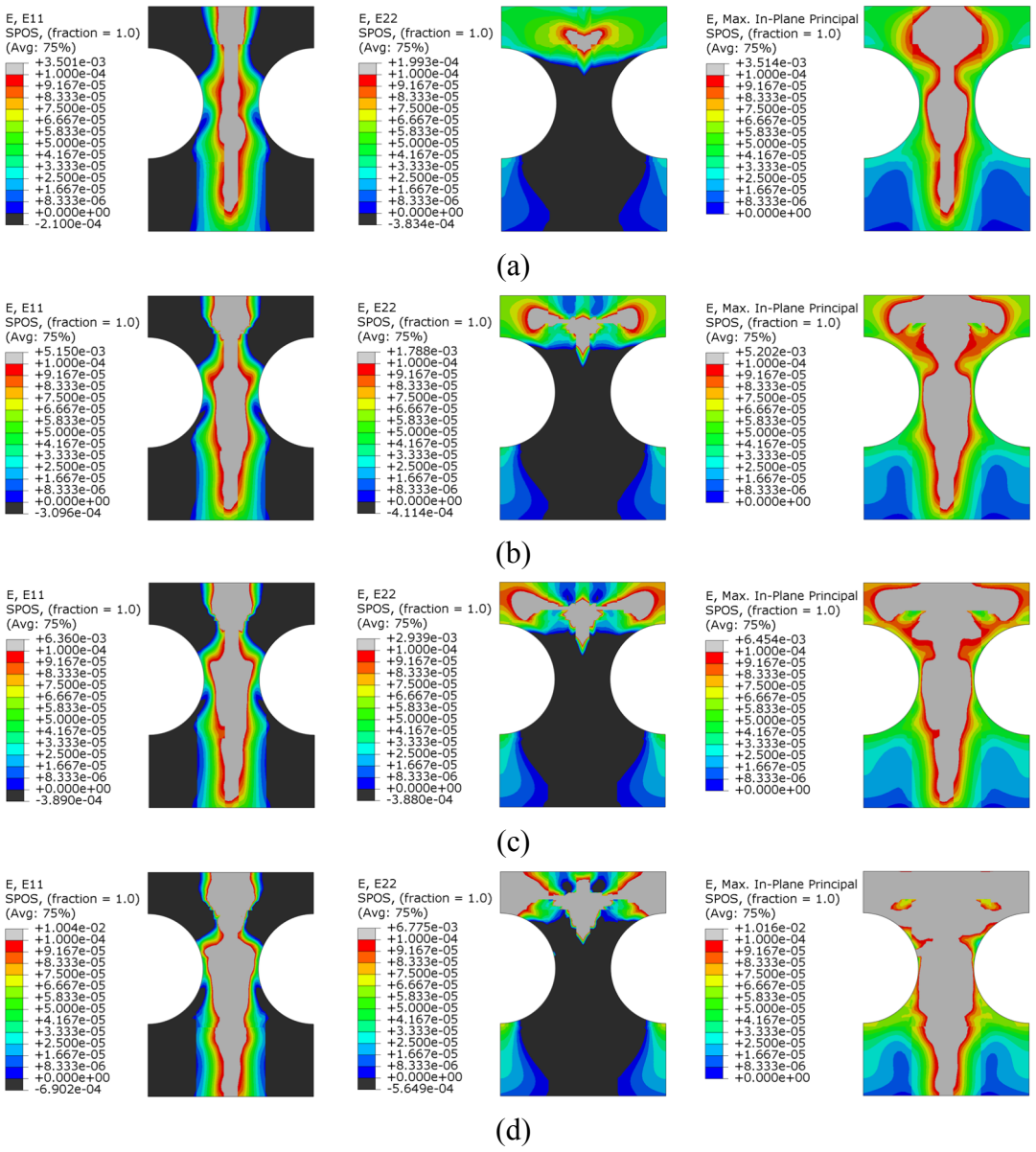

Figure 5.43 Strains in the top of the thick slab for load levels: (a) 525 kN/m^2; (b) 625 kN/m^2; (c) 670 kN/m^2; (d) 760 kN/m^2.

To indicate when the reinforcement starts to yield, the load levels for which reinforcement in different parts of the thick slab and the beam start to yield was studied. These load levels can be seen in Table 5.14 as well as indication of a widespread yielding for the reinforcement in the transversal direction of the slab in the top between the slab openings, which showed earlier signs of yielding than the rest of the structure.

Table 5.14 Yielding loads of reinforcement at different locations, with positional reference to Table 5.10.

Reinforcement location	Bottom/top	Direction	Yielding load [kN/m^2]	Widespread yielding [kN/m^2]
Left of openings	Bottom	Longitudinal	840	-
		Transversal	-	-
	Top	Longitudinal	-	-
Between openings	Bottom	Longitudinal	765	-
		Transversal	-	-
	Top	Longitudinal	895	-
		Transversal	455	735
Right of openings	Bottom	Longitudinal	850	-
		Transversal	-	-
	Top	Longitudinal	930	-
Beam	Bottom	Longitudinal	840	-

The structure and especially the slab appears to be fully cracked for a load level of 760 kN/m^2, this corresponds well with the load levels for which the reinforcement start to yield. Further, there is one region, the top reinforcement in the transversal direction between the openings, which indicates earlier yielding, at a load level of around 455 kN/m^2. This is confirmed in the load-displacement curve where an indentation in the stiffness can be seen between 400 and 550 kN/m^2. Per definition, the state II limit will thus be at a load level of 455 kN/m^2. However, so called widespread yielding was observed for this exceptive reinforcement region for load levels around which other reinforcement regions also started to yield. As such, around a load level of 760 kN/m^2 it can be said that yielding is spreading across the slab.

Additional results are presented as follows:

- Global deformation picture at different load levels, Figure 5.44.
- Transverse shear flow in the slab at different load levels, Figure 5.45.

Figure 5.44 presents contour plots of the vertical deformation on deformed models for different load levels.

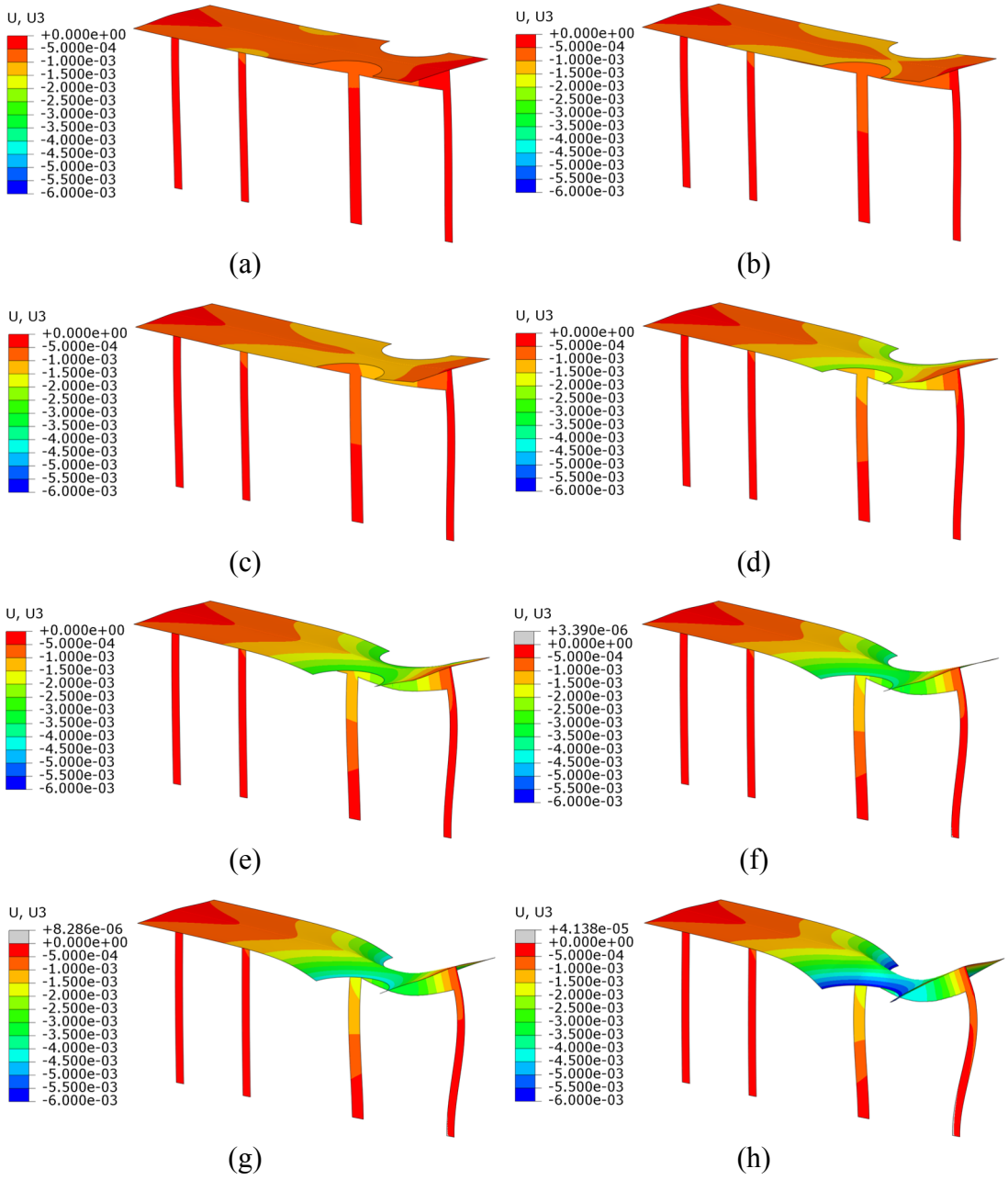

Figure 5.44 *Global deformation picture with units in m for load levels: (a) 0 kN/m^2; (b) 150 kN/m^2; (c) 250 kN/m^2; (d) 400 kN/m^2; (e) 525 kN/m^2; (f) 625 kN/m^2; (g) 670 kN/m^2; (h) 760 kN/m^2.*

Figure 5.45 presents contour plots of the transverse shear force (SF4) in the 0.41 m slab for the different load levels. The results have been limited so that the previously determined shear resistance is the maximum value in both positive and negative magnitude. Black and grey colours indicate values exceeding the resistance. The graphs show that the shear resistance is exceeded at a load level of 250 kN/m2.

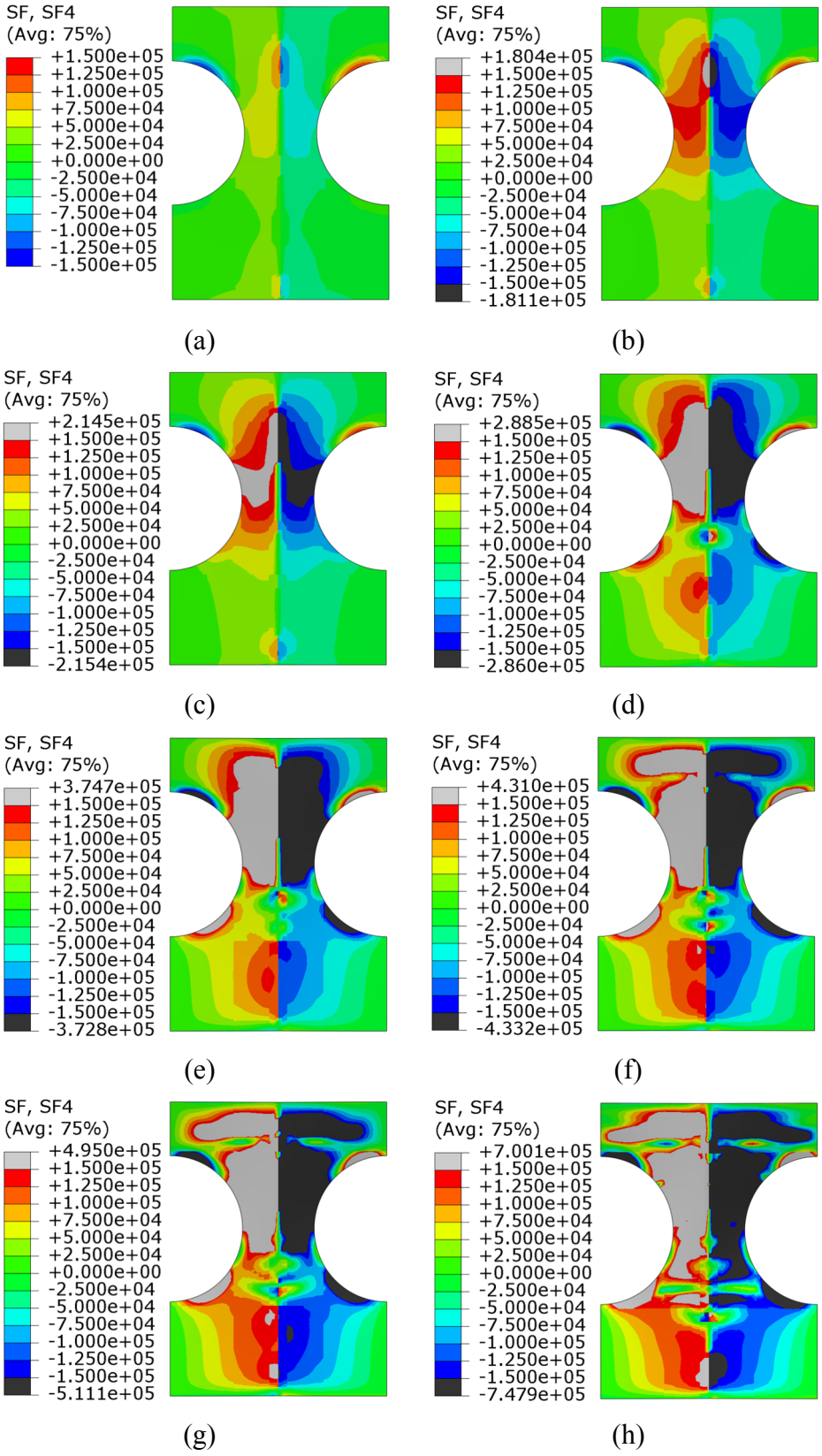

Figure 5.45 Transverse shear flow in the thick slab with units in N for load levels: (a) 0 kN/m^2; (b) 150 kN/m^2; (c) 250 kN/m^2; (d) 400 kN/m^2; (e) 525 kN/m^2; (f) 625 kN/m^2; (g) 670 kN/m^2; (h) 760 kN/m^2.

Load controlled analysis

The load-controlled non-linear analysis, the level III main analysis, served as a comparison against the level I and level II analyses for the silo variable load of 350 kN/m2. As such, the results obtained in the level III analysis are studied in the same manner as the results obtained in the level II analysis in order to identify possible differences. The same limits as for the level II results were chosen, when pertinent, i.e. resistances used for contour plots. The results from the level III analysis were compared to the level II – shells model, hereon referred to as level II, as this was the model also used in level III.

- Global deformation picture, Figure 5.46. These pictures are meant to display possible differences in behaviour between the level II and level III analyses.
- Vertical deformation in a path along the centre of the beam, Figure 5.47. This figure shows that the non-linear model behaves differently, this is due to the model taking into account concrete in state II.
- Bending moment in the slab along a path above the centre of the beam, Figure 5.48. This figure also displays a difference in behaviour of the non-linear model due to concrete in state II being accounted for.
- Shear membrane force along the centre of the beam, Figure 5.49. This figure displays a similar behaviour of the level III model, except for a dent at around 2.8 m, which can be explained by a crack in the beam.

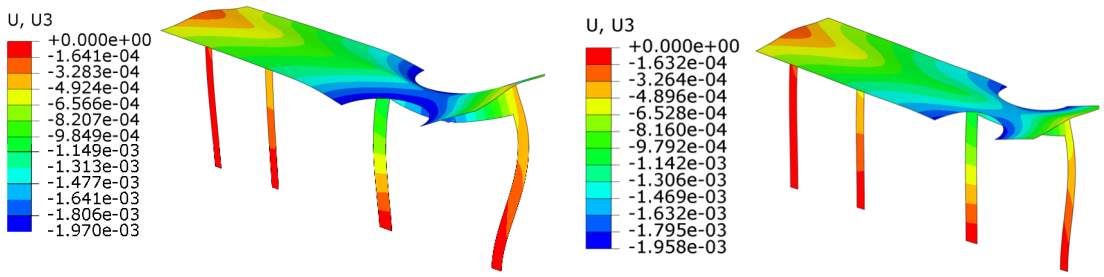

(a) (b)

Figure 5.46 Global deformation picture [m] for: (a) Level III; (b) Level II.

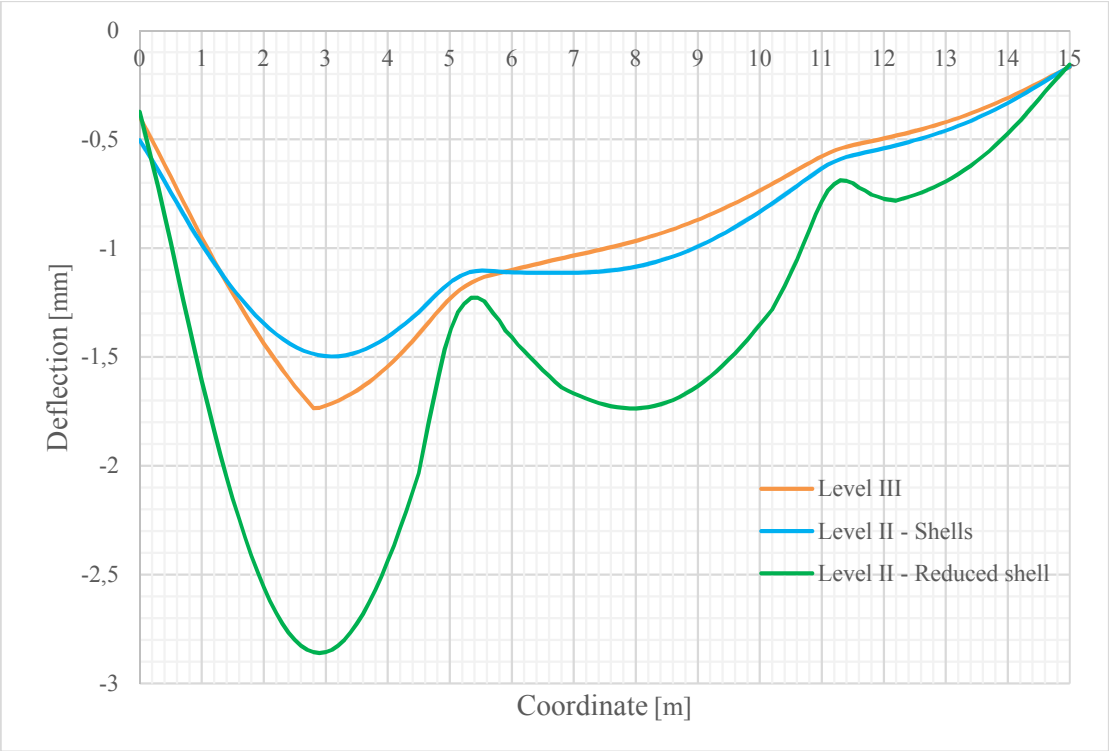

Figure 5.47 Vertical deformation along the centre of the beam.

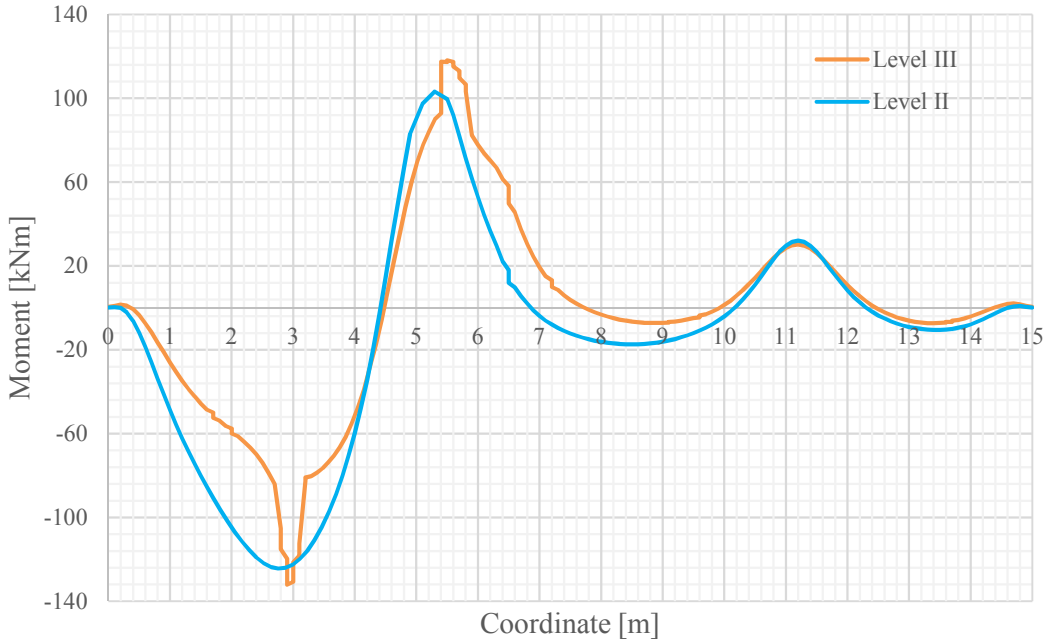

Figure 5.48 Bending moment in the slab above the beam.

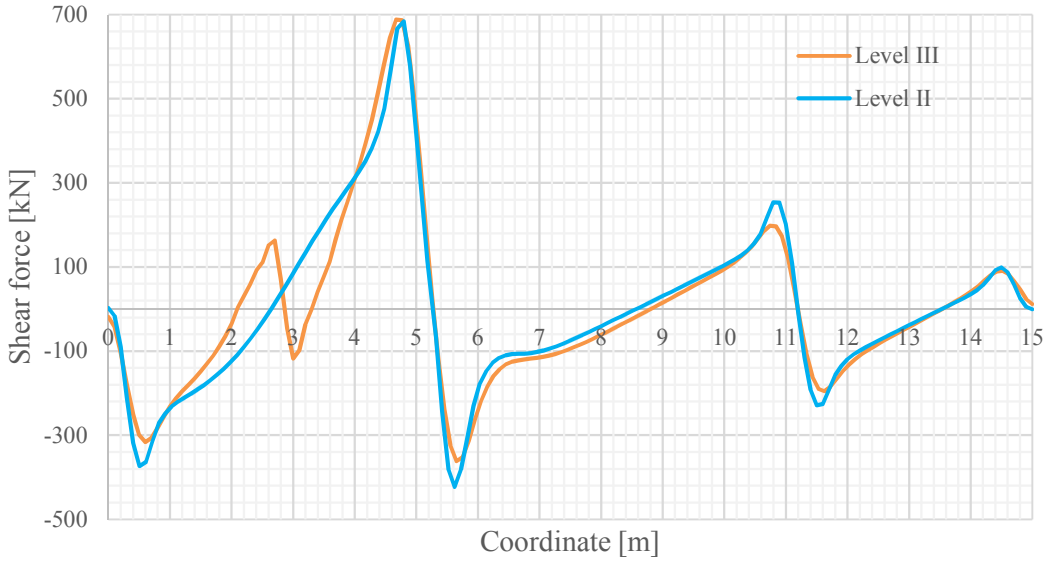

Figure 5.49 Shear membrane force in the beam.

The results and figures presenting global deformation, vertical deformation, bending moment and shear membrane force are meant to display differences and similarities between the different levels of analyses. The main results of interest for the study, i.e. shear in the slab, are presented next.

Figure 5.46 displays contour plots of the shear flow in the 0.41 m thick part of the slab, for the level II models and the level III model. The results have been limited in the same way as was done for the level II results, with a determined shear resistance of 151 kN as a maximum value in both positive and negative magnitude. Black and grey colours indicate values exceeding the resistance. A difference in the shear flow of the non-linear model can be observed, this can be explained by the model treating the concrete in state II. The three paths, A, B and C shown in Figure 5.16, that were studied in the level II analyses were plotted in the following figures as well, in order to further study differences between the linear and non-linear analyses.

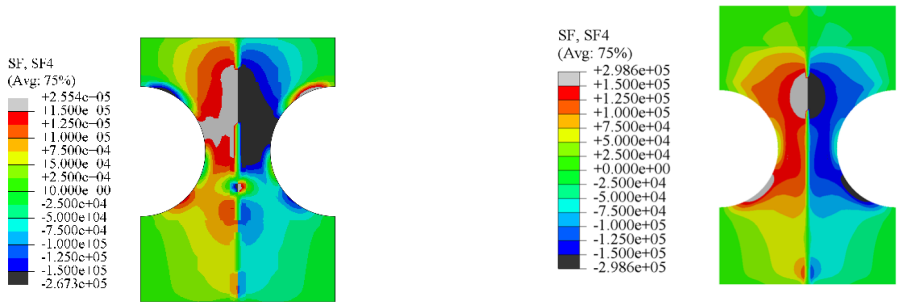

(a) (b)

Figure 5.50 Transverse shear flow in slab [N] for: (a) Level III; (b) Level II.

Figure 5.51 displays the shear force in the slab along path A, for all the levels of analysis. Figure 5.52 and Figure 5.53 show the shear force in the slab along paths B and C respectively. Some difference in behaviour can be observed between the different

levels. The level III analysis treats the 3D-behaviour in the same way as the level II analysis, but it also takes into account the cracking of the concrete, i.e. concrete in state II. This can explain the difference in the plots in the outermost parts of Figure 5.51. Otherwise, good agreement can be seen between level II and level III regarding maximum values. The shear force pattern in level III is not completely symmetrical around the middle of the studied path in Figure 5.52, which as well could be due to the cracking of the concrete.

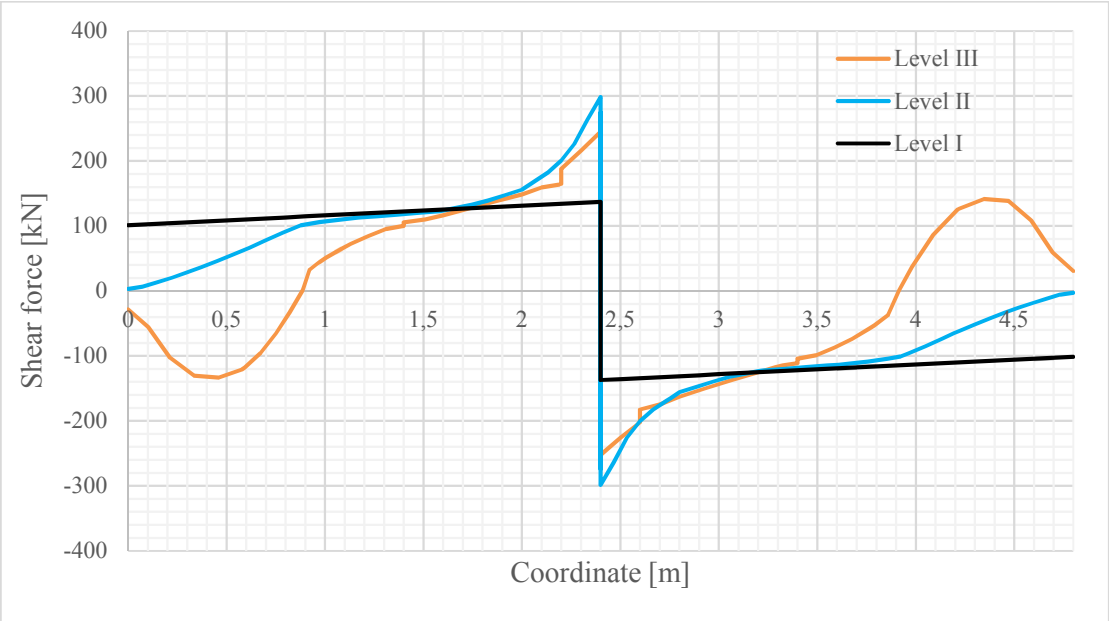

Figure 5.51 Transverse shear force in the slab between nodes at the top of the slab openings, path A.

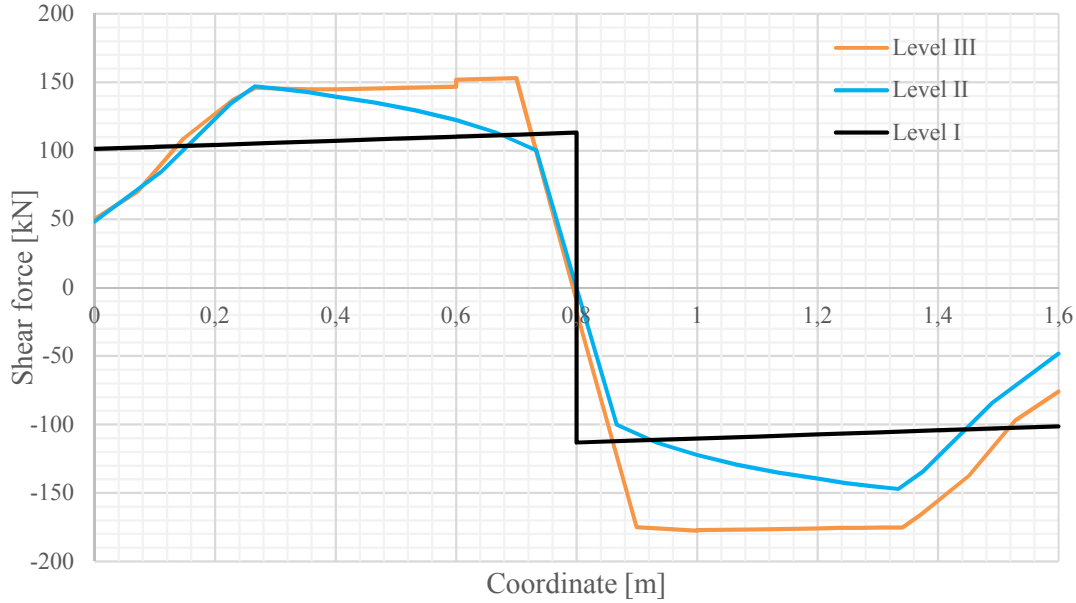

Figure 5.52 Transverse shear force in the slab between the centre of the slab openings, path B.

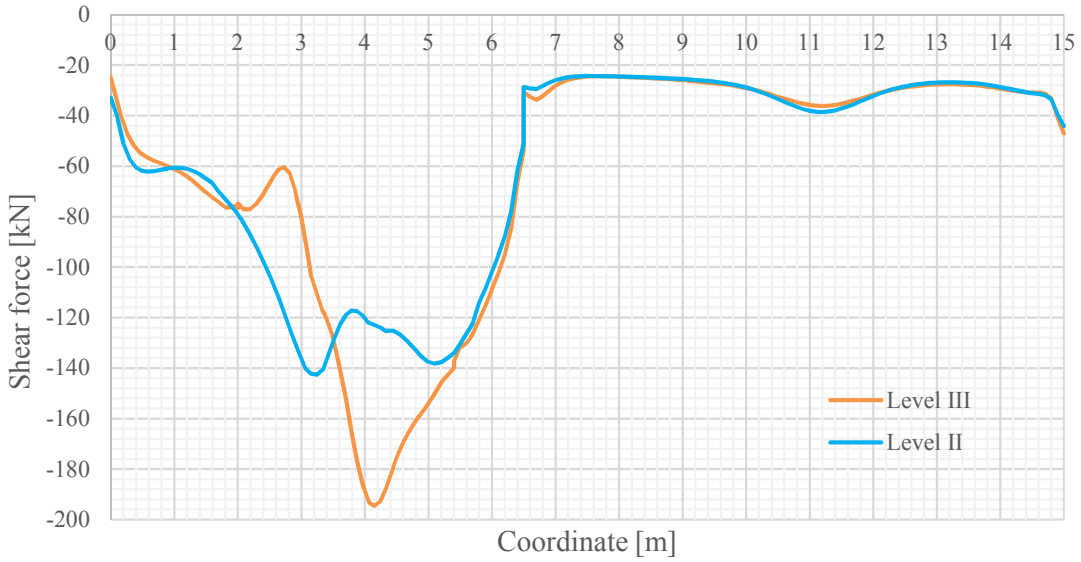

Figure 5.53 Transverse shear force in the slab parallel to the beam with an offset of 610 mm, path C.

5.1.3.2 Conclusions for the level III analysis

The main analysis in level III showed similarities to the results of level II, in the way shear was distributed along the studied paths. However, with some discrepancies, especially in the middle between the first and second column and around the slab openings. An explanation for this could be the cracking of the concrete, which would require a redistribution of the section forces in order to still fulfil equilibrium. The discrepancies correspond well with areas that appear to crack. Therefore, the differences observed are considered reasonable.

The results themselves from the level III main analysis show an actual need for shear strengthening, in contrast to what the previous two levels have indicated. As previously mentioned in Section 4.5.3, the level III analysis will not capture shear failure because of the element type used in this level of assessments. However, when comparing the load values with the previously determined capacity, the results indicate a need for strengthening in an area between the upper part of the slab openings and the adjacent column, to acquire a shear capacity of around 200 kN. This result differs a lot compared to previous levels of assessment. These areas correspond well with areas that are also affected by cracking, thus it raises a concern of whether the cracking (i.e. its distribution and cracking loads) can be considered correct or if the cracking in the level III analysis has affected the outcome in some unfavourable way.

An objective was to assess a pre-cracked structure, something that was not fulfilled. A discussion about this can be seen in Section 5.1.4. The structure was loaded as uncracked and was hence allowed to crack during the loading process. Discrete cracks and their location will greatly influence the distribution of shear forces within the concrete, which means that a pre-cracked structure would have yielded different results.

However, the result itself, that the structure needs shear strengthening, is still relevant. In general, the shear load observed increases for higher assessment level. Thus, as the

level II analysis showed shear loads close to the capacity, almost any increase in the shear load for the level III analysis would result in a need for shear strengthening. Since nothing else can be said regarding specific numbers in this case than those that have been presented in the results, the conclusion is that a shear strengthening is indeed needed and should ensure a capacity of around 200 kN for the area between the upper part of the slab openings and the adjacent column, see the black and grey areas in Figure 5.50(a).

5.1.4 Conclusions of the assessment of the structural behaviour

For the level I analysis, consisting of hand calculations, the shear load in the slab amounted to a magnitude of around 85% of the capacity. Thus, if only a level I analysis is performed, no concerns due to shear would be expected. However, it can be stated that a level I analysis in this case would not be expected to reflect reality particularly well, due to the complexity of the structure. 3D effects because of slab openings, varying T-section geometry in the slab-beam intersection, and distribution of the load in two-way rather than only one-way are in this case coveted traits.

When progressing to the level II analysis, the 3D linear FE analysis, the shear in the slab reached levels almost of the determined capacity, around 95%. However, the full capacity was still not reached, and no shear failure should be expected. This observation applies regardless of the model elements used in the analyses. In addition, it is worth noting the fact that the model with reduced stiffness displayed almost no difference in shear forces along the studied paths when compared with the models with regular stiffness.

The most critical areas for shear, according to both level II and level III analyses, were observed as the perimeters of the circular openings and towards the closest column, which is also the largest column. This was an expected behaviour, since the perimeters of the openings are in this case subjected to the governing load and this region is close to a support column. As mentioned, the differences between the two levels of assessment is that the calculated shear load values are within the calculated capacity of the slab for level II (however not with a large margin), but well above the capacity for level III. Level III analysis yielded larger shear loads in the slab, which leads to the conclusion that the slab should be strengthened for shear.

As stated in the introduction of Section 5, the motivation for the case study was to assess whether or not an increase in the load from the hanged silos would lead to concerns with regard to shear for an existing cracked structure. As such, it was important to capture the structural behaviour, accounting for the existing cracks. However, as described in section 5.1.3, due to the limitations of the chosen material model, it was not possible to model the pre-cracking of the structure. In the analysis, the concrete reached cracking before the load level of interest was applied, but if the structure would have been already cracked before the load application, which was the case in reality, some variation of the result would have been expected. For the linear elastic FE analysis, a model with reduced stiffness was made in order to reflect a pre-cracked structure in a linear analysis. However, this model did not appear to be stiff enough, which may be explained by the fact that the complete structure was assumed to be cracked. In comparison, the non-linear analysis showed that only certain parts of the structure were cracked for the same load. As previously mentioned, this method will

not be able to describe the behaviour in the ultimate state, but only in the serviceability state.

Regarding which level of assessment should be used in daily practice, it can be seen that different levels of assessment of the structure gave different results. In the studied case, the complexity of the structure and specifically its reinforcement layout may be a reason for the need of strengthening that was evident in the level III analysis. However, some additional arrangement of reinforcement around the slab openings, both stirrups and surface reinforcement, was omitted in this study for simplicity reasons, which would have contributed to the capacity and thus, reduced the need for strengthening. Additionally, the cracking process of the structure and specifically the crack pattern, greatly influences the way the shear forces are spread. A shear strengthening need may be present, but to a lesser extent than what is shown in this study, as a higher level of assessment normally produces results closer to reality, according to Plos et al. (2016) and as is shown in Figure 4.4.

In conclusion, the level that is the most applicable for use depends on each situation's relevant project parameters. A level III analysis should be used with caution. It requires a great level of detail in the modelling, which in turn demands both time, effort and expertise. In addition, a deep knowledge of the software used is needed. However, when done correctly, a level III analysis will give the most reliable results. It should be stated, however, that the difference in the required effort compared with the result acquired from level II and level III analyses may not always be worth the extra attention. In this case study, though, only the level III analysis showed a clear need for strengthening. Therefore, the extra effort in this particular case study resulted in a difference between a yes- or no-answer to the question whether or not strengthening is needed. Due to the proven need of shear strengthening of the structure, an evaluation of the shear strengthening methods presented in Section 3 was made, previously mentioned as part 2 of the case study.

5.2 Evaluation of strengthening methods

Part 2 of the study consisted of further assessing the shear strengthening methods and performing an evaluation of to which extent they are applicable to the case study. As a result of the assessment previously performed, it was determined that strengthening is needed in the areas between the upper part of the slab openings and the adjacent column, shown as the black and grey areas in Figure 5.50(a). The required shear capacity for the slab was 200 kN and the existing capacity was 150 kN. The relevant strengthening methods were compared to each other based upon how much increase in shear capacity for the slab they could provide, their respective cost and also applicability to the structure. Not all methods described in Chapter 3 are suitable, because some of them are more appropriate for beams rather than slabs or punching rather one-way shear. In Table 5.15 the methods are presented together with their intended area of usage.

Table 5.15 Reinforcement methods and their area of usage.

Method number	Reinforcement technique	Applicability
1	Drilled in steel bars	Beams and slabs
2	Vertical steel bolts	Slabs
3	External steel plates	Slabs
4	Externally bonded FRP	Beams and slabs
5	Near surface mounted FRP	Beams
6	Embedded through section FRP	Beams and slabs
7	Textile reinforced mortar	Beams
8	Steel fibre reinforced concrete	Beams
9	Shape memory alloys	Beams

The first step in further evaluating the introduced methods was assessing which methods would be applicable on the studied slab. The methods developed solely for beams would not be suitable for the studied case, this ruled out methods 5, 7, 8 and 9. Method number 3, the reinforcement technique using external steel plates, emphasizes on the resistance against punching failure. As shown in the first part of the case study, Section 5.1, punching failure is not of concern in the structure, and method number 3 was therefore omitted.

Four of the methods brought up in Table 5.15, namely methods 1, 2, 4 and 6, were found suitable as they could be applied to slabs and hence, be applicable to the structure in the case study. These methods also provide resistance against one-way failure, which is the most critical type of shear in the studied structure. The methods to be further assessed were therefore:

- Drilled-in steel bars, described in Section 3.1.1.
- Vertical or angled bolts, described in Section 3.1.2.
- Externally bonded FRP, described in Section 3.2.1.
- Embedded through section FRP, described in Section 3.2.3.

As for the the externally bonded FRP method, the proposed application for slabs was implemented.

5.2.1 Analytical expressions

This section aims to present useful analytical expressions for determining the capacity of a strengthened RC slab. The presented expressions have been adopted from studies evaluating the respective methods. In order to be comparable to each other and compatible with Eurocode, some adjustments have been made to the expressions presented in the studies. In these calculations, it was assumed that the existing concrete capacity could be added together with the extra capacity determined by strengthenings. This is not the case when designing according to Eurocode, as was described in Section 2.6.2, where the concrete capacity should be neglected as soon as some shear reinforcement is introduced to the member.

5.2.1.1 Drilled-in steel bars

In the study carried out by Breveglieri et al. (2014), the added shear capacity of a member from ETS bars is suggested to be determined according to equation (5.1). This expression may then be combined with the concrete contribution determined according to Eurocode 2 ('SS-EN 1992-1-1', 2008), calculated with equation (2.6) to provide the total shear resistance of the member.

$$V_{R,f} = \frac{A_{fw} f_{yt} (\sin\alpha + \cos\alpha) d}{s_{fw}} \tag{5.1}$$

where

A_{fw} is the cross sectional area of the ETS bars
f_{yt} is the yield stress of the ETS bars
α is the inclination of the bars with respect to the longitudinal axis of the slab
d is the effective depth
s_{fw} is the spacing of the ETS bars

As can be seen in equation (5.1), the additional shear strength added from the strengthening techniques are calculated in the same way as the contribution of an already existing shear reinforcement. This observation is confirmed, when comparing the method used by Fiset et al. (2017), who utilises the same expressions for calculating the added shear strength from the drilled-in steel bars.

However, equation (5.1) assumes that shear reinforcement is capable of reaching its yield capacity, which is not always the case. As it is brought up in Section 3.1.1, the bars tend to fail by debonding before yielding, which is therefore important to take into account. A more detailed calculation method is proposed by Breveglieri, Aprile, & Barros (2015), which takes into account whether the reinforcement fails due to yielding of the bars or by debonding. The force developed in a single ETS bar after the yield force has been reached may be calculated with equation (5.2).

$$V_{fy} = \frac{\pi \phi_{ETS}^2}{4} f_{yt} \tag{5.2}$$

where

ϕ_{ETS} is the ETS bar diameter

The resisting bond force, in the same method, is calculated with equation (5.3).

$$V_{fbd} = L_p \frac{1}{J_1} \lambda \left(\delta_1 \sin\left(\lambda L_{Rfi.eq} \right) \right) \tag{5.3}$$

where

L_p is the bar perimeter
J_1 is a bond modelling constant
λ is a bond modelling constant
δ_1 is the bond slip
$L_{Rfi.eq}$ is the equivalent value of the average resisting bond length

The final contribution of the bars, according to the proposed method, is then calculated with equation (5.4).

$$V_{R,f} = n_{bar} N_{f,int}^{l} V_{fi,eff}^{max} \sin \alpha \tag{5.4}$$

where

n_{bar} is the number of installed bars
$N_{f,int}^{l}$ is the minimum number of bars that can cross the shear crack
$V_{fi,eff}^{max}$ is the maximum capacity of the average length bar along the shear crack and is taken as the minimum value between the resisting bond force and yield force
α is the inclination of the ETS bar with respect to the longitudinal axis of the slab

5.2.1.2 Vertical or inclined steel bolts

For vertical or inclined steel bols, as for the drilled-in bars, the capacity may be considered as a sum of both a concrete contribution and a bolt contribution (Baig, Alsayed, & Abbas, 2015; Polak & Bu, 2013). In accordance with Section 2.6.2, the bolt capacity determined according to equation (5.5), may then be added to the original capacity (due to shear reinforcement of concrete only). A detailed assessment may as well consider the fact that concrete is removed for the bolts.

$$V_{R,f} = \frac{A_s f_{yt}(\sin\alpha + \cos\alpha)d}{s_{fw}} \quad (5.5)$$

where

f_{yt} is the yield strength of the bolt
A_s is the cross-sectional area of the bolt stem
α is the inclination of the bars with respect to the longitudinal axis of the slab

5.2.1.3 Externally bonded FRP

In essence, strengthening with externally bonded FRP according to the method proposed by Binici & Bayrak (2006), consisting of wrapping FRP strips through predrilled holes, is applicable to the slab. However, in order to make the method more suitable for one-way shear, some modifications were needed. This was done by treating the area between the drilled holes as a wrapped beam. Formulations from the study performed by Jung et al. (2015), see equation (5.6), could then be adapted in order to assess the capacity increase of the method. In their study, a certain consideration is taken to the concern of debonding. However, as it is brought up in Section 3.2.1, this is not an issue of wrapped beams. Binici & Bayrak (2006) further suggest using a reduction factor, β, for taking into account that the usable strength of the FRP material is smaller than the ultimate strength.

$$V_{R,f} = \frac{\beta n_{layer} A_f f_{fv} d}{s_{ebr}} \quad (5.6)$$

where

β is a reduction factor with regard to the usable FRP strength
n_{layer} is the number of layers of FRP strips
A_f is the cross-sectional area of the FRP strip
f_{fv} is the tensile strength of the FRP material
d is the effective depth of the reinforcement
s_{ebr} is the spacing of FRP reinforcement

5.2.1.4 Embedded through section FRP

This method works in principle the same as for method 1, with drilled-in steel bars, but rather than using steel, bars are made of FRP. Thus, the capacities are calculated in the same way using equation (5.1). The difference is the material properties of steel and FRP, where FRP has a higher ultimate strength, as mentioned in Section 3.2.

5.2.2 Calculated capacities

In order to compare the performance of the presented methods, the analytical expressions were applied for the studied slab. The calculations were performed with as identical conditions as possible. All calculations together with assumptions are

presented in Appendix E. The results are presented in Table 5.16. The calculations are done for a meter strip of the slab.

When performing the calculations, the same spacing and bar diameter was assumed for method 1 and 2, i.e., the methods using steel. The assumptions were a spacing of 300 mm and a bar diameter of 12 mm respectively. Additionally, the same yield strength of steel, 500 MPa, was used for these methods. For the methods using bars, an inclination of 45 degrees were assumed as this provides a greater increase than a vertical configuration. Figure 5.54(a) presents the assumed layout for drilled-in steel bars, bolts and ETS FRP, Figure 5.54(b) presents the assumed layout for the externally bonded FRP strips.

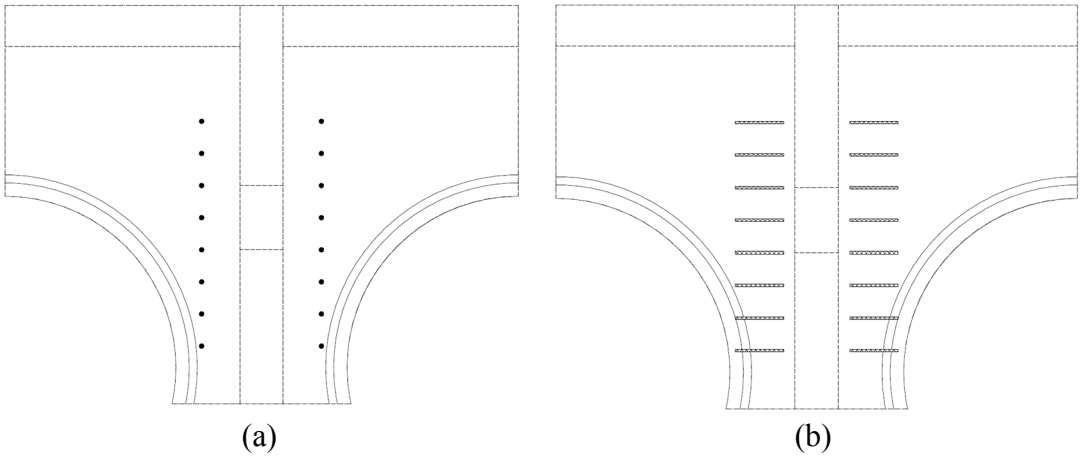

Figure 5.54 Proposed layout for the shear strengthening of the slab with: (a) Drilled-in steel bars, bolts and ETS FRP; (b) Externally bonded FRP.

As for the FRP material, the same material used in the study by Binici & Bayrak (2003) was assumed. This was a CFRP with an ultimate tensile strength of 876 MPa and an ultimate tensile strain of 0.0121. The strips were assumed to be 25 mm wide, 3.04 mm thick and to consist of 2 layers of strengthening. The reduction factor, β, was taken as $1/3$, which was further suggested by Binici & Bayrak (2006). This suggestion is also supported in the study performed by Jung et al. (2015), who bring up that the tensile design strain should not be greater than 0.004, which happens to correspond to $1/3$ of the ultimate strain of the used material.

Table 5.16 Increase of shear capacity for the different methods.

Method	Increased net capacity [kN]	Total capacity [kN]
Drilled-in steel bars (debonding not included)	101	252
Drilled-in steel bars (debonding included)	80	231
Vertical or inclined steel bolts	101	252
Externally bonded FRP	56	207
Embedded through section FRP	59	210

It was determined in the level III analysis, Section 5.2.2, that the shear capacity of the slab would need to be increased to a total shear capacity of around 200 kN. The current shear capacity of the slab was, according to the level I analysis around 150 kN, thus an additional capacity of 50 kN was required. All methods were able to provide this increase and it is rather the quantity of material that will determine the increase of capacity. The calculated capacities displayed in Table 5.16 are determined for roughly the same area of strengthening material but could be optimized to ensure only a capacity increase of up to 200 kN.

5.2.3 Practical application and cost

As for the applicability between these different methods, there were no great differences between methods 1, 2 and 6, as they resemble each other both in the method of installation and the way they interact with the concrete. As mentioned in the review of the state-of-practice today, see Section 3.5, vertical installation will be easier to perform than inclined, though at the expense of potential capacity loss. Additionally, the state-of-practice today is that steel is more common than FRP due to the novelty of FRP in the building sector. When evaluating the externally bonded FRP, it was considered less applicable due to several reasons. Firstly, it is a method most commonly used for beams which was adjusted to better suit slabs. Secondly, it is a method more intrusive into the existing concrete than the other methods as more holes are required. Because of this, the risk of damaging the existing flexural reinforcement increases. Thirdly, this method is still at an experimental stage and therefore rather uncertain in itself.

Regarding the cost of performing these respective strengthening methods, a comparative matrix was established. The matrix puts into relation the costs of labour for performing the different strengthening methods and their respective material costs. As a result, a perspective of the total cost of each method is produced. The methods were graded from 1 to 3, in which 3 is the most expensive. For methods 1, 2 and 6, it can be stated that the cost of labour is similar. A small addition was included for the method with bolts, as these require some extra effort with the nuts. Meanwhile, the externally bonded FRP requires more holes, which themselves are larger as well. The risk of encountering problems with the flexural reinforcement is therefore much greater, which is regarded as a cost in this case. The material cost was surveyed from Swedish building department stores as:

- The cost of reinforcement bars for drilled in steel bars
- The cost of threaded rods and nuts for vertical or angled bolts
- The cost of CFRP sheets for the externally bonded FRP
- The cost of CFRP rods for the embedded through section FRP

The resulting cost matrix is presented in Table 5.17.

Table 5.17 Cost matrix for the strengthening methods.

Method	Labour cost	Material cost	Total cost
Drilled in steel bars	1	1	2
Vertical or angled bolts	1	2	3
Externally bonded FRP	3	3	6
Embedded through section FRP	1	3	4

These methods have been studied further by means of analytical expressions that may be used in order to evaluate the resulting capacity after strengthening.

5.2.4 Contribution of flexural strengthening

The structure has previously been strengthened with regard to its flexural capacity in a project carried out by ÅF. Although the intent of this strengthening was to increase only the flexural capacity, it will have an impact on the shear capacity as well. This strengthening was performed using FRP-strips glued to the soffit of the slab. The impact of this strengthening on the shear capacity was in this study examined as well. By studying equation (2.6a), more specifically the ρ_l factor, which is the ratio between the cross-sectional reinforcement area and the concrete area, it can be seen that the cross-sectional reinforcement area has an impact on the shear capacity.

$$V_{Rd,c} = \left[C_{Rd,c}k(100\rho_l f_{ck})^{\frac{1}{3}} + k_1\sigma_{cp}\right]b_w d \qquad (2.6a)$$

The increase of shear capacity was then calculated by expressing an equivalent area of the FRP strengthening by using equation (5.6) and modifying the ρ_l factor accordingly.

$$A_{eq.s} = A_{FRP}\frac{E_{FRP}}{E_s} \qquad (5.6)$$

where

A_{FRP} is the cross-sectional area of the FRP reinforcement
E_{FRP} is the Young's modulus for the FRP material
E_s is the Young's modulus for steel

The dimensions and material data of the FRP strengthening was provided from the previous project and consisted of strips with a width of 150 mm and a thickness of 1.2 mm, thus yielding a cross-sectional area 180 mm^2 per strip. The Young's modulus of the material was given as 240 GPa. A strip of the concrete slab, with a width of 1 m, strengthened with two FRP strips, was studied.
Using expression (2.6a) the calculated shear capacity of the slab without the shear strengthening is 122 kN, see Appendix C. This can be compared to the flexurally strengthened slab which obtains a shear capacity of 147 kN, see Appendix E. The increase of shear capacity due to the flexural strengthening was then 25 kN which corresponds to almost 21%. However, as is brought up in Section 2.6.2, there is a minimum value for concrete members, which are not reinforced with regard to shear, see equation (2.6b). This minimum value was calculated to 151 kN, see Appendix C, and will therefore be the design value of the slab, regardless of the flexural strengthening. It is worth noting that if more strips were to be added to the flexural strengthening the shear capacity calculated from equation (2.6a) would exceed the minimum value and thus yield a higher resistance for the slab.

5.2.5 Conclusion & discussion of the evaluation of the strengthening methods

The increase in shear capacities presented in Table 5.16 were calculated for roughly the same cross-sectional area of the strengthening material. By just studying the results, the drilled-in steel bars method, calculated with the simple expression, seems to provide the most additional shear capacity. When comparing the simple and detailed expressions of the drilled-in steel bars method, it is worth noting that the simple expression does not take the bonding between steel bars and the concrete into consideration. This might leave some scepticism for the expression as debonding has been shown to be the most common failure mode for this strengthening method. Therefore, the more detailed expression might be more appropriate as this takes the issue of debonding into account. With regard to application, the drilled-in steel bars method was deemed to be as intrusive as the methods using vertical bolts or ETS FRP, however, the fact that it is one of the more common methods used today favours this method. It is also the method with the lowest total cost.

Vertical steel bolts method uses the same expression as the simple method for the drilled-in steel bars. This method does not experience failure due to debonding as the nuts keep the bars in place. The applicability of vertical steel bolts is in level with the drilled-in steel bars method and the ETS FRP method, but it has a slightly higher total cost than the drilled-in steel bars.

The externally bonded FRP method provides, according to the assessment, the lowest increase in capacity. However, the fact that the properties of the used FRP material will have a large impact, as mentioned for the embedded through section method, is highly relevant for this method as well. This method is brought up as the most expensive method, and even though this is true, it is worth noting that for larger capacity increases, it is significantly easier to add an additional layer of wrapping than it is to make space for additional bars, as would be the case for the other methods. This could affect the choice in this case study where, should the strengthening be designed strictly according to Eurocode, the concrete contribution may not be included. Consequently, the needed capacity of the strengthening would have been 200 kN instead of 50 kN, which could have been accomplished more easily with this method than the others. However, as the method is still at an experimental stage, it is difficult to evaluate its efficiency. Combined with the higher costs, it is suggested that further studies should be performed to evaluate the applicability of the method before it is used in practice.

When studying the layout presented in Figure 5.54(b) it can be seen that the capacity could, depending on the crack behaviour, in fact be doubled. This would be the case if the spacing, l_1, between the drilled holes are shorter than the projected length of the crack, l_2, see Figure *5.55*. This was not assumed to be the case here.

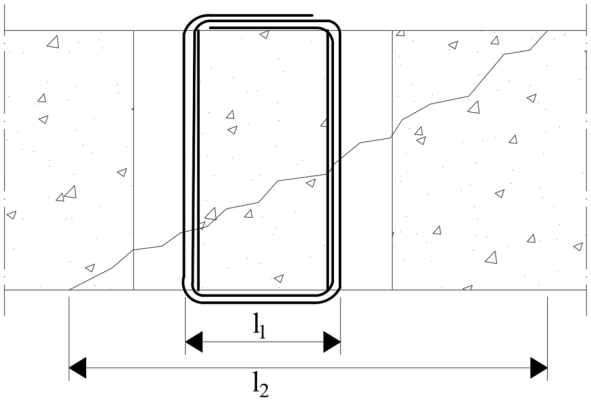

Figure 5.55 Relation between length l_1 and l_2 with regard to double capacity from the externally bonded FRP method.

The expression for embedded through section FRP strengthening provided a fairly low increase of capacity. This could be credited to the type of FRP material employed. There are many types of FRP materials and the properties of those will differ. The capacity of the method is also influenced by the suggested reduction factor, which dictates that only $1/3$ of the ultimate tensile strength can be utilised. The applicability of this method is ranked the same as the method using vertical bolts, with the exception of steel being a more traditionally used material and it is therefore slightly favoured in this evaluation. However, the cost of FRP rods is higher than the cost for steel bolts.

The evaluation of the influence of the flexural strengthening showed that this strengthening indeed has an impact on the shear capacity. However, for the case study, this increase was not enough to provide shear capacity beyond the designated minimum expression, following Eurocode recommendations. With this said, it is still worth evaluating the contribution of the flexural strengthening on the shear capacity. In the presented case study, two strips increased the capacity by 25 kN. If the slab would have been strengthened even further in bending, the contribution to shear capacity would have exceeded the minimum threshold and actually increased the capacity of the slab. For the flexural strengthening to contribute enough to the shear capacity that no additional shear strengthening would be needed, i.e. $V_{Rd,c}$ equal to 200 kN, the total area of flexural strengthening must be increased to 1620 mm^2 instead of the current 360 mm^2.

However, in order to verify the analytical expressions, experimental testing would have to be performed.

In conclusion, the method using drilled-in steel bars was deemed the most appropriate for the case study. The reasons for this are:

- It is the cheapest and most applicable method
- The procedure is well known and the expertise in its implementation is high
- By using the detailed analytical expression, the concern of debonding can be taken into account, which as it is shown, this failure mode is the major concern when using such strengthening methods

6 General Conclusions and suggestions for further studies

This study has reviewed the shear behaviour of RC slabs and investigated differences that are apparent between the current and previous design codes with regard to shear capacity in RC slabs and design loads. Comparisons were made between the current design code, Eurocode, and two previous Swedish design codes, BKR (Boverkets Konstruktionsregler) and SBN (Svensk Byggnorm). Further, several different strengthening methods that are applicable to both beams and slabs were reviewed. Some methods are still at an experimental stage, whereas some methods such as the post-installation of shear reinforcement may be considered as standard methods of choice today.

A case study in two parts was conducted for an existing industrial building, in which the subjected load were to be increased. Part 1 of the case study used a structural assessment strategy, proposed by Plos et al. (2016), to determine whether or not a need for shear strengthening was apparent. The structural assessment strategy consisted of three levels:

- Level I – analytical calculations according to Eurocode
- Level II – 3D linear FE analyses
- Level III – 3D non-linear FE analyses

By performing continuous comparisons and evaluations of the different levels of the structural assessment strategy, a recommendation was produced for the treatment of future similar cases. Part 2 of the case study consisted of choosing and designing an appropriate strengthening method for the case study, where soft values were based on costs and applicability.

The main conclusions that were drawn in these topics were:

- Eurocode provides a lower shear capacity than previous design codes. This arises from the fact that shear reinforcement may not be added as a complementary capacity to the capacity of the plain concrete according to Eurocode. In a calculated example for a simply supported beam with shear reinforcement, the shear capacity according to Eurocode was around 70% of the shear capacities according to BBK (Boverkets Handbok om Betongkonstruktioner) and SBN.
- Loads are treated with the partial factor safety method both in Eurocode and BKR, but not in SBN. The treatment of loads and actions are similar between all codes. However, the partial factors that are utilised by Eurocode and BKR for the load combinations and safety classes differ. When all factors are applied, i.e. the product of partial factors for both load combination and safety class, they yield similar results.
- A review of the state-of-practice today concluded that both steel and FRP is used for the shear strengthening of slabs and beams, though steel is still more common due to the relative novelty of FRP in the building sector. Soft values, i.e. values other than pure resistance gained due to the strengthening, often determine which method is chosen.
- In Part 1 of the case study, levels I and II of the structural assessment strategy which consisted of analytical calculations and 3D linear FE analyses, showed

that the shear capacity of the structure was sufficient. However, level III which consisted of 3D non-linear FE analyses, showed a need for strengthening the structure with an additional shear need of 50 kN. The non-linear FE analysis captured load redistributions due to cracking in the concrete, which led to high local shear forces around an interior column.

- For similar cases, i.e. composite slab-beam structures, it is sufficient to use shell elements throughout the entirety of the structure. A level III assessment, 3D non-linear FE analyses, may in some cases be worth the extra effort to perform, since it will give a better approximation to reality than the common standard of practice in industry today, level II which consists of 3D linear FE analyses. However, high demands are put for a level III assessment and should as such be approached with caution.
- Part 2 of the case study concluded that strengthening with drilled-in steel bars would be the most appropriate for this structure due to its low cost, easy implementation and precision in determining the capacity that is gained.
- The study showed that a flexural strengthening by means of FRP laminates may contribute to the shear capacity. However, for this particular case study, the flexural strengthening applied would not be enough to increase the shear capacity of the structure. The shear capacity of the slab was determined from a minimum value based on the gross concrete section according to Eurocode, the flexural strengthening was not able to raise the capacity above this minimum value.

To complement the conclusions from this study, it is suggested to further perform levels IV and V of the structural assessment strategy. A method to modelling a pre-cracked structure for the level III analysis should also be studied. Additionally, the reinforcement in the slab that was omitted may be included, both when determining the shear capacity and modelling the behaviour. Thus, both validating the model used in this study and providing further accuracy for recommendations on how to perform similar assessments. Further experimental studies should as well be made, in order to validate the analytical expressions that were used to determine additional capacities of different strengthening methods in this study. The subject of prestressed slabs have not been regarded, which could be the subject to future studies.

7 References

AB Svensk Byggtjänst. (1990). *Betonghandbok Konstruktion* (2nd ed.). Solna: AB Svensk Byggtjänst.

Abaqus/CAE User's Manual. (2016). Dassault Systèmes.

Adetifa, B., & Polak, M. A. (2005). Retrofit of Slab Column Interior Connections Using Shear Bolts. *ACI Structural Journal; Farmington Hills*, *102*(2), 268–274.

Al-Emrani, M., Engström, B., Johansson, M., & Johansson, P. (2013). *Bärande Konstruktioner Del 1* (No. Report 2013:1). Göteborg, Sweden: Division of Structural Engineering, Chalmers University of Technology.

Askar, H. S. (2015). Usage of prestressed vertical bolts for retrofitting flat slabs damaged due to punching shear. *Alexandria Engineering Journal*, *54*(3), 509–518.

Baig, Z. I., Alsayed, S. H., & Abbas, H. (2015). Punching of slab–column connections strengthened using external steel shear bolts. *Magazine of Concrete Research*, *68*(2), 55–68.

Barros, J. a. O., & Dalfré, G. M. (2013). Assessment of the Effectiveness of the Embedded Through-Section Technique for the Shear Strengthening of Reinforced Concrete Beams. *Strain*, *49*(1), 75–93.

Beverly, P., & International Federation for Structural Concrete (fib) (Eds.). (2013). fib model code for concrete structures 2010. Ernst & Sohn.

Binici, B., & Bayrak, O. (2003). Punching Shear Strengthening of Reinforced Concrete Flat Plates Using Carbon Fiber Reinforced Polymers. *Journal of Structural Engineering*, *129*(9), 1173–1182.

Binici, B., & Bayrak, O. (2006). FRP retrofitting of reinforced concrete two-way slabs.

BKR från 1994 till 2010. (2014, June 24). Retrieved 31 January 2018, from http://www.boverket.se/sv/lag--ratt/aldre-lagar-regler--handbocker/aldre-regler-om-byggande/bkr-fran-1994-till-2010/

Boverket. (1989). *Boverkets nybyggnadsregler* (1:2). Stockholm: Boverket.

Boverket. (2003). *Regelsamling för konstruktion - Boverkets konstruktionsregler, BKR, byggnadsverkslagen och byggnadsverksförordningen* (1st ed.). Boverket.

Boverket. (2004). *Boverkets handbok om betongkonstruktioner BBK 04*. Boverket.

Breveglieri, M., Aprile, A., & Barros, J. (2015). RC beams strengthened in shear using the Embedded Through-Section technique: Experimental results and analytical formulation. *Composites Part B: Engineering*, *89*.

Breveglieri, M., Aprile, A., & Barros, J. A. O. (2014). Shear strengthening of reinforced concrete beams strengthened using embedded through section steel bars. *Engineering Structures*, *81*, 76–87.

Broo, H. (2008). *Shear and Torsion in Concrete Structures Non-linear Finte Element Analysis in Design and Assessment* (Doctoral thesis). Chalmers University of Technology.

Broo, H., Lundgren, K., & Plos, M. (2008). *A guide to non-linear finite element modelling of shear and torsion in concrete bridges*. Göteborg, Sweden: Division of Structural Engineering, Chalmers University of Technology.

Chaallal, O., Mofidi, A., Benmokrane, B., & Neale, K. (2011). Embedded Through-Section FRP Rod Method for Shear Strengthening of RC Beams: Performance and Comparison with Existing Techniques. *Journal of Composites for Construction*, *15*(3).

Davidson, M. (2003). *Strukturanalys av brokonstruktioner med finit elementmetoden*. Göteborg, Sweden: Brosamverkan Väst.

De Lorenzis, L., & Nanni, A. (2001). Shear Strengthening of Reinforced Concrete Beams with Near-Surface Mounted Fiber-Reinforced Polymer Rods. *Structural Journal*, *98*(1), 60–68.

EKS från 2008. (2014, June 24). Retrieved 31 January 2018, from http://www.boverket.se/sv/lag--ratt/aldre-lagar-regler--handbocker/aldre-regler-om-byggande/aldre-eks/

Elbakry, H. M. F., & Allam, S. M. (2015). Punching strengthening of two-way slabs using external steel plates. *Alexandria Engineering Journal*, *54*(4), 1207–1218. https://doi.org/10.1016/j.aej.2015.09.005

Engström, B. (2014). *Design and analysis of slabs and flat slabs* (No. Report 2011-5, Edition 2014). Göteborg, Sweden: Division of Structural Engineering, Chalmers University of Technology.

Esfahani, M. R., Kianoush, M. R., & Moradi, A. R. (2009). Punching shear strength of interior slab–column connections strengthened with carbon fiber reinforced polymer sheets. *Engineering Structures*, *31*(7), 1535–1542. https://doi.org/10.1016/j.engstruct.2009.02.021

Eurocode 1: Actions on structures - Part 1: General actions - Densities, self-weight, imposed loads for buildings. (2011, January 26). Swedish Standards Institute.

Eurocode 2: Design of concrete structures - Part 1: General rules and rules for buildings. (2008, October 6). Swedish Standards Institute.

Fernández Ruiz, M., Muttoni, A., & Kunz, J. (2011). Strengthening of Flat Slabs Against Punching Shear Using Post-Installed Shear Reinforcement. *ACI Structural Journal*, *107*.

Ferreira, D., Oller, E., Marí, A., & Bairán, J. (2016). Analysis of FRP Shear Strengthening Solutions for Reinforced Concrete Beams Considering Debonding Failure. *Journal of Composites for Construction*, *20*(5), 04016018.

Fiset, M., Bastien, J., & Mitchell, D. (2017). Methods for Shear Strengthening of Thick Concrete Slabs. *Journal of Performance of Constructed Facilities*, *31*(3), 04016103.

Hendriks, M. A. N., de Boer, A., & Belletti, B. (2017). *Guidelines for Nonlinear Finite Element Analysis of Concrete Structures*. Rijkswaterstaat Centre for Infrastructure.

Jung, K., Hong, K., Han, S., Park, J., & Kim, J. (2015). Shear Strengthening Performance of Hybrid FRP-FRCM. *Advances in Materials Science and Engineering*, *2015*.

Koppitz, R., Kenel, A., & Keller, T. (2013). Punching shear of RC flat slabs – Review of analytical models for new and strengthening of existing slabs. *Engineering Structures*, *52*, 123–130. https://doi.org/10.1016/j.engstruct.2013.02.014

Lantsoght, E. O. L., de Boer, A., & van der Veen, C. (2017). Distribution of peak shear stress in finite element models of reinforced concrete slabs. *Engineering Structures*, *148*, 571–583.

Mari, A., & Cladera, A. (2007). Shear strength in the new Eurocode 2. A step forward? *Structural Concrete*, *8*, 57–66.

Meisami, M. H., Mostofinejad, D., & Nakamura, H. (2013). Punching shear strengthening of two-way flat slabs using CFRP rods. *Composite Structures*, *99*, 112–122.

Monti, G. (2006). *Modelling aspects and design issues for anchorages, shear strengthening and confinement* (Technical Report No. 35) (p. 220). Lausanne, Switzerland: International Federation for Structural Concrete (fib).

Nováček, J., & Zich, M. (2016). Study of Flat Slabs Strengthening against Punching Shear. *Solid State Phenomena*, *249*, 221–226.

Pacoste, C., Plos, M., & Johansson, M. (2012). *Recommendations for finite element analysis for the design of reinforced concrete slabs*. KTH Royal Institute of Tchnology.

Plos, M. (2000). *Finite element analyses of reinforced concrete structures*. Göteborg, Sweden: Chalmers University of Technology.

Plos, M., Shu, J., & Lundgren, K. (2016). A multi-level structural assessment strategy for analysis of RC bridge deck slabs. *19th IABSE Congress Stockholm (Pp. 1559–1566). Stockholm, Sweden*, 1564–1571.

Polak, M. A., & Bu, W. (2013). Design Considerations for Shear Bolts in Punching Shear Retrofit of Reinforced Concrete Slabs. *ACI Structural Journal; Farmington Hills*, *110*(1), 15–25.

Regelhierarki – från lag till allmänt råd. (2014, August 24). Retrieved 29 January 2018, from http://www.boverket.se/sv/lag--ratt/forfattningssamling/regelhierarki/

Rius, J., Cladera, A., Ribas, C., & Mas, B. (2017). Active shear strengthening of RC beams using shape memory alloys.

Rombach, G., & Kohl, M. (2013). Shear Design of RC Bridge Deck Slabs according to Eurocode 2. *Journal of Bridge Engineering*, *18*(12), 1261–1269.

Ruano, G., Isla, F., Pedraza, R. I., Sfer, D., & Luccioni, B. (2014). Shear retrofitting of reinforced concrete beams with steel fiber reinforced concrete. *Construction and Building Materials*, *54*, 646–658.

SBN från 1968 till 1989. (2014, June 25). Retrieved 30 January 2018, from http://www.boverket.se/sv/lag--ratt/aldre-lagar-regler--handbocker/aldre-regler-om-byggande/sbn-fran-1968-till-1989/

Sherwood, E., Lubell, A., Bentz, E., & P Collins, M. (2006). One-Way Shear Strength of Thick Slabs and Wide Beams. *Aci Structural Journal*, *103*, 794–802.

Statens Betongkommitté. (1964). *Förslag till bestämmelser för dimensionering av betongplattor på pelare jämte utdrag ur kommentarer*. Stockholm: Statens Betongkommitté.

Statens Betongkommitté. (1969). *Bestämmelser för betongkonstruktioner - Allmänna konstruktionsbestämmelser*. Stockholm: Statens Betongkommitté.

Statens planverk. (1983). *Svensk Byggnorm 1980* (2nd ed.). Stockholm: Statens Planverk.

Täljsten, B. (2002). *CFRP-Strengthening-Concrete-Structures-Strengthened-With-Near-Surface-Mounted-CFRP-Laminates.pdf*. Luleå, Sweden: Department of Civil Engineering, Luleå University of Technology.

Tetta, Z. C., Koutas, L. N., & Bournas, D. A. (2018). Shear strengthening of concrete members with TRM jackets: Effect of shear span-to-depth ratio, material and amount of external reinforcement. *Composites Part B: Engineering*, *137*, 184–201.

Triantafillou, T. C., & Papanicolaou, C. G. (2006). Shear strengthening of reinforced concrete members with textile reinforced mortar (TRM) jackets. *Materials and Structures*, *39*(1), 93–103.

Vaz Rodrigues, R. (2007). Shear strength of reinforced concrete bridge deck slabs.

Walraven, J., Belletti, B., & Esposito, R. (2013). Shear Capacity of Normal, Lightweight, and High-Strength Concrete Beams according to Model Code 2010. I: Experimental Results versus Analytical Model Results. *Journal of Structural Engineering*, *139*(9), 1593–1599.

Appendix A – Example shear capacities

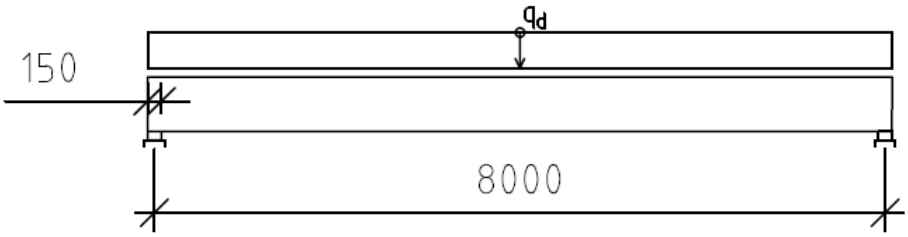

Geometries

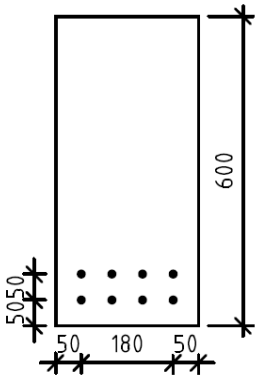

$L := 8m$

$h := 600mm$

$c := 50mm$

$b_w := 280mm$

$d := h - c = 550 \cdot mm$

$b_s := 150mm$

$d_{sl} := 20mm$ Reinforcement diameter

Material, assume concrete C25/30

$f_{ck} := 25MPa$

$f_{ctk.0.05} := 1.8MPa$

Load

$q_d := 55 \frac{kN}{m}$

Design according to Eurocode 2

All references to Section 6.2 ('SS-EN 1992-1-1', 2008) unless stated otherwise

$R_A := \frac{q_d \cdot L}{2} = 220 \cdot kN$ Support reaction due to load

$V_{Ed.x} = R_A - q_d \cdot x$

$V_{Ed} := R_A$

Safety parameters & constants

$\alpha_{cc} := 1.0$ ('SS-EN 1992-1-1', 2008) section 3.1.6

$\alpha_{ct} := 1.0$ ('SS-EN 1992-1-1', 2008) section 3.1.6

$\gamma_c := 1.5$ ('SS-EN 1992-1-1', 2008) section 2.4.2.4, Table 2.1N)

Material

$f_{cd} := \frac{\alpha_{cc} \cdot f_{ck}}{\gamma_c} = 16.667 \cdot MPa$ ('SS-EN 1992-1-1', 2008) section 3.1.6, eq. (3.15)

$f_{ctd} := \frac{\alpha_{ct} \cdot f_{ctk.0.05}}{\gamma_c} = 1.2 \cdot MPa$ ('SS-EN 1992-1-1', 2008) section 3.1.6, eq. (3.16)

$f_{ywd} := 435MPa$ Assume reinforcing steel, S500

Control against web shear compression failure

$V_{Ed} \le 0.5 b_w \cdot d \cdot \nu \cdot f_{cd}$ Eq. (6.5)

$\nu := 0.6 \cdot \left(1 - \frac{f_{ck}}{250MPa} \right) = 0.54$ Eq. (6.6)

$V_{Ed} = 220 \cdot kN$

$0.5 b_w \cdot d \cdot \nu \cdot f_{cd} = 693 \cdot kN$

$$\text{Control}_{wscf} := \begin{cases} \text{"OK!"} & \text{if } V_{Ed} \le 0.5 b_w \cdot d \cdot \nu \cdot f_{cd} \\ \text{"Not OK"} & \text{otherwise} \end{cases} = \text{"OK!"}$$

Control if shear reinforcement is needed

Capacity is controlled at a distance *0.9d* from support face.

$$x := \frac{b_s}{2} + 0.9d = 0.57\,\text{m}$$

$$V_{Ed.x} := R_A - q_d \cdot x = 188.65 \cdot \text{kN}$$

$$V_{Ed.red.x} := V_{Ed.x} - \frac{(2d - x)^2}{4d} q_d = 181.627 \cdot \text{kN}$$

The load is reduced due to loading near support, see 6.2.2 (6)

$$V_{Rd.c} = \max\left(\left[C_{Rd.c} \cdot k \cdot \left(100 \rho_l \cdot f_{ck}\right)^{\frac{1}{3}}\right] b_w \cdot d, v_{min} \cdot b_w \cdot d\right)$$

Eq. (6.2)

$$C_{Rd.c} := \frac{0.18}{\gamma_c} = 0.12$$

Section 6.2.2

$$k := \min\left(1 + \sqrt{\frac{200\,\text{mm}}{d}}, 2.0\right) = 1.603$$

Section 6.2.2

$$\rho_l = \min\left(\frac{A_{sl}}{b_w \cdot d}, 0.02\right)$$

Section 6.2.2

$$A_{sl} := 8 \cdot \frac{\pi \cdot d_{sl}^2}{4} = 2.513 \times 10^{-3}\,\text{m}^2$$

Section 6.2.2

$$\rho_l := \min\left(\frac{A_{sl}}{b_w \cdot d}, 0.02\right) = 0.016$$

$$v_{min} := 0.035 \cdot k^{\frac{3}{2}} \cdot \left(\frac{f_{ck}}{\text{MPa}}\right)^{\frac{1}{2}} = 0.355$$

Section 6.2.2

$$V_{Rd.c} := \max\left(\left[C_{Rd.c}\cdot k\cdot\left(100\rho_l\cdot\frac{f_{ck}}{MPa}\right)^{\frac{1}{3}}\right]\frac{b_w\cdot d}{mm^2}\cdot N, v_{min}\cdot\frac{b_w\cdot d}{mm^2}N\right) = 101.983\cdot kN$$

$$Control_{reinf} := \begin{cases} \text{"No reinforcement is needed"} & \text{if } V_{Ed.red.x} \le V_{Rd.c} \\ \text{"Reinforcement is needed"} & \text{otherwise} \end{cases} = \text{"Reinforcement is needed"}$$

Design of reinforcement

Choose a crack inclination of 40°.

$\theta := 40deg$

$\cot(\theta) = 1.192$

$\cot(\theta)\cdot 0.9d = 0.59\,m$

$x := 75mm + .59m = 0.665\,m$

$V_{Ed.x} := R_A - x\cdot q_d = 183.425\cdot kN$

$V_{Ed.red.x} := V_{Ed.x} - \frac{(2d - x)^2}{4d}q_d = 178.694\cdot kN$

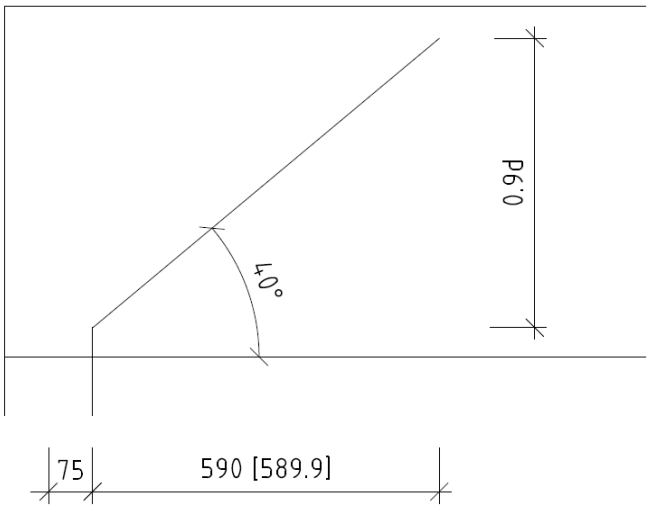

Control against web shear compression failure

$$V_{Rd.max} = \alpha_{cw} \cdot b_w \cdot z \cdot \nu_1 \cdot \frac{f_{cd}}{\cot(\theta) + \tan(\theta)} \qquad \text{Eq. (6.9)}$$

$\alpha_{cw} := 1$

$z := 0.9d = 0.495\ \text{m}$

$\nu_1 := \nu = 0.54$

$$V_{Rd.max} := \alpha_{cw} \cdot b_w \cdot z \cdot \nu_1 \cdot \frac{f_{cd}}{\cot(\theta) + \tan(\theta)} = 614.225 \cdot \text{kN}$$

Design of shear reinforcement

Assume vertical stirrups

$$V_{Rd.s} = \frac{A_{sw}}{s} \cdot z \cdot f_{ywd} \cdot \cot(\theta) \qquad \text{Eq. (6.8)}$$

$V_{Rd.s} \geq V_{Ed.red.x}$

$$z \cdot f_{ywd} \cdot \cot(\theta) = 2.566 \times 10^8 \frac{\text{kg}}{\text{s}^2}$$

$$\frac{A_{sw}}{s} \geq \frac{V_{Ed.red.x}}{z \cdot f_{ywd} \cdot \cot(\theta)}$$

$$\frac{V_{Ed.red.x}}{z \cdot f_{ywd} \cdot \cot(\theta)} = 696.354 \cdot \frac{\text{mm}^2}{\text{m}}$$

Assume shear reinforcement diameter 8 mm

$$A_{sw} := 2 \cdot \frac{\pi \cdot (8\text{mm})^2}{4} = 100.531 \cdot \text{mm}^2$$

$$s := A_{sw} \cdot \frac{z \cdot f_{ywd} \cdot \cot(\theta)}{V_{Ed.red.x}} = 0.144\ \text{m}$$

Choose shear reinforcement φ8 s140

$s := 140\text{mm}$

$$V_{Rd.s} := \frac{A_{sw}}{s} \cdot z \cdot f_{ywd} \cdot \cot(\theta) = 184.269 \cdot \text{kN}$$

Resistance according to BBK 04

The reinforcement designed in previous section will be used as input. Methods are described in BBK 04 Section 3.7 unless stated otherwise.

The crack inclination must be chosen to 45°.

$\theta := 45deg$

$V_{Ed.red.x} := V_{Ed.x} - \frac{(3d - x)^2}{6d} \cdot q_d = 167.255 \cdot kN$ Reduction of load according to Betonghandbok Konstruktion (AB Svensk Byggtjänst, 1990) Section 3.7 eq. (8)

Shear capacity

$V_{Sd} \le V_c + V_i + V_s$ Eq. (3.7.4.1a)

$V_d - V_i \le 0.25 b_w \cdot d \cdot f_{cd}$ Eq. (3.7.4.1b)

$V_c = b_w \cdot d \cdot f_v$ Eq. (3.7.3.2a)

$f_v = \xi \cdot (1 + 50\rho) \cdot 0.30 f_{ctd}$ Eq. (3.7.3.2b)

$$\rho := \min\left(\frac{8 \frac{\pi \cdot d_{sl}^2}{4}}{b_w \cdot d}, 0.02 \right) = 0.016$$

$$\xi := \begin{cases} 1.4 & \text{if } d \le 0.2m \\ \left(1.6 - \frac{d}{m}\right) & \text{if } 0.2m < d \le 0.5m \\ \left(1.3 - 0.4\frac{d}{m}\right) & \text{if } 0.5m < d \le 1.0m \\ 0.9 & \text{if } d > 1.0m \end{cases} = 1.08$$

$f_{ctd} = 1.2 \cdot MPa$ Assume same as for Eurocode 2, C25/30

$f_v := \xi \cdot (1 + 50\rho)\, 0.30 f_{ctd} = 0.706 \cdot MPa$

$V_c := b_w \cdot d \cdot f_v = 108.733 \cdot kN$

$V_i := 0$ No inclination

$V_s = A_{sw} \cdot f_{ywd} \cdot \frac{0.9d}{s} \cdot (\sin(\beta) + \cos(\beta))$ Eq. (3.7.4.2a)

$\beta := 90deg$ Angle between shear reinforcement and longitudinal axis of beam

$s = 140 \cdot mm$ Designed value according to Eurocode

$A_{sw} = 100.531 \cdot mm^2$ Designed value according to Eurocode

$V_s := A_{sw} \cdot f_{ywd} \cdot \frac{0.9d}{s} \cdot (\sin(\beta) + \cos(\beta)) = 154.62 \cdot kN$

$V_{Rd} := \min\left(V_c + V_i + V_s, 0.25 b_w \cdot d \cdot f_{cd}\right) = 263.353 \cdot kN$

Resistance according to SBN 80

The resistance may either be assumed to A) consist of the resistance coming from the shear reinforcement or it may B) be assumed to consist of both the resistance coming from the shear reinforcement and contributing concrete. Assumption B) is used here to resemble previous checks as much as possible. References in this section refer to "Bestämmelser för betongkonstruktioner - Allmänna konstruktionsbestämmelser" (Statens Betongkommitté, 1969) which is referred to from SBN specifically for concrete design.

$kp := 9.81N$ Conversion of unit

$R = \tau_{bo} \cdot b_w \cdot h + h \cdot A \cdot \sigma_a \cdot (\sin(\beta) + \cos(\beta))$ Section 2:2 eq. (12)

$A_{sw} = 1.005 \times 10^{-4} m^2$ Designed value according to Eurocode

$s = 140 \cdot mm$ Designed value according to Eurocode

$A := \frac{A_{sw}}{s} = 7.181 \times 10^{-4} \cdot \frac{m^2}{m}$ Amount of shear reinforcement per unit length

$\sigma_a := f_{ywd} = 435 \cdot MPa$

$\beta = 90 \cdot deg$

Assume concrete class K350, which yields similar strength values as C25/30

$\tau_{bo} := 4.7 \frac{kp}{cm^2} = 0.461 \cdot MPa$ Table 2:261

$R := \tau_{bo} \cdot b_w \cdot h + h \cdot A \cdot \sigma_a \cdot (\sin(\beta) + \cos(\beta)) = 264.878 \cdot kN$

Appendix B – Reinforcement layout

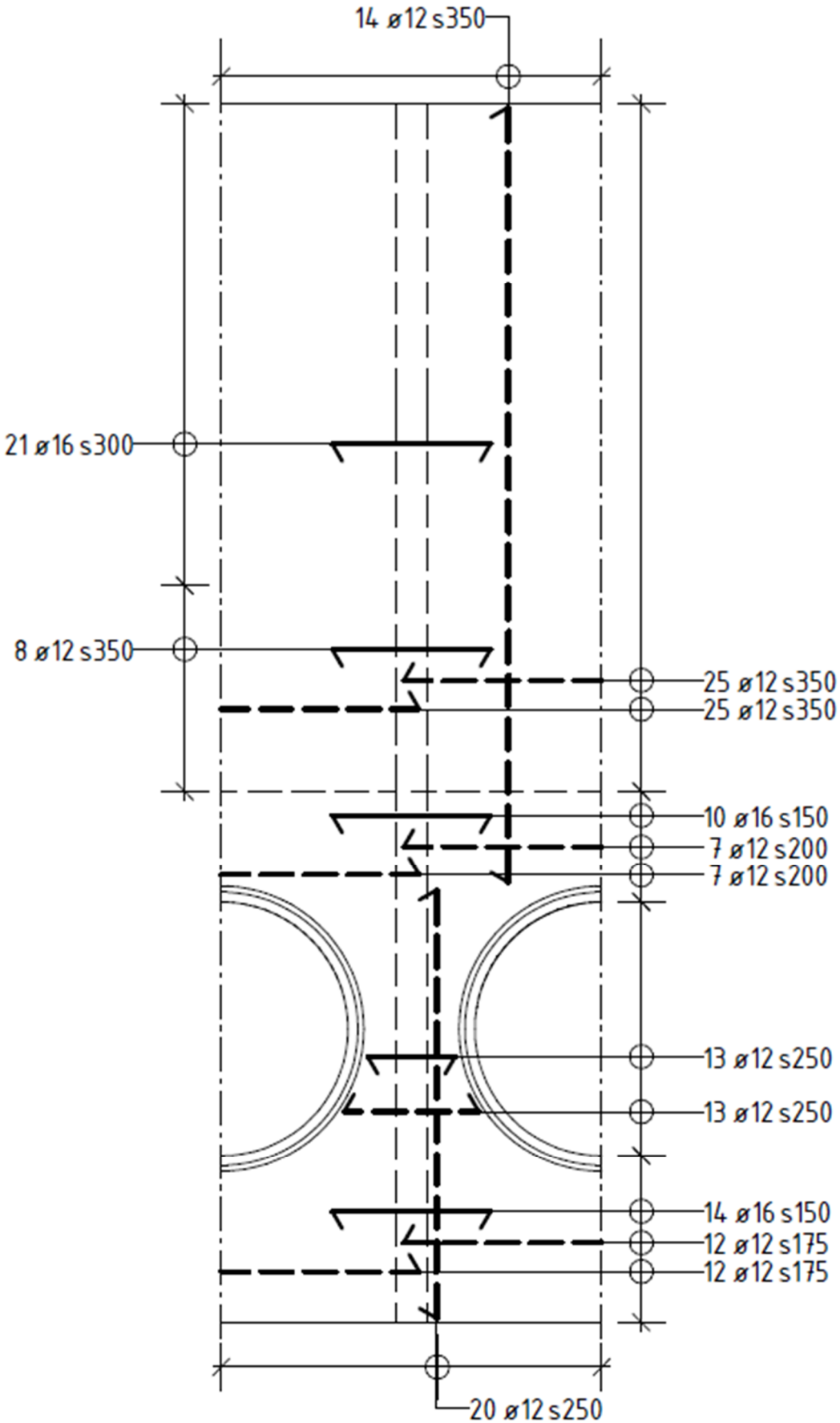
14 ø12 s350
21 ø16 s300
8 ø12 s350
25 ø12 s350
25 ø12 s350
10 ø16 s150
7 ø12 s200
7 ø12 s200
13 ø12 s250
13 ø12 s250
14 ø16 s150
12 ø12 s175
12 ø12 s175
20 ø12 s250

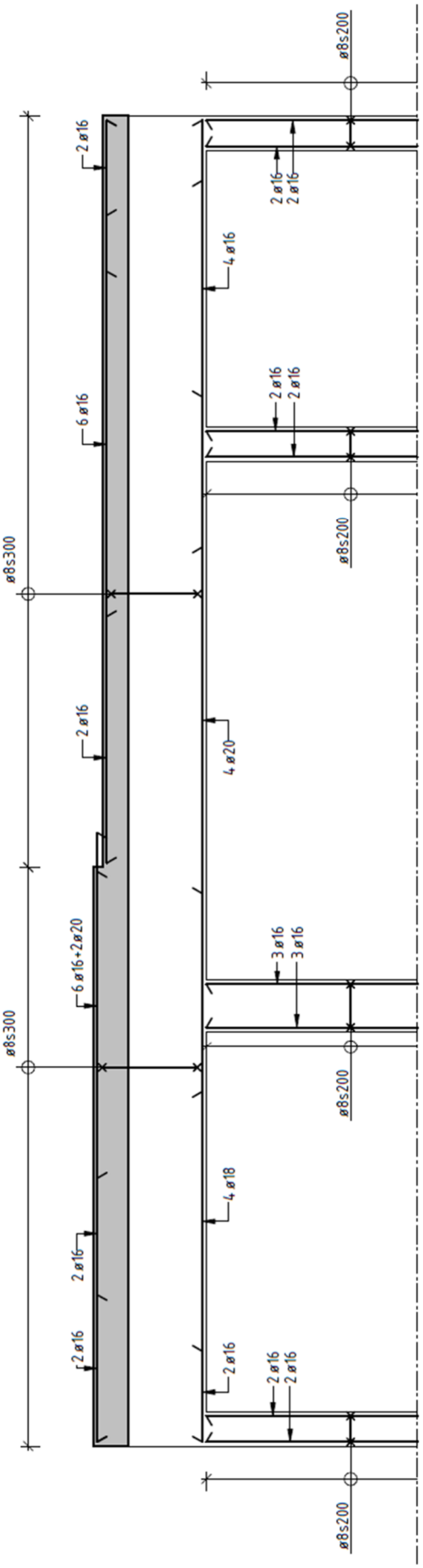
ø8s200
2 ø16
2 ø16
2 ø16
4 ø16
2 ø16
2 ø16
6 ø16
ø8s200
ø8s300
2 ø16
4 ø20
3 ø16
3 ø16
6 ø16+2ø20
ø8s200
ø8s300
4 ø18
2 ø16
2 ø16
2 ø16
2 ø16
ø8s200

Appendix C – Level I analysis

Geometry

Slab

$h_1 := 410mm$ Thicker part of the slab

$h_2 := 300mm$ Thinner part of the slab

$b := 1000mm$ consider 1m strip

Reinforcement

$r_{reinf} := 6mm$ radius of reinforcement bars

$A_{si} := r_{reinf}^2 \cdot \pi = 113.097 \cdot mm^2$

$s := 200mm$ spacing between bars

$A_s := \frac{A_{si} \cdot b}{s} = 565.487 \cdot mm^2$

$c_{cover} := 30mm$

$d_1 := h_1 - c_{cover} = 380 \cdot mm$ distance to reinforcement

$d_2 := h_2 - c_{cover} = 270 \cdot mm$

Material input

Concrete C25/30

$f_{ck} := 25MPa$

$\gamma_c := 1.5$

$f_{cd} := \frac{f_{ck}}{\gamma_c} = 16.667\,MPa$

$\rho_c := 2500 \frac{kg}{m^3}$ density of concrete

Shear Capacity

Slab thickness 410mm

$k_1 := \min\left[1 + \left(\frac{200 \cdot mm}{d_1}\right)^{0.5}, 2.0\right] = 1.725$

$\rho_{l1} := \min\left(\frac{A_s}{b \cdot d_1}, 0.02\right) = 1.488 \times 10^{-3}$

$$C_{Rd.c} := \frac{0.18}{\gamma_c} = 0.12$$

$$v_{min1} := 0.035 \cdot k_1^{\frac{3}{2}} \cdot \left(\frac{f_{ck}}{MPa} \right)^{0.5} = 0.397$$

$$V_{Rd.c1} := \left[C_{Rd.c} \cdot k_1 \cdot \left(100 \cdot \rho_{l1} \cdot \frac{f_{ck}}{MPa} \right)^{\frac{1}{3}} \right] \cdot \frac{b \cdot d_1}{mm^2} \cdot N = 121.918 \cdot kN$$

$$V_{Rd.c1.min} := v_{min1} \cdot \frac{b \cdot d_1}{mm^2} \cdot N = 150.725 \cdot kN$$

$$V_{Rd.c1} := \max\left(V_{Rd.c1}, V_{Rd.c1.min} \right)$$

$V_{Rd.c1} = 150.725 \cdot kN$

Slab thickness 300mm

$$k_2 := \min\left[1 + \left(\frac{200 \cdot mm}{d_2} \right)^{0.5}, 2.0 \right] = 1.861$$

$$\rho_{l2} := \min\left(\frac{A_s}{b \cdot d_2}, 0.02 \right) = 2.094 \times 10^{-3}$$

$$v_{min2} := 0.035 \cdot k_2^{\frac{3}{2}} \cdot \left(\frac{f_{ck}}{MPa} \right)^{0.5} = 0.444$$

$$V_{Rd.c2} := \left[C_{Rd.c} \cdot k_1 \cdot \left(100 \cdot \rho_{l2} \cdot \frac{f_{ck}}{MPa} \right)^{\frac{1}{3}} \right] \cdot \frac{b \cdot d_2}{mm^2} \cdot N = 97.078 \cdot kN$$

$$V_{Rd.c2.min} := v_{min2} \cdot \frac{b \cdot d_2}{mm^2} \cdot N$$

$$V_{Rd.c2} := \max\left(V_{Rd.c2}, V_{Rd.c2.min} \right)$$

$V_{Rd.c2} = 119.923 \cdot kN$

Capacity with regard to crushing

The capacity of the concrete with regard to crushing is calculated according to EC2 eq. 6.5

$\upsilon := 0.6 \cdot \left(1 - \frac{f_{ck}}{250\text{MPa}}\right) = 0.54$ Reduction factor

$V_{Ed.crush.410} := 0.5 \cdot b \cdot d_1 \cdot \upsilon \cdot f_{cd} = 1.71 \times 10^3\,\text{kN}$

$V_{Ed.crush.410} = 1.71 \times 10^3\,\text{kN}$

$V_{Ed.crush.300} := 0.5 \cdot b \cdot d_2 \cdot \upsilon \cdot f_{cd} = 1.215 \times 10^3\,\text{kN}$

$V_{Ed.crush.300} = 1.215 \times 10^3\,\text{kN}$

Shear in slab

Geometry

$l_m := 1.6\text{m}$ length of path over holes

$l_t := 4.8\text{m}$ length of path top of holes

$a := 0.4\text{m}$ width beam

$d := 0.41\text{m}$ thickness slab

Loads

$q_{self} := d \cdot 1\text{m} \cdot 1 \cdot \rho_c \cdot g = 10.052 \cdot \frac{\text{kN}}{\text{m}}$ Self weight

$q_d := 4.91\,\frac{\text{kN}}{\text{m}}$ distributed load on slab

$q_{silo} := 450\,\frac{\text{kN}}{\text{m}}$ distributed load from silo

$l_{silo} := 0.225\text{m}$ length on which distributed load from silo operate

$P_{silo} := q_{silo} \cdot l_{silo} = 101.25 \cdot \text{kN}$

Shear in slab with a distance a/2+d from centre

$$x_m := \frac{l_m}{2} - \left(\frac{a}{2} + d\right) = 0.19\,m$$

$$V_m := -P_{silo} - x_m \cdot \left(q_d + q_{self}\right) = -104.093 \cdot kN$$

$V_m = -104.093 \cdot kN$ Shear in slab path over holes

$$x_t := \frac{l_t}{2} - \left(\frac{a}{2} + d\right) = 1.79\,m$$

$$V_t := -P_{silo} - x_t \cdot \left(q_d + q_{self}\right) = -128.032 \cdot kN$$

$V_t = -128.032 \cdot kN$ Shear in slab path top of holes

Appendix D – Stiffness reductions for cracked concrete

Equivalent stiffness slab t=410 mm field

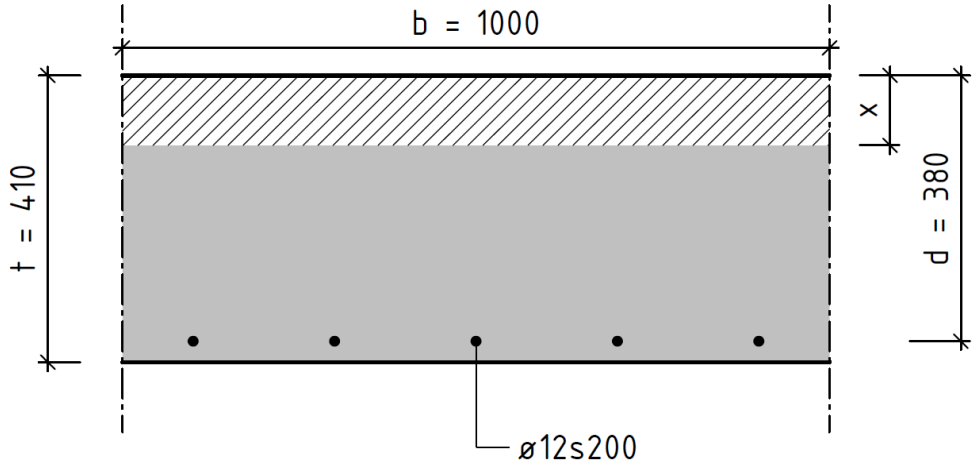

Concrete geometry

$b := 1m$

$t := 410mm$

Reinforcement geometry

$\varphi := 12mm$ Bar diameter

$s := 200mm$ Bar spacing

$A_s := \frac{\pi \cdot \varphi^2}{4} \cdot \frac{b}{s} = 5.655 \times 10^{-4} \cdot m^2$

$d := 380mm$ Distance from top of slab to reinforcement

Materials

$E_{cm} := 31GPa$ $f_{cm} := 33MPa$ Concrete C25/30

Creep

$\varphi_{inf.t0} = \beta_c \cdot \varphi_0$ Final creep coefficient

$\varphi_0 = \varphi_{RH} \cdot \beta_{fcm} \cdot \beta_{t0}$ Notional creep coefficient

$RH := 75\%$ BBK 04, Section 2.4.6, non-heated indoor

$A_c := b \cdot t = 0.41\,m^2$ Concrete area

$u := b = 1\,m$ Perimeter exposed to drying, assumed underside of slab

$$h_0 := \frac{2A_c}{u} = 0.82\,m$$

$$\varphi_{RH} := 1 + \frac{1 - \frac{RH \cdot 100}{100}}{0.1 \cdot \left(\frac{h_0 \cdot 1000}{m}\right)^{\frac{1}{3}}} = 1.267$$

$\beta_{fcm} := 2.93$

$\beta_{t0} := \frac{1}{0.1 + 15^{0.2}} = 0.55$ Assume load is applied at t=15 days

$\varphi_0 := \varphi_{RH} \cdot \beta_{fcm} \cdot \beta_{t0} = 2.041$

$$\beta_c = \left[\frac{t - t_0}{\beta_H + (t - t_0)}\right]^{0.3}$$

$$\beta_H := \min\left[1.5 \cdot \left[1 + (0.012 \cdot RH)^{18}\right] \cdot \frac{h_0 \cdot 1000}{m} + 250, 1500\right] = 1.48 \times 10^3$$

$$\beta_c := \left[\frac{50 \cdot 365 - 1}{\beta_H + (50 \cdot 365 - 1)}\right]^{0.3} = 0.977$$

$\varphi_{inf.t0} := \beta_c \cdot \varphi_0 = 1.994$ Final creep coefficient

Steel

$E_s := 200GPa$

$$\alpha_{ef} := \frac{E_s}{E_{cm}} \cdot \left(1 + \varphi_{inf.t0}\right) = 19.317$$

Calculate second moment of inertia in stadium I

$$I_I := \frac{b \cdot t^3}{12} = 5.743 \times 10^{-3}\,m^4$$

Calculate second moment of inertia in stadium II

$x := 0.1m$ First guess

Given

$$b \cdot x \cdot \frac{x}{2} = \alpha_{ef} \cdot A_s \cdot (d - x)$$

$x := \text{Find}(x)$

$x = 0.081\,m$

$$I_{II} := \frac{b \cdot x^3}{12} + \alpha_{ef} \cdot A_s \cdot (d - x)^2 = 1.022 \times 10^{-3}\,m^4$$

Stiffness reduction

$$E_{slab.410.field} := \frac{I_{II}}{I_I} = 0.178$$

Equivalent stiffness slab t=300 mm field

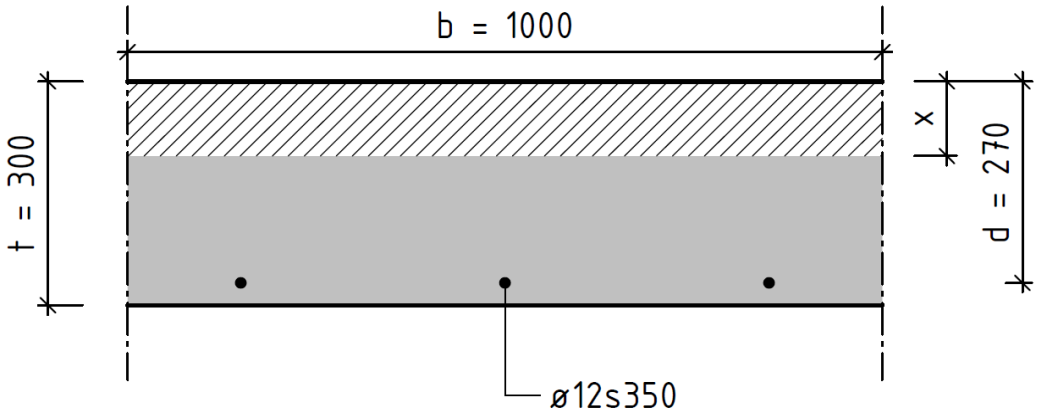

Concrete geometry

$b := 1m$

$t := 300mm$

Reinforcement geometry

$\varphi := 12mm$

$s := 350mm$

$A_{sx} := \frac{\pi \cdot \varphi^2}{4} \cdot \frac{b}{s} = 3.231 \times 10^{-4} \cdot m^2$

$d := 270mm$

Materials

$E_{cm} := 31GPa$ $f_{cm} := 33MPa$ Concrete C25/30

Creep

$\varphi_{inf.t0} = \beta_c \cdot \varphi_0$ Final creep coefficient

$\varphi_0 = \varphi_{RH} \cdot \beta_{fcm} \cdot \beta_{t0}$ Notional creep coefficient

$RH := 75\%$ BBK 04, Section 2.4.6, non-heated indoor

$A_c := b \cdot t = 0.3\,m^2$ Concrete area

$u := b = 1\,m$ Perimeter exposed to drying, assumed underside of slab

$$h_0 := \frac{2A_c}{u} = 0.6\,m$$

$$\varphi_{RH} := 1 + \frac{1 - \frac{RH \cdot 100}{100}}{0.1 \cdot \left(\frac{h_0 \cdot 1000}{m}\right)^{\frac{1}{3}}} = 1.296$$

$\beta_{fcm} := 2.93$

$\beta_{t0} := \frac{1}{0.1 + 15^{0.2}} = 0.55$ Assume load is applied at t=15 days

$\varphi_0 := \varphi_{RH} \cdot \beta_{fcm} \cdot \beta_{t0} = 2.088$

$$\beta_c = \left[\frac{t - t_0}{\beta_H + (t - t_0)}\right]^{0.3}$$

$$\beta_H := \min\left[1.5 \cdot \left[1 + (0.012 \cdot RH)^{18}\right] \cdot \frac{h_0 \cdot 1000}{m} + 250, 1500\right] = 1.15 \times 10^3$$

$$\beta_c := \left[\frac{50 \cdot 365 - 1}{\beta_H + (50 \cdot 365 - 1)}\right]^{0.3} = 0.982$$

$\varphi_{inf.t0} := \beta_c \cdot \varphi_0 = 2.051$ Final creep coefficient

Steel

$E_s := 200GPa$

$$\alpha_{ef} := \frac{E_s}{E_{cm}} \cdot \left(1 + \varphi_{inf.t0}\right) = 19.681$$

Calculate second moment of inertia in stadium I

$$I_I := \frac{b \cdot t^3}{12} = 2.25 \times 10^{-3}\,m^4$$

Calculate second moment of inertia in stadium II

$x := 0.1m$ First guess

Given

$$b \cdot x \cdot \frac{x}{2} = \alpha_{ef} \cdot A_s \cdot (d - x)$$

$x := \text{Find}(x)$

$x = 0.053\,m$

$$I_{II} := \frac{b \cdot x^3}{12} + \alpha_{ef} \cdot A_s \cdot (d - x)^2 = 3.127 \times 10^{-4}\,m^4$$

Stiffness reduction

$$E_{slab.300.field} := \frac{I_{II}}{I_I} = 0.139$$

Equivalent stiffness T-section 0<x<4.5m (compressed top)

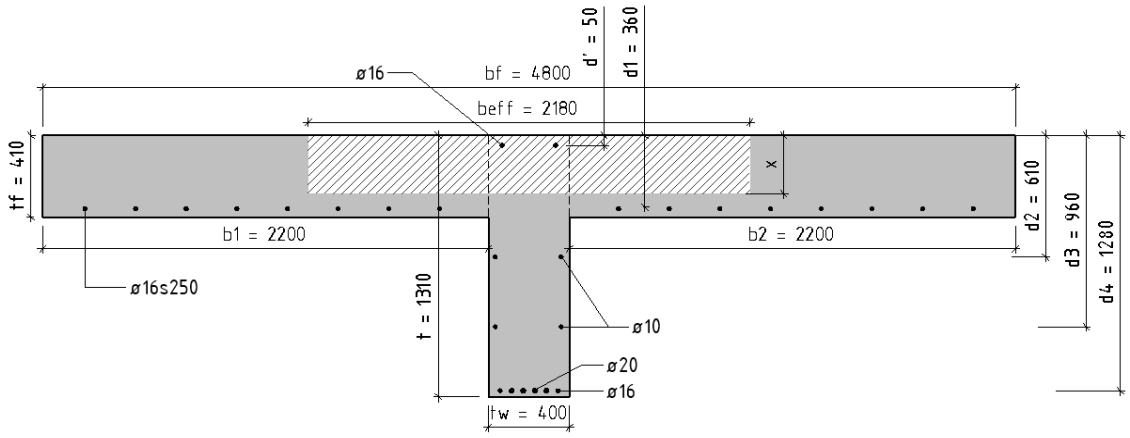

Concrete geometry

$b_f := 4800mm$

$t_f := 410mm$

$h_w := 900mm$

$t_w := 400mm$

$b_1 := \frac{b_f - t_w}{2} = 2.2\,m$

$b_2 := b_1$

$l_0 := 4.5m$ From Abaqus model with shells

$b_{eff.1} := \min\left(0.2b_1 + 0.1l_0, 0.2l_0\right) = 0.89\,m$

$b_{eff.2} := b_{eff.1}$

$b_{eff} := b_{eff.1} + b_{eff.2} + t_w = 2.18\,m$

Reinforcement geometry

$\varphi' := 16mm$ $n' := 2$ $d' := 50mm$

$\varphi_1 := 16mm$ $n_1 := 6$ $d_1 := 360mm$

$\varphi_2 := 10mm$ $n_2 := 2$ $d_2 := 610mm$

$\varphi_3 := 10mm$ $n_3 := 2$ $d_3 := 960mm$

$\varphi_{41} := 16mm$ $n_{41} := 2$ $\varphi_{42} := 20mm$ $n_{42} := 4$ $d_4 := 1280mm$

$$A'_s := n' \cdot \frac{\pi \cdot \varphi'^2}{4} = 4.021 \times 10^{-4}\, m^2$$

$$A_{s1} := n_1 \cdot \frac{\pi \cdot \varphi_1^2}{4} = 1.206 \times 10^{-3}\, m^2$$

$$A_{s2} := n_2 \cdot \frac{\pi \cdot \varphi_2^2}{4} = 1.571 \times 10^{-4}\, m^2$$

$$A_{s3} := n_3 \cdot \frac{\pi \cdot \varphi_3^2}{4} = 1.571 \times 10^{-4}\, m^2$$

$$A_{s4} := n_{41} \cdot \frac{\pi \cdot \varphi_{41}^2}{4} + n_{42} \cdot \frac{\pi \cdot \varphi_{42}^2}{4} = 1.659 \times 10^{-3}\, m^2$$

Materials

$E_{cm} = 31 \cdot GPa$ $f_{cm} := 33MPa$ Concrete C25/30

Creep

$\varphi_{inf.t0} = \beta_c \cdot \varphi_0$ Final creep coefficient

$\varphi_0 = \varphi_{RH} \cdot \beta_{fcm} \cdot \beta_{t0}$ Notional creep coefficient

$RH := 75\%$ BBK 04, Section 2.4.6, non-heated indoor

$A_c := b_{eff} \cdot t_f + t_w \cdot h_w = 1.254\,m^2$ Concrete area

$u := b_{eff.1} + b_{eff.2} + 2 \cdot h_w + t_w = 3.98\,m$ Perimeter exposed to drying, assumed underside of slab and complete beam

$$h_0 := \frac{2A_c}{u} = 0.63\,m$$

$$\varphi_{RH} := 1 + \frac{1 - \frac{RH \cdot 100}{100}}{0.1 \cdot \left(\frac{h_0 \cdot 1000}{m}\right)^{\frac{1}{3}}} = 1.292$$

$\beta_{fcm} := 2.93$

$\beta_{t0} := \frac{1}{0.1 + 15^{0.2}} = 0.55$ Assume load is applied at t=15 days

$\varphi_0 := \varphi_{RH} \cdot \beta_{fcm} \cdot \beta_{t0} = 2.081$

$$\beta_c = \left[\frac{t - t_0}{\beta_H + (t - t_0)}\right]^{0.3}$$

$$\beta_H := \min\left[1.5 \cdot \left[1 + (0.012 \cdot RH)^{18}\right] \cdot \frac{h_0 \cdot 1000}{m} + 250, 1500\right] = 1.195 \times 10^3$$

$$\beta_c := \left[\frac{50 \cdot 365 - 1}{\beta_H + (50 \cdot 365 - 1)}\right]^{0.3} = 0.981$$

$\varphi_{inf.t0} := \beta_c \cdot \varphi_0 = 2.042$ Final creep coefficient

Steel

$E_s := 200GPa$

$$\alpha_{ef} := \frac{E_s}{E_{cm}} \cdot \left(1 + \varphi_{inf.t0}\right) = 19.623$$

Calculate position of neutral layer, assume one layer of reinforcement in compression zone

$x := 0.1\,m$ First guess

Given

$$b_{eff}\cdot x\cdot\frac{x}{2} + (\alpha_{ef}-1)\cdot A'_s\cdot(x-d') = \alpha_{ef}\cdot A_{s1}\cdot(d_1-x) + \alpha_{ef}\cdot A_{s2}\cdot(d_2-x) + \alpha_{ef}\cdot A_{s3}\cdot(d_3-x) \ldots + \alpha_{ef}\cdot A_{s4}\cdot(d_4-x)$$

$x := \text{Find}(x)$

$x = 0.196\,m$

"OK, assumption is correct " if $x < d_1$ = "OK, assumption is correct "

"Not OK" otherwise

Second moment of inertia of slab part

$$I_{II.slab} := \frac{b_{eff}\cdot x^3}{12} + (\alpha_{ef}-1)\cdot A'_s\cdot(x-d')^2 \ldots + \alpha_{ef}\cdot A_{s1}\cdot(d_1-x)^2 = 2.159\times 10^{-3}\,m^4$$ Stadium II

$$I_{I.slab} := \frac{b_{eff}\cdot t_f^3}{12} + (\alpha_{ef}-1)\cdot A'_s\cdot(x-d')^2 \ldots + (\alpha_{ef}-1)\cdot A_{s1}\cdot(d_1-x)^2 = 0.013\,m^4$$ Stadium I

Second moment of inertia of beam part

$$I_{II.beam} := \alpha_{ef}\cdot A_{s2}\cdot(d_2-t_f)^2 + \alpha_{ef}\cdot A_{s3}\cdot(d_3-t_f)^2 + \alpha_{ef}\cdot A_{s4}\cdot(d_4-t_f)^2 = 0.026\,m^4$$

$$I_{I.beam} := \frac{t_w\cdot h_w^3}{12} + (\alpha_{ef}-1)\cdot A_{s2}\cdot(d_2-t_f)^2 + (\alpha_{ef}-1)\cdot A_{s3}\cdot(d_3-t_f)^2 \ldots + (\alpha_{ef}-1)\cdot A_{s4}\cdot(d_4-t_f)^2 = 0.049\,m^4$$

Stiffness reduction

$$E_{slab.support.1} := \frac{I_{II.slab}}{I_{I.slab}} = 0.162$$

$$E_{beam.1} := \frac{I_{II.beam}}{I_{I.beam}} = 0.528$$

Equivalent stiffness T-section 4.5<x<6.8m (compressed bottom)

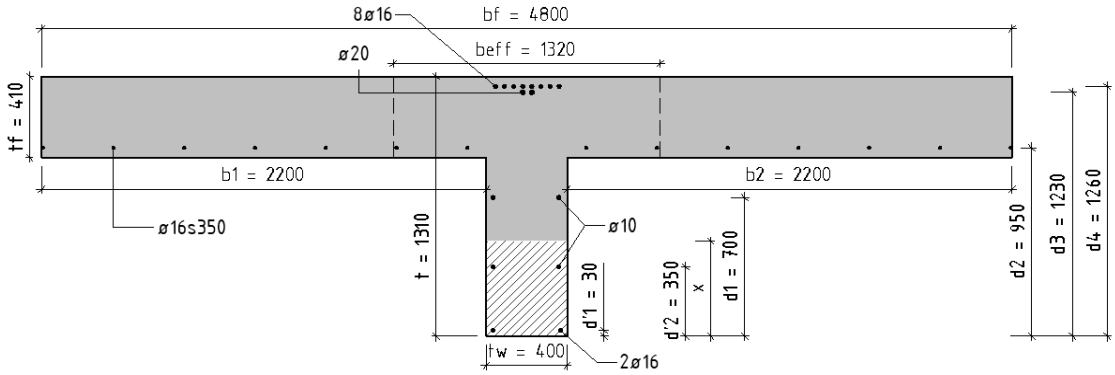

Concrete geometry

$b_f = 4.8\,\text{m}$

$t_f = 0.41\,\text{m}$

$h_w = 0.9\,\text{m}$

$t_w = 0.4\,\text{m}$

$b_1 = 2.2\,\text{m}$

$b_2 = 2.2\,\text{m}$

$l_0 := 2.3\text{m}$ From Abaqus model with shells

$b_{eff.1} := \min\left(0.2b_1 + 0.1l_0, 0.2l_0\right) = 0.46\,\text{m}$

$b_{eff.2} := b_{eff.1}$

$b_{eff} := b_{eff.1} + b_{eff.2} + t_w = 1.32\,\text{m}$

Reinforcement geometry

$\varphi'_1 := 16mm$ $n'_1 := 2$ $d'_1 := 30mm$

$\varphi'_2 := 10mm$ $n'_2 := 2$ $d'_2 := 350mm$

$\varphi_1 := 10mm$ $n_1 := 2$ $d_1 := 700mm$

$\varphi_2 := 16mm$ $n_2 := 4$ $d_2 := 950mm$

$\varphi_3 := 20mm$ $n_3 := 2$ $d_3 := 1230mm$

$\varphi_4 := 16mm$ $n_4 := 8$ $d_4 := 1260mm$

$$A'_{s1} := n'_1 \cdot \frac{\pi \cdot \varphi'^{2}_1}{4} = 4.021 \times 10^{-4}\, m^2$$

$$A'_{s2} := n'_2 \cdot \frac{\pi \cdot \varphi'^{2}_2}{4} = 1.571 \times 10^{-4}\, m^2$$

$$A_{s1} := n_1 \cdot \frac{\pi \cdot \varphi_1^{2}}{4} = 1.571 \times 10^{-4}\, m^2$$

$$A_{s2} := n_2 \cdot \frac{\pi \cdot \varphi_2^{2}}{4} = 8.042 \times 10^{-4}\, m^2$$

$$A_{s3} := n_3 \cdot \frac{\pi \cdot \varphi_3^{2}}{4} = 6.283 \times 10^{-4}\, m^2$$

$$A_{s4} := n_4 \cdot \frac{\pi \cdot \varphi_4^{2}}{4} = 1.608 \times 10^{-3}\, m^2$$

Materials

$E_{cm} = 31 \cdot GPa$ $f_{cm} = 33 \cdot MPa$ Concrete C25/30

Creep

$\varphi_{inf.t0} = \beta_c \cdot \varphi_0$ Final creep coefficient

$\varphi_0 = \varphi_{RH} \cdot \beta_{fcm} \cdot \beta_{t0}$ Notional creep coefficient

$RH = 75 \cdot \%$ BBK 04, Section 2.4.6, non-heated indoor

$A_c := b_{eff} \cdot t_f + t_w \cdot h_w = 0.901\,m^2$ Concrete area

$u := b_{eff.1} + b_{eff.2} + 2 \cdot h_w + t_w = 3.12\,m$ Perimeter exposed to drying, assumed underside of slab and complete beam

$$h_0 := \frac{2A_c}{u} = 0.578\,m$$

$$\varphi_{RH} := 1 + \frac{1 - \frac{RH \cdot 100}{100}}{0.1 \cdot \left(\frac{h_0 \cdot 1000}{m}\right)^{\frac{1}{3}}} = 1.3$$

$\beta_{fcm} := 2.93$

$\beta_{t0} := \frac{1}{0.1 + 15^{0.2}} = 0.55$ Assume load is applied at t=15 days

$\varphi_0 := \varphi_{RH} \cdot \beta_{fcm} \cdot \beta_{t0} = 2.095$

$$\beta_c = \left[\frac{t - t_0}{\beta_H + (t - t_0)}\right]^{0.3}$$

$$\beta_H := \min\left[1.5 \cdot \left[1 + (0.012 \cdot RH)^{18}\right] \cdot \frac{h_0 \cdot 1000}{m} + 250, 1500\right] = 1.117 \times 10^3$$

$$\beta_a := \left[\frac{50 \cdot 365 - 1}{\beta_H + (50 \cdot 365 - 1)}\right]^{0.3} = 0.982$$

$\varphi_{inf.t0} := \beta_c \cdot \varphi_0 = 2.058$ Final creep coefficient

Steel

$E_s = 200 \cdot GPa$

$\alpha_{ef} := \frac{E_s}{E_{cm}} \cdot \left(1 + \varphi_{inf.t0}\right) = 19.726$

Calculate position of neutral layer, assume two layers of reinforcement in compression zone

$x := 0.1m$ First guess

Given

$$t_w \cdot x \cdot \frac{x}{2} + \left(\alpha_{ef} - 1\right) \cdot A'_{s1} \cdot \left(x - d'_1\right) + \left(\alpha_{ef} - 1\right) \cdot A'_{s2} \cdot \left(x - d'_2\right) = \alpha_{ef} \cdot A_{s1} \cdot \left(d_1 - x\right) \ldots + \alpha_{ef} \cdot A_{s2} \cdot \left(d_2 - x\right) \ldots + \alpha_{ef} \cdot A_{s3} \cdot \left(d_3 - x\right) \ldots + \alpha_{ef} \cdot A_{s4} \cdot \left(d_4 - x\right)$$

$x := Find(x)$

$x = 0.45\,m$

"OK, assumption is correct" if $d'_2 < x < d_1$ = "OK, assumption is correct"

"Not OK" otherwise

Second moment of inertia of slab part

$I_{II.slab} := \alpha_{ef} \cdot A_{s2} \cdot \left(d_2 - h_w\right)^2 + \alpha_{ef} \cdot A_{s3} \cdot \left(d_3 - h_w\right)^2 \ldots + \alpha_{ef} \cdot A_{s4} \cdot \left(d_4 - h_w\right)^2 = 5.502 \times 10^{-3}\,m^4$ Stadium II

$I_{I.slab} := \frac{b_{eff} \cdot t_f^3}{12} + \left(\alpha_{ef} - 1\right) \cdot A_{s2} \cdot \left(d_2 - h_w\right)^2 \ldots + \left(\alpha_{ef} - 1\right) \cdot A_{s3} \cdot \left(d_3 - h_w\right)^2 + \left(\alpha_{ef} - 1\right) \cdot A_{s4} \cdot \left(d_4 - x\right)^2 = 0.029\,m^4$ Stadium I

Second moment of inertia of beam part

$$I_{II.beam} := \frac{t_w \cdot x^3}{12} + (\alpha_{ef} - 1) \cdot A'_{s1} \cdot (x - d'_1)^2 + (\alpha_{ef} - 1) \cdot A'_{s2} \cdot (x - d'_2)^2 + \alpha_{ef} \cdot A_{s1} \cdot (d_1 - x)^2 \ldots = 4.601 \times 10^{-3}\,\mathrm{m}^4$$

$$I_{I.beam} := \frac{t_w \cdot h_w^3}{12} + (\alpha_{ef} - 1) \cdot A'_{s1} \cdot (t_f - d'_1)^2 + (\alpha_{ef} - 1) \cdot A'_{s2} \cdot (t_f - d_3)^2 + (\alpha_{ef} - 1) \cdot A_{s1} \cdot (t_f - d_4)^2 \ldots = 0.029\,\mathrm{m}^4$$

Stiffness reduction

$$E_{slab.support.2} := \frac{I_{II.slab}}{I_{I.slab}} = 0.192$$

$$E_{beam.2} := \frac{I_{II.beam}}{I_{I.beam}} = 0.156$$

Equivalent stiffness T-section 6.8<x<10.2m (compressed top), assuming beam 900mm high

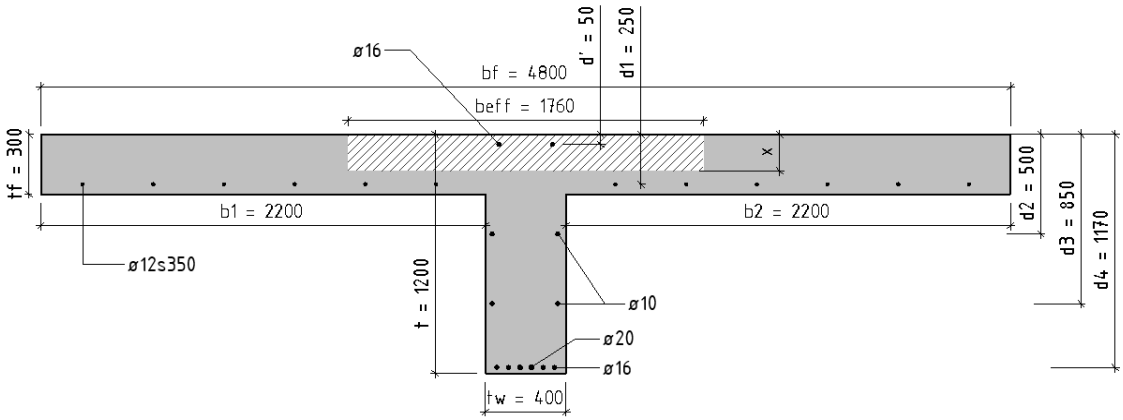

Concrete geometry

$b_f := 4800mm$

$t_f := 300mm$

$h_w := 900mm$

$t_w := 400mm$

$b_1 := \frac{b_f - t_w}{2} = 2.2\,m$

$b_2 := b_1$

$l_0 := 3.4m$ From Abaqus model with shells

$b_{eff.1} := \min\left(0.2b_1 + 0.1l_0, 0.2l_0\right) = 0.68\,m$

$b_{eff.2} := b_{eff.1}$

$b_{eff} := b_{eff.1} + b_{eff.2} + t_w = 1.76\,m$

Reinforcement geometry

$\varphi' := 16mm$ $n' := 2$ $d' := 50mm$

$\varphi_1 := 12mm$ $n_1 := 4$ $d_1 := 250mm$

$\varphi_2 := 10mm$ $n_2 := 2$ $d_2 := 500mm$

$\varphi_3 := 10mm$ $n_3 := 2$ $d_3 := 850mm$

$\varphi_{41} := 16mm$ $n_{41} := 4$ $\varphi_{42} := 20mm$ $n_{41} := 2$ $d_4 := 1170mm$

$$A'_s := n' \cdot \frac{\pi \cdot \varphi'^2}{4} = 4.021 \times 10^{-4}\, m^2$$

$$A_{s1} := n_1 \cdot \frac{\pi \cdot \varphi_1^2}{4} = 4.524 \times 10^{-4}\, m^2$$

$$A_{s2} := n_2 \cdot \frac{\pi \cdot \varphi_2^2}{4} = 1.571 \times 10^{-4}\, m^2$$

$$A_{s3} := n_3 \cdot \frac{\pi \cdot \varphi_3^2}{4} = 1.571 \times 10^{-4}\, m^2$$

$$A_{s4} := n_{41} \cdot \frac{\pi \cdot \varphi_{41}^2}{4} + n_{42} \cdot \frac{\pi \cdot \varphi_{42}^2}{4} = 1.659 \times 10^{-3}\, m^2$$

Materials

$E_{cm} = 31 \cdot GPa$ $f_{cm} := 33MPa$ Concrete C25/30

Creep

$\varphi_{inf.t0} = \beta_c \cdot \varphi_0$ Final creep coefficient

$\varphi_0 = \varphi_{RH} \cdot \beta_{fcm} \cdot \beta_{t0}$ Notional creep coefficient

$RH := 75\%$ BBK 04, Section 2.4.6, non-heated indoor

$A_c := b_{eff} \cdot t_f + t_w \cdot h_w = 0.888\,m^2$ Concrete area

$u := b_{eff.1} + b_{eff.2} + 2 \cdot h_w + t_w = 3.56\,m$ Perimeter exposed to drying, assumed underside of slab and complete beam

$$h_0 := \frac{2A_c}{u} = 0.499\,m$$

$$\varphi_{RH} := 1 + \frac{1 - \frac{RH \cdot 100}{100}}{0.1 \cdot \left(\frac{h_0 \cdot 1000}{m}\right)^{\frac{1}{3}}} = 1.315$$

$\beta_{fcm} := 2.93$

$\beta_{t0} := \frac{1}{0.1 + 15^{0.2}} = 0.55$ Assume load is applied at t=15 days

$\varphi_0 := \varphi_{RH} \cdot \beta_{fcm} \cdot \beta_{t0} = 2.119$

$$\beta_c = \left[\frac{t - t_0}{\beta_H + (t - t_0)}\right]^{0.3}$$

$$\beta_H := \min\left[1.5 \cdot \left[1 + (0.012 \cdot RH)^{18}\right] \cdot \frac{h_0 \cdot 1000}{m} + 250, 1500\right] = 998.315$$

$$\beta_c := \left[\frac{50 \cdot 365 - 1}{\beta_H + (50 \cdot 365 - 1)}\right]^{0.3} = 0.984$$

$\varphi_{inf.t0} := \beta_c \cdot \varphi_0 = 2.085$ Final creep coefficient

Steel

$E_s := 200GPa$

$\alpha_{ef} := \frac{E_s}{E_{cm}} \cdot \left(1 + \varphi_{inf.t0}\right) = 19.905$

Calculate position of neutral layer, assume one layer of reinforcement in compression zone

$x := 0.1\,m$ First guess

Given

$$b_{eff}\cdot x\cdot\frac{x}{2} + (\alpha_{ef} - 1)\cdot A'_s\cdot(x - d') = \alpha_{ef}\cdot A_{s1}\cdot(d_1 - x) + \alpha_{ef}\cdot A_{s2}\cdot(d_2 - x) + \alpha_{ef}\cdot A_{s3}\cdot(d_3 - x) \ldots + \alpha_{ef}\cdot A_{s4}\cdot(d_4 - x)$$

$x := \text{Find}(x)$

$x = 0.198\,m$

"OK, assumption is correct " if $x < d_1$ = "OK, assumption is correct "

"Not OK" otherwise

Second moment of inertia of slab part

$$I_{II.slab} := \frac{b_{eff}\cdot x^3}{12} + (\alpha_{ef} - 1)\cdot A'_s\cdot(x - d')^2 + \alpha_{ef}\cdot A_{s1}\cdot(d_1 - x)^2 = 1.326\times 10^{-3}\,m^4$$ Stadium II

$$I_{I.slab} := \frac{b_{eff}\cdot t_f^3}{12} + (\alpha_{ef} - 1)\cdot A'_s\cdot(x - d')^2 \ldots = 4.151\times 10^{-3}\,m^4$$ Stadium I
$$+ \alpha_{ef}\cdot A_{s1}\cdot(d_1 - x)^2$$

Second moment of inertia of beam part

$$I_{II.beam} := \alpha_{ef}\cdot A_{s2}\cdot(d_2 - t_f)^2 + \alpha_{ef}\cdot A_{s3}\cdot(d_3 - t_f)^2 + \alpha_{ef}\cdot A_{s4}\cdot(d_4 - t_f)^2 = 0.026\,m^4$$

$$I_{I.beam} := \frac{t_w\cdot h_w^3}{12} + (\alpha_{ef} - 1)\cdot A_{s2}\cdot(d_2 - t_f)^2 + (\alpha_{ef} - 1)\cdot A_{s3}\cdot(d_3 - t_f)^2 \ldots = 0.049\,m^4$$
$$+ (\alpha_{ef} - 1)\cdot A_{s4}\cdot(d_4 - t_f)^2$$

Stiffness reduction

$$E_{slab.support.3} := \frac{I_{II.slab}}{I_{I.slab}} = 0.319$$

$$E_{beam.3} := \frac{I_{II.beam}}{I_{I.beam}} = 0.531$$

Equivalent stiffness T-section 10.2<x<12.2m (compressed bottom), assuming beam 900mm high

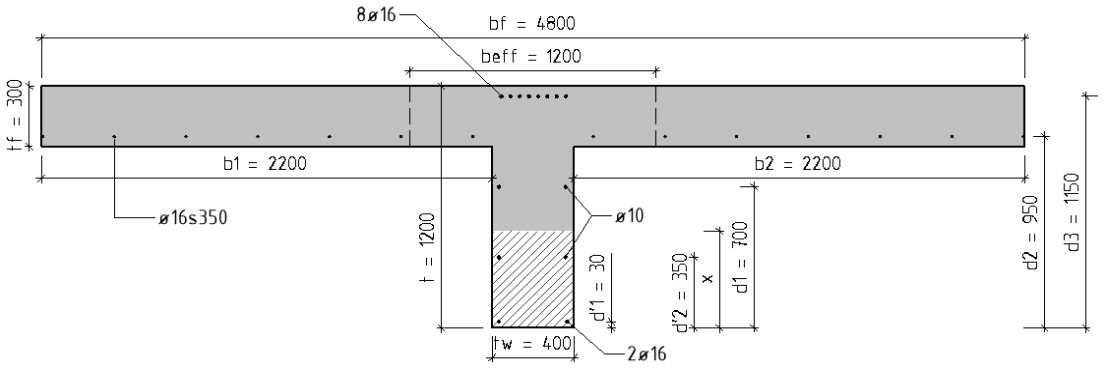

Concrete geometry

$b_f = 4.8\,\text{m}$

$t_f = 0.3\,\text{m}$

$h_w = 0.9\,\text{m}$

$t_w = 0.4\,\text{m}$

$b_1 = 2.2\,\text{m}$

$b_2 = 2.2\,\text{m}$

$l_0 := 2\text{m}$ From Abaqus model with shells

$b_{eff.1} := \min\left(0.2b_1 + 0.1l_0, 0.2l_0\right) = 0.4\,\text{m}$

$b_{eff.2} := b_{eff.1}$

$b_{eff} := b_{eff.1} + b_{eff.2} + t_w = 1.2\,\text{m}$

Reinforcement geometry

$\varphi'_1 := 16mm$ $n'_1 := 2$ $d'_1 := 30mm$

$\varphi'_2 := 10mm$ $n'_2 := 2$ $d'_2 := 350mm$

$\varphi_1 := 10mm$ $n_1 := 2$ $d_1 := 700mm$

$\varphi_2 := 12mm$ $n_2 := 2$ $d_2 := 950mm$

$\varphi_3 := 16mm$ $n_3 := 8$ $d_3 := 1150mm$

$$A'_{s1} := n'_1 \cdot \frac{\pi \cdot \varphi'^{2}_1}{4} = 4.021 \times 10^{-4}\, m^2$$

$$A'_{s2} := n'_2 \cdot \frac{\pi \cdot \varphi'^{2}_2}{4} = 1.571 \times 10^{-4}\, m^2$$

$$A_{s1} := n_1 \cdot \frac{\pi \cdot \varphi^{2}_1}{4} = 1.571 \times 10^{-4}\, m^2$$

$$A_{s2} := n_2 \cdot \frac{\pi \cdot \varphi^{2}_2}{4} = 2.262 \times 10^{-4}\, m^2$$

$$A_{s3} := n_3 \cdot \frac{\pi \cdot \varphi^{2}_3}{4} = 1.608 \times 10^{-3}\, m^2$$

Materials

$E_{cm} = 31 \cdot GPa$ $f_{cm} = 33 \cdot MPa$ Concrete C25/30

Creep

$\varphi_{inf.t0} = \beta_c \cdot \varphi_0$ Final creep coefficient

$\varphi_0 = \varphi_{RH} \cdot \beta_{fcm} \cdot \beta_{t0}$ Notional creep coefficient

$RH = 75 \cdot \%$ BBK 04, Section 2.4.6, non-heated indoor

$A_c := b_{eff} \cdot t_f + t_w \cdot h_w = 0.72\,m^2$ Concrete area

$u := b_{eff.1} + b_{eff.2} + 2 \cdot h_w + t_w = 3\,m$ Perimeter exposed to drying, assumed underside of slab and complete beam

$$h_0 := \frac{2A_c}{u} = 0.48\,m$$

$$\varphi_{RH} := 1 + \frac{1 - \frac{RH \cdot 100}{100}}{0.1 \cdot \left(\frac{h_0 \cdot 1000}{m}\right)^{\frac{1}{3}}} = 1.319$$

$\beta_{fcm} := 2.93$

$\beta_{t0} := \frac{1}{0.1 + 15^{0.2}} = 0.55$ Assume load is applied at t=15 days

$\varphi_0 := \varphi_{RH} \cdot \beta_{fcm} \cdot \beta_{t0} = 2.125$

$$\beta_c = \left[\frac{t - t_0}{\beta_H + (t - t_0)}\right]^{0.3}$$

$$\beta_H := \min\left[1.5 \cdot \left[1 + (0.012 \cdot RH)^{18}\right] \cdot \frac{h_0 \cdot 1000}{m} + 250, 1500\right] = 970$$

$$\beta_a := \left[\frac{50 \cdot 365 - 1}{\beta_H + (50 \cdot 365 - 1)}\right]^{0.3} = 0.985$$

$\varphi_{inf.t0} := \beta_c \cdot \varphi_0 = 2.093$ Final creep coefficient

Steel

$E_s = 200 \cdot GPa$

$\alpha_{ef} := \frac{E_s}{E_{cm}} \cdot \left(1 + \varphi_{inf.t0}\right) = 19.952$

Calculate position of neutral layer, assume two layers of reinforcement in compression zone

$x := 0.1m$ First guess

Given

$$t_w \cdot x \cdot \frac{x}{2} + \left(\alpha_{ef} - 1\right) \cdot A'_{s1} \cdot \left(x - d'_1\right) + \left(\alpha_{ef} - 1\right) \cdot A'_{s2} \cdot \left(x - d'_2\right) = \alpha_{ef} \cdot A_{s1} \cdot \left(d_1 - x\right) \ldots + \alpha_{ef} \cdot A_{s2} \cdot \left(d_2 - x\right) \ldots + \alpha_{ef} \cdot A_{s3} \cdot \left(d_3 - x\right)$$

$x := Find(x)$

$x = 0.363\,m$

"OK, assumption is correct" if $d'_2 < x < d_1$ = "OK, assumption is correct"

"Not OK" otherwise

Second moment of inertia of slab part

$I_{II.slab} := \alpha_{ef} \cdot A_{s2} \cdot \left(d_2 - h_w\right)^2 + \alpha_{ef} \cdot A_{s3} \cdot \left(d_3 - h_w\right)^2 = 2.017 \times 10^{-3}\,m^4$ Stadium II

$$I_{I.slab} := \frac{b_{eff} \cdot t_f^3}{12} + \left(\alpha_{ef} - 1\right) \cdot A_{s2} \cdot \left(d_2 - h_w\right)^2 \ldots + \left(\alpha_{ef} - 1\right) \cdot A_{s3} \cdot \left(d_3 - h_w\right)^2 = 4.616 \times 10^{-3}\,m^4$$ Stadium I

Second moment of inertia of beam part

$$I_{II.beam} := \frac{t_w \cdot x^3}{12} + (\alpha_{ef} - 1) \cdot A'_{s1} \cdot (x - d'_1)^2 + (\alpha_{ef} - 1) \cdot A'_{s2} \cdot (x - d'_2)^2 \ldots + \alpha_{ef} \cdot A_{s1} \cdot (d_1 - x)^2 = 2.799 \times 10^{-3}\,\mathrm{m}^4$$

$$I_{I.beam} := \frac{t_w \cdot h_w^3}{12} + (\alpha_{ef} - 1) \cdot A'_{s1} \cdot (x - d'_1)^2 + (\alpha_{ef} - 1) \cdot A'_{s2} \cdot (x - d'_2)^2 \ldots + (\alpha_{ef} - 1) \cdot A_{s1} \cdot (d_1 - x)^2 = 0.025\,\mathrm{m}^4$$

Stiffness reduction

$$E_{slab.support.4} := \frac{I_{II.slab}}{I_{I.slab}} = 0.437$$

$$E_{beam.4} := \frac{I_{II.beam}}{I_{I.beam}} = 0.11$$

Equivalent stiffness T-section 12.2<x<15m (compressed top), assuming beam 900mm high

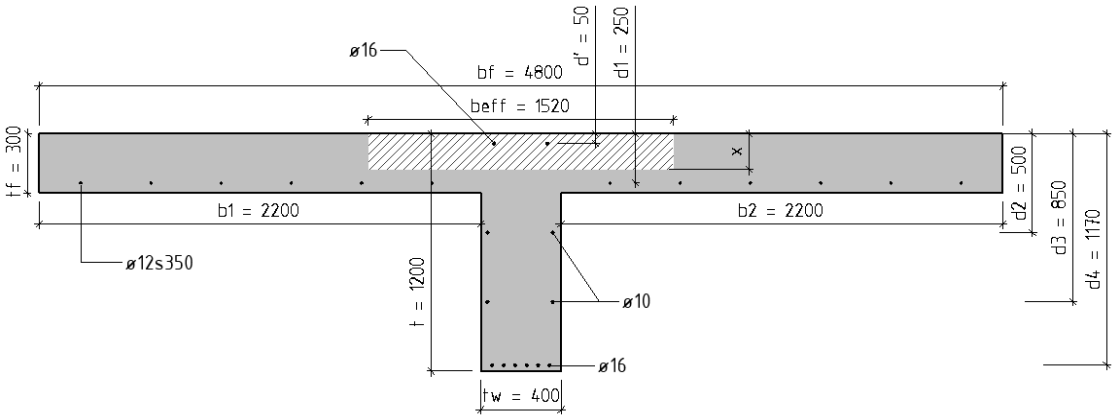

Concrete geometry

$b_f := 4800mm$

$t_f := 300mm$

$h_w := 900mm$

$t_w := 400mm$

$b_1 := \frac{b_f - t_w}{2} = 2.2\,m$

$b_2 := b_1$

$l_0 := 2.8m$ From Abaqus model with shells

$b_{eff.1} := \min\left(0.2b_1 + 0.1l_0, 0.2l_0\right) = 0.56\,m$

$b_{eff.2} := b_{eff.1}$

$b_{eff} := b_{eff.1} + b_{eff.2} + t_w = 1.52\,m$

Reinforcement geometry

$\varphi' := 16mm$ $n' := 2$ $d' := 50mm$

$\varphi_1 := 12mm$ $n_1 := 2$ $d_1 := 250mm$

$\varphi_2 := 10mm$ $n_2 := 2$ $d_2 := 500mm$

$\varphi_3 := 10mm$ $n_3 := 2$ $d_3 := 850mm$

$\varphi_4 := 16mm$ $n_{41} := 6$ $d_4 := 1170mm$

$$A'_s := n' \cdot \frac{\pi \cdot \varphi'^2}{4} = 4.021 \times 10^{-4}\, m^2$$

$$A_{s1} := n_1 \cdot \frac{\pi \cdot \varphi_1^2}{4} = 2.262 \times 10^{-4}\, m^2$$

$$A_{s2} := n_2 \cdot \frac{\pi \cdot \varphi_2^2}{4} = 1.571 \times 10^{-4}\, m^2$$

$$A_{s3} := n_3 \cdot \frac{\pi \cdot \varphi_3^2}{4} = 1.571 \times 10^{-4}\, m^2$$

$$A_{s4} := n_4 \cdot \frac{\pi \cdot \varphi_4^2}{4} = 1.608 \times 10^{-3}\, m^2$$

Materials

$E_{cm} = 31 \cdot GPa$ $f_{cm} := 33MPa$ Concrete C25/30

Creep

$\varphi_{inf.t0} = \beta_c \cdot \varphi_0$ Final creep coefficient

$\varphi_0 = \varphi_{RH} \cdot \beta_{fcm} \cdot \beta_{t0}$ Notional creep coefficient

$RH := 75\%$ BBK 04, Section 2.4.6, non-heated indoor

$A_c := b_{eff} \cdot t_f + t_w \cdot h_w = 0.816\,m^2$ Concrete area

$u := b_{eff.1} + b_{eff.2} + 2 \cdot h_w + t_w = 3.32\,m$ Perimeter exposed to drying, assumed underside of slab and complete beam

$$h_0 := \frac{2A_c}{u} = 0.492\,m$$

$$\varphi_{RH} := 1 + \frac{1 - \frac{RH \cdot 100}{100}}{0.1 \cdot \left(\frac{h_0 \cdot 1000}{m}\right)^{\frac{1}{3}}} = 1.317$$

$\beta_{fcm} := 2.93$

$\beta_{t0} := \frac{1}{0.1 + 15^{0.2}} = 0.55$ Assume load is applied at t=15 days

$\varphi_0 := \varphi_{RH} \cdot \beta_{fcm} \cdot \beta_{t0} = 2.121$

$$\beta_c = \left[\frac{t - t_0}{\beta_H + (t - t_0)}\right]^{0.3}$$

$$\beta_H := \min\left[1.5 \cdot \left[1 + (0.012 \cdot RH)^{18}\right] \cdot \frac{h_0 \cdot 1000}{m} + 250, 1500\right] = 987.349$$

$$\beta_c := \left[\frac{50 \cdot 365 - 1}{\beta_H + (50 \cdot 365 - 1)}\right]^{0.3} = 0.984$$

$\varphi_{inf.t0} := \beta_c \cdot \varphi_0 = 2.088$ Final creep coefficient

Steel

$E_s := 200GPa$

$\alpha_{ef} := \frac{E_s}{E_{cm}} \cdot \left(1 + \varphi_{inf.t0}\right) = 19.923$

Calculate position of neutral layer, assume one layer of reinforcement in compression zone

$x := 0.1\,m$ First guess

Given

$$b_{eff}\cdot x\cdot\frac{x}{2} + (\alpha_{ef} - 1)\cdot A'_s\cdot(x - d') = \alpha_{ef}\cdot A_{s1}\cdot(d_1 - x) + \alpha_{ef}\cdot A_{s2}\cdot(d_2 - x) + \alpha_{ef}\cdot A_{s3}\cdot(d_3 - x) \ldots + \alpha_{ef}\cdot A_{s4}\cdot(d_4 - x)$$

$x := \text{Find}(x)$

$x = 0.208\,m$

"OK, assumption is correct " if $x < d_1$ = "OK, assumption is correct "

"Not OK" otherwise

Second moment of inertia of slab part

$$I_{II.slab} := \frac{b_{eff}\cdot x^3}{12} + (\alpha_{ef} - 1)\cdot A'_s\cdot(x - d')^2 \ldots + \alpha_{ef}\cdot A_{s1}\cdot(d_1 - x)^2 = 1.331\times 10^{-3}\,m^4$$ Stadium II

$$I_{I.slab} := \frac{b_{eff}\cdot t_f^3}{12} + (\alpha_{ef} - 1)\cdot A'_s\cdot(x - d')^2 \ldots + (\alpha_{ef} - 1)\cdot A_{s1}\cdot(d_1 - x)^2 = 3.617\times 10^{-3}\,m^4$$ Stadium I

Second moment of inertia of beam part

$$I_{II.beam} := \alpha_{ef}\cdot A_{s2}\cdot(d_2 - t_f)^2 + \alpha_{ef}\cdot A_{s3}\cdot(d_3 - t_f)^2 + \alpha_{ef}\cdot A_{s4}\cdot(d_4 - t_f)^2 = 0.025\,m^4$$

$$I_{I.beam} := \frac{t_w\cdot h_w^3}{12} + (\alpha_{ef} - 1)\cdot A_{s2}\cdot(d_2 - t_f)^2 + (\alpha_{ef} - 1)\cdot A_{s3}\cdot(d_3 - t_f)^2 \ldots + (\alpha_{ef} - 1)\cdot A_{s4}\cdot(d_4 - t_f)^2 = 0.048\,m^4$$

Stiffness reduction

$$E_{slab.support.5} := \frac{I_{II.slab}}{I_{I.slab}} = 0.368$$

$$E_{beam.5} := \frac{I_{II.beam}}{I_{I.beam}} = 0.524$$

Results

$E_{slab.410.field} = 0.178$

$E_{reduced.slab.410.field} := E_{cm} \cdot E_{slab.410.field} = 5.514 \cdot GPa$

$E_{slab.300.field} = 0.139$

$E_{reduced.slab.300.field} := E_{cm} \cdot E_{slab.300.field} = 4.309 \cdot GPa$

$E_{slab.support.1} = 0.162$ 0<x<=4.5m

$E_{reduced.slab.support.1} := E_{cm} \cdot E_{slab.support.1} = 5.037 \cdot GPa$

$E_{slab.support.2} = 0.192$ 4.5<x<=6.8m

$E_{reduced.slab.support.2} := E_{cm} \cdot E_{slab.support.2} = 5.955 \cdot GPa$

$E_{slab.support.3} = 0.319$ 6.8<x<=10.2m

$E_{reduced.slab.support.3} := E_{cm} \cdot E_{slab.support.3} = 9.901 \cdot GPa$

$E_{slab.support.4} = 0.437$ 10.2<x<=12.2m

$E_{reduced.slab.support.4} := E_{cm} \cdot E_{slab.support.4} = 13.546 \cdot GPa$

$E_{slab.support.5} = 0.368$ 12.2<x<=15m

$E_{reduced.slab.support.5} := E_{cm} \cdot E_{slab.support.5} = 11.405 \cdot GPa$

$E_{beam.1} = 0.528$ 0<x<=4.5m

$E_{reduced.beam.1} := E_{cm} \cdot E_{beam.1} = 16.36 \cdot GPa$

$E_{beam.2} = 0.156$ 4.5<x<=6.8m

$E_{reduced.beam.2} := E_{cm} \cdot E_{beam.2} = 4.836 \cdot GPa$

$E_{beam.3} = 0.531$ 6.8<x<=10.2m

$E_{reduced.beam.3} := E_{cm} \cdot E_{beam.3} = 16.47 \cdot GPa$

$E_{beam.4} = 0.11$ 10.2<x<=12.2m

$E_{reduced.beam.4} := E_{cm} \cdot E_{beam.4} = 3.404 \cdot GPa$

$E_{beam.5} = 0.524$ 12.2<x<=15m

$E_{reduced.beam.5} := E_{cm} \cdot E_{beam.5} = 16.237 \cdot GPa$

Appendix E – Shear strengthening calculations

In all methods a one metre wide strip in the thicker part of the slab is studied

Geometry

$h_w := 410mm$

$b_w := 1000mm$

$\theta := 40deg$ shear crack inclination

$\alpha_{45} := 45deg$ 45 deg inclination of ETS bar

$\alpha_{90} := 90deg$ 90 deg inclination of ETS bar

$d := 380mm$ effective depth of slab

$\phi_{ETS} := 12mm$ consider ETS bar diameter 12mm

$n_{bar} := 1$ number of bars

$A_{fw} := \pi \cdot \left(\frac{\phi_{ETS}}{2} \right)^2 \cdot n_{bar} = 1.131 \times 10^{-4} m^2$

$s_{fw} := 300mm$ spacing of ETS bars

$L_f := \frac{h_w}{\sin(\alpha_{45})} = 0.58\,m$ ETS bar length

$A_c := s_{fw} \cdot \frac{b_w}{2} = 0.15\,m^2$

$n_{FRP} := 2$ number of layers of FRP-strips

$t_{FRP} := 3.04mm$ thickness FRP strip

$w_{FRP} := 25mm$ width FRP strip

$A_{FRP} := t_{FRP} \cdot w_{FRP} = 7.6 \times 10^{-5} \cdot m^2$ width of FRP-strips used

Material data

Steel

$f_{yt} := 500MPa$ yield strength of steel bar

$E_{fw} := 200GPa$ youngs's modulus for ETS steel

Concrete

$f_{cm} := 28MPa$ average concrete compressive strength

$f_{ck} := 25MPa$

$$f_{ctm} := 1.4 \cdot \left(\frac{\frac{f_{cm}}{MPa} - 8}{10} \right)^{\frac{2}{3}} \cdot MPa = 2.222 \cdot MPa$$

$$E_c := 2.15 \cdot 10000 \cdot \left(\frac{\frac{f_{cm}}{MPa}}{10} \right)^{\frac{1}{3}} \cdot MPa = 30.303 \cdot GPa$$

$$\gamma_c := 1.5$$

FRP

$f_{u.FRP} := 876MPa$ ultimate tensile strength of CFRP used by Binici & Bayrak (2006)

$$\beta := \frac{1}{3}$$

$$f_{y.FRP} := \beta \cdot f_{u.FRP} = 292 \cdot MPa$$

Drilled-in steel bars method (simple)

Calculation carried out according to equation proposed by Breveglieri et al. (2014).

Shear capacity

$$V_{f.simple} := \frac{A_{fw} \cdot f_{yt} \cdot \left(\sin(\alpha_{45}) + \cos(\alpha_{45}) \right) \cdot d}{s_{fw}} = 101.298 \cdot kN$$

$V_{f.simple} = 101.298 \cdot kN$

Drilled-in steel bars method (detailed)

Same calculation procedure as in the study by Breveglieri et. al (2015) is used

Model parameters

$\beta_a := 28.5deg$ angle between bar and concrete conical surface

$\tau_0 := 16MPa$ bond stress

$\delta_1 := 6mm$ bond slip

Shear contribution

$$N_{fint} := \text{floor}\left(h_w \cdot \frac{\cot(\theta) + \cot(\alpha_{45})}{s_{fw}}\right) = 2$$

$$x_{fi} := N_{fint} \cdot s_{fw} = 0.6\,\text{m}$$

$$L_{fi} := \begin{cases} \left(N_{fint} \cdot s_{fw} \cdot \frac{\sin(\theta)}{\sin(\theta + \alpha_{45})}\right) & \text{if } x_{fi} < \frac{h_w}{2} \cdot \left(\cot(\theta) + \cot(\alpha_{45})\right) \\ \left(L_f - N_{fint} \cdot s_{fw} \cdot \frac{\sin(\theta)}{\sin(\theta + \alpha_{45})}\right) & \text{otherwise} \end{cases} = 0.193$$

$$L_{Rfi} := \frac{1}{N_{fint}} \cdot \sum_{i=1}^{N_{fint}} L_{fi} = 0.193\,\text{m}$$ Average value of availble bond length

$$L_p := \phi_{ETS} \cdot \pi = 0.038\,\text{m}$$ Bar perimeter

$$J_1 := \frac{L_p}{A_{fw}} \cdot \left(\frac{1}{E_{fw}} + \frac{A_{fw}}{A_c \cdot E_c}\right) = 1.675 \times 10^{-9}\,\frac{s^2}{kg}$$ Bond modelling constant

$$\lambda := \sqrt{\frac{\tau_0 \cdot J_1}{\delta_1}} = 2.113\,\frac{1}{m}$$ Bond modelling constant

$$L_{Rfe} := \frac{\pi}{2 \cdot \lambda} = 0.743\,\text{m}$$ Effective resisting bond length

$$V_{f.bd1} := \frac{L_p \cdot \lambda \cdot \delta_1}{J_1} = 285.407 \cdot \text{kN}$$ Corresponding maximum bond force

$$V_{f.y} := \frac{\pi \cdot \phi_{ETS}^{\,2}}{4} \cdot f_{yt} = 56.549 \cdot \text{kN}$$ Force developed by single ETS bar after yield force is reached

$$f_{ctm.s} := \frac{L_p \cdot \lambda \cdot \delta_1 \cdot \sin(\lambda \cdot L_{Rfi})}{J_1 \cdot \pi \cdot \min\left(L_{Rfi} \cdot \tan(\beta_a), \frac{b_w}{4}\right) \cdot \frac{\sin(\theta + \alpha_{45})}{2} \cdot \left(\begin{array}{l} \min\left(\frac{s_{fw} \cdot \sin(\alpha_{45})}{2 \cdot \sin(\theta + \alpha_{45})}, \frac{L_{Rfi} \cdot \sin(\beta_a)}{\sin(\alpha_{45} + \theta + \beta_a)}\right) \ldots \\ + \min\left(\frac{s_{fw} \cdot \sin(\alpha_{45})}{2 \cdot \sin(\theta + \alpha_{45})}, \frac{L_{Rfi} \cdot \sin(\beta_a)}{\sin(\alpha_{45} + \theta + \beta_a)}\right) \end{array}\right)}$$

$f_{ctm.s} = 3.444 \cdot MPa$ Value of average concrete tensile strength for values larger than for which concrete fracture does not occur

$$\eta := \begin{cases} \sqrt{\frac{f_{ctm}}{f_{ctm.s}}} & \text{if } f_{ctm} < f_{ctm.s} \\ 1 & \text{otherwise} \end{cases} = 0.803$$

$L_{Rfi.eq} := L_{Rfi} \cdot \eta = 0.155\ m$ equivalent value of average resisting bond length

$V_{f.bd} := L_p \cdot \frac{1}{J_1} \cdot \lambda \cdot \left(\delta_1 \cdot \sin\left(\lambda \cdot L_{Rfi.eq}\right)\right) = 91.71 \cdot kN$ Resisting bond force

$V_{f.eff} := \min\left(V_{f.bd}, V_{f.y}\right) = 56.549 \cdot kN$

$V_{f.detail} := n_{bar} \cdot N_{fint} \cdot V_{f.eff} \cdot \sin\left(\alpha_{45}\right) = 79.972 \cdot kN$

$V_{f.detail} = 79.972 \cdot kN$

Vertical or angled bolts method

Calculations carried out according to equation proposed by Baig, Alsayed, & Abbas (2015)

$$V_{f.bolt} := \frac{f_{yt} \cdot A_{fw} \cdot \left(\sin\left(\alpha_{45}\right) + \cos\left(\alpha_{45}\right)\right) \cdot d}{s_{fw}} = 101.298 \cdot kN$$

$V_{f.bolt} = 101.298 \cdot kN$

Externally bonded FRP

Calculations carried out according to equation proposed by Jung et al. (2015)
with assumptions taken from Binici & Bayrak (2006)

$$V_{f.ebr} := \frac{\beta \cdot n_{FRP} \cdot A_{FRP} \cdot f_{u.FRP} \cdot d}{s_{fw}} = 56.22 \cdot kN$$

$V_{f.ebr} = 56.22 \cdot kN$

Embedded through section FRP

Calculations carried out in the same way as for drilled-in steel bar but with different material parameters

$$V_{f.ets} := \frac{A_{fw} \cdot f_{y.FRP} \cdot \left(\sin\left(\alpha_{45}\right) + \cos\left(\alpha_{45}\right)\right) \cdot d}{s_{fw}} = 59.158 \cdot kN$$

$V_{f.ets} = 59.158 \cdot kN$

Strengthening due to flexural reinforcement

Longitudinal reinforcement area

$r_{reinf} := 6mm$ radius of reinforcement bars

$A_{si} := r_{reinf}^{2} \cdot \pi = 113.097 \cdot mm^2$

$s_l := 200mm$ spacing longitudinal reinforcement bars

$A_s := \frac{A_{si} \cdot b_w}{s_l} = 565.487 \cdot mm^2$

Addition from Flexural strengthening

$b_{FRP.l} := 150mm$ width of longitudinal reinforcement

$t_{FRP.l} := 1.2mm$ thickness of longitudinal reinforcement

$n_{FRP.l} := 2$ number of strengthening strips

$A_{FRP.l} := n_{FRP.l} b_{FRP.l} \cdot t_{FRP.l} = 3.6 \times 10^{-4} m^2$ cross-sectional area of flexural strengthening

$E_{FRP} := 240GPa$ Young's modulus of flexural strengthening

$A_{eq.s} := A_{FRP.l} \cdot \frac{E_{FRP}}{E_{fw}} = 432 \cdot mm^2$

$A_{s.tot} := A_s + A_{eq.s} = 997.487 \cdot mm^2$

Shear capacity of slab with flexural strengthening

$$k := \min\left[1 + \left(\frac{200\cdot mm}{d}\right)^{0.5}, 2.0\right] = 1.725$$

$$\rho_l := \min\left(\frac{A_{s.tot}}{b_w\cdot d}, 0.02\right) = 2.625 \times 10^{-3}$$

$$C_{Rd.c} := \frac{0.18}{\gamma_c} = 0.12$$

$$v_{min1} := 0.035\cdot k^{\frac{3}{2}}\cdot\left(\frac{f_{ck}}{MPa}\right)^{0.5} = 0.397$$

$$V_{Rd.c} := \left[C_{Rd.c}\cdot k\cdot\left(100\cdot\rho_l\cdot\frac{f_{ck}}{MPa}\right)^{\frac{1}{3}}\right]\cdot\frac{b_w\cdot d}{mm^2}\cdot N = 147.309\cdot kN$$

$$V_{Rd.c.min} := v_{min1}\cdot\frac{b_w\cdot d}{mm^2}\cdot N = 150.725\cdot kN$$

$$V_{Rd.c} := \max\left(V_{Rd.c}, V_{Rd.c.min}\right)$$

$V_{Rd.c} = 150.725\cdot kN$

Number of strips needed for $V_{Rd.c}$ = 200 kN

$n_{FRP.l} := 9$ Increase number of strips until $V_{Rd.c}$ > 200 kN

$$A_{FRP.l} := n_{FRP.l}\, b_{FRP.l}\cdot t_{FRP.l} = 1.62 \times 10^{-3}\cdot m^2$$

$$A_{eq.s} := A_{FRP.l}\cdot\frac{E_{FRP}}{E_{fw}} = 1.944 \times 10^{3}\cdot mm^2$$

$$A_{s.tot} := A_s + A_{eq.s} = 2.509 \times 10^{3}\cdot mm^2$$

$$\rho_l := \min\left(\frac{A_{s.tot}}{b_w \cdot d}, 0.02\right) = 6.604 \times 10^{-3}$$

$$V_{Rd.c} := \left[C_{Rd.c} \cdot k \cdot \left(100 \cdot \rho_l \cdot \frac{f_{ck}}{MPa}\right)^{\frac{1}{3}}\right] \cdot \frac{b_w \cdot d}{mm^2} \cdot N = 200.349 \cdot kN$$

$$V_{Rd.c.min} := v_{min1} \cdot \frac{b_w \cdot d}{mm^2} \cdot N = 150.725 \cdot kN$$

$$V_{Rd.c} := \max\left(V_{Rd.c}, V_{Rd.c.min}\right)$$

$$V_{Rd.c} = 200.349 \cdot kN$$